Universiteit Utrecht

Department of Earth Science

Master's Thesis

Reconstructing the eruption history of El Chichón volcano from river terraces (Chiapas, Mexico)

Author:
Bocaj Post

Supervisors:
Dr. M.J. van Bergen
Ir. C.A.M. Nooren

Fieldwork supervisors:
Prof. dr. H. Middelkoop
Dr. W.Z. Hoek

28 October 2016
Academic Year 2015/2016

Abstract

El Chichón volcano (Chiapas, Mexico) is known for its devastating eruption in 1982. This event instigated more research to improve our knowledge on its eruption history. Although 12 eruptions have been recognized over the last 8000 years, the data are incomplete and leave uncertainties concerning frequency and impacts of the eruptive events, specifically for the early history of the volcano. Because El Chichón eruptions often have an explosive character, much of the activity record is represented by tephra deposits. A distal archive has recently become available from tephra-fall deposits collected in drill core from a swampy area in the Usumacinta-Grijalva delta. Based on the chemical signature of glass shards, the distinguished eruptive events could generally be attributed to activity of El Chichón, except for relatively silica-rich tephra which has a deviating composition not recognized in the volcano so far.

In order to further explore the eruption history of El Chichón with proximal deposits, river terraces of the Platanar and Magdalena rivers were investigated, assuming that they formed during or shortly after an eruption of El Chichón and thus are “event related”.

This thesis addresses the following research questions: 1. Are river terraces that largely consist of pyroclastic material suitable for tephrochronology? 2. Does each terrace level of the Magdalena and Platanar rivers represent a single eruption? Are they so-called ‘event terraces’? 3. Does the SiO_2-rich distal tephra from the delta plain area have an equivalent in the river terraces and could it therefore be linked to El Chichón or not?

To answer these questions, fieldwork was carried out to collect pumice and matrix samples from terraces in the valleys of the Magdalena and Platanar rivers, in close proximity to El Chichón. Electron microprobe analysis of glass shards, mineral phases and microliths of pumices and matrix material was used to obtain geochemical fingerprint of each terrace. A total of eight eruption-related terraces were distinguished using evidence from Lidar images, reports on hyper-concentrated and debris flows in the river valleys, existing maps of eruption deposits, and C-14 dating of charcoal. Morphological features in the terrace stratigraphy, inverse grading, and intervals of coarse-grained pumice-rich layers were useful as additional indicators.

The river terraces of the Magdalena and Platanar rivers appeared suitable for tephrochronology and geochemical fingerprinting, although the limited compositional variability of the volcanic products of El Chichón through time make it difficult to distinguish the different eruptions. Four terraces represented the 1982 eruption and three had developed during older eruptions with unknown ages. All of the analysed glasses from pumices and shards in terrace matrix showed a fairly uniform geochemistry. Nonetheless, the results of this thesis demonstrate that geochemical fingerprinting of river terraces around active, tephra-producing volcanoes can be used as an additional tool to reconstruct eruption histories in cases where primary deposits are lacking or inaccessible.

The source of the high SiO_2 cluster found in the delta plain of Tabasco, Mexico is most likely the 84 ka Los Chocoyos eruption of the Guatemalan Atitlan volcano. Major and trace-element compositions of glasses from this cluster are similar to air fall tephra of this eruption, and are distinct from the signatures of El Chichón products.

Acknowledgement

I am grateful to the following people for their assistance throughout the project:

Dr. Manfred van Bergen for the time and work he has put into my research, his proofreading and his patience.

Ir. Kees Nooren, Dr. Wim Hoek and Prof. dr. Hans Middelkoop for their guidance during fieldwork and for their opinions and advice.

Dr. Paul Mason for his encouragement and advice.

Tilly Bouten and Dr. Sergey Matveev of Geolab, Utrecht University for their help with microprobe analysis, kind discussion, advice and assistance in processing the data.

Őzlem Ersoy and Alejandro Rodríguez for providing me with new insights when I had to solve scientific problems.

I am very thankful to Karlijn Smits who has been of great encouragement throughout this work, during the fieldwork, both scientifically and personally.

Finally, my sincere gratitude goes to Annika Huizinga for assisting me during the project, her curiosity for the results and appreciation.

Table of Content

Page

Contents

1. Introduction

In Chiapas, Mexico, the volcano El Chichón erupted in 1982. Before that eruption El Chichón was a relatively unimportant volcano, one of the many volcanoes present in Mexico. The 1982 eruption had dramatic consequences for the inhabitants of Chiapas and Tabasco, over 2000 people died from the eruption that lasted for 6 days (Carey and Sigurdsson, 1986). It caused tremendous economic damage to the area. Since then the government of Mexico along with many scientists paid more attention to the Central Volcanic Arc, the volcanic system of El Chichón. During the eruption huge amounts of fine ash with high sulphur concentrations were ejected into the atmosphere which had a global cooling effect on the earth. These ash layers were also found in an ice core on the North Pole (Palais et al., 1992).

Despite numerous studies the eruptive history of the volcano is not well known. Espíndola et al. (2000) reported at least twelve eruptions in the last 8000 years, four of them occurred in the last 2000 years. Duffield et al. (1984) reported that the entire dome of the volcano consists of pyroclastic rocks. Tephra layers in flood basin deposits of the Usumacinta-Grijalva delta plain were identified by Nooren et al. (2009) and were linked to past eruptions of El Chichón.

A Master student from the Utrecht University (Huizinga, 2013, unpub. MSc thesis) was the first to derive a detailed petrological and geochemical record of the eruption history of El Chichón for the last 3000 years. In the swamps of the Tabasco delta plain at the Gulf of Mexico a core was drilled. Distal tephra-fall deposits within the organic flood basin deposits were isolated from the drill core and analysed for chemical fingerprinting. The tephra layers were dated using ^{14}C dating of organic material found in the core. The distal tephra showed a range of chemical compositions. Based on their SiO_2 composition they were divided into three groups. Two groups were linked to the proximal deposits at slopes of El Chichón, but the third group with the highest SiO_2 content (77-79 wt.%) could not be linked. This third group was mainly present in the deeper parts of the drill core, whereas the other two groups were mainly present the upper layers of the drill core. It is suggested that this high SiO_2 cluster might represent an old eruption of El Chichón.

1.1 Eruption related river terraces

This thesis has two main research questions: 1. Are river terraces suitable for tephrochronology and does each river terrace of the Magdalena and Platanar river represents one eruption? 2. Is the high SiO_2 content tephra group (3^{th} group, 77-79%) from the distal delta plain area in Tabasco, Mexico also found in the river terraces and linked to El Chichón?

Therefor the river valleys near El Chichón were visited to collect tephra and look for geomorphic features indicating eruption related terraces. Preliminary research from height altitude maps suggests that the river terraces are events terraces formed during or after an eruption. The hypothesis is that river terraces in close distance to the volcano formed during or after an eruption. After an eruption there is much new material which is deposited in the river valleys as one thick layer of new material. With time erosion removes most of the deposits and what remains forms the event terrace. after a consequent eruption new material is deposited and a new terrace forms after erosion, but at a lower level than the previous eruption. In the time between eruptions incision by the river cuts down into the river valley below the old event terrace. Therefor the new event terrace

will be at a lower level than the previous one. Older terraces will be higher and further away from the river and young terrace closer to the river.

1.2 High SiO_2 swamp core tephra

Earlier work conducted by Nooren et al. (2009) and Huizinga (2013, unpub. MSc thesis) shows the importance of this high SiO_2 cluster tephra. The results will not only contribute to a more detailed understanding of the eruption history of El Chichón volcano, but also contributes to the reconstruction of the evolution of the Usumacinta-Grijalva delta plain. Volcanoclastic sediments are an important component of the alluvial deposits in the delta and the beach ridges at the Mexican coast. This study will provide essential information for geographers studying the beach ridge development and the influence of past eruptions on the climate. Another important aspect is the impact of past eruptions on Maya cultures present in the area.

In order to investigate this, fieldwork was conducted to collect tephra from the river terraces of the Tabasco delta plain; in proximity of 30 km of El Chichón (fig. 5). River terraces of Magdalena and (North) Platanar were sampled. The Platanar has two branches, the North and South Platanar rivers; the main branch is the North Platanar river. The South Platanar river is a small stream of minor importance. For convenience, the North Platanar river will be mentioned as the Platanar river. These two rivers starting near El Chichón and transport most of the eruption material downstream into the Tabasco delta plain area. The chemical composition of the tephra was derived using electron microprobe analysis. Tephra from the distal area in the swamp core of the Tabasco delta plain was compared to the proximal river terrace tephra.

In summary, this research is done to provide new knowledge on the eruption history and answering the following questions.

Two main research questions:

> Are river terraces suitable for tephrochronology and does each river terrace level of the Magdalena and Platanar river represents one eruption?
>
> Is the high SiO_2 content tephra group (3^{th} group, 77-79 wt.%) from the distal delta plain area in Tabasco, Mexico also found in the river terraces and linked to El Chichón?

Subquestions:

> Are these 'event' river terraces formed during or shortly after an eruption?
>
> Is tephra composition from the river terraces uniform or do different events have different chemical compositions?
>
> Is there a difference between proximal and distal tephra?

1.3 Structure

The outline of this thesis is as follows. First the geological settings are described with the most recent events and available tephra data. In the research strategy the river terrace setting, theory of terrace formation and its surrounding are described. Next the approach taken for field sampling, research strategies, definitions and sample preparation. Section 4 describes the sample quality, contamination

and other sources of errors. In the results the terrace conditions, content of the individual terrace, sample pairs, clusters, microliths and enclosed minerals are reported.

The importance of river terraces and the source of the high SiO_2 cluster tephra are described in the discussion. The eruption history of El Chichón is further improved, the uniformity of the volcano is discussed and the origin of the volcanic deposits in the Grijalva and Usumacinta delta plain is derived. The chapters are subdivided into smaller paragraphs notated with numbers. The figures in the Appendix are named after their order; the first appendix is named A so the figures all get noted as A-1, A-2, etc.

2. Background and geological settings

El Chichón is a plinian volcano with trachandesites volcanic rocks, located on the north-western part of the Chiapas province (7°22'N, 93°14'W, altitude of 1260 m), Mexico. It is the last active volcano of the Chiapanecan Volcanic Arc (CVA). The volcano has unusual high potassic and sulphur rich andesitic rocks. The Cardenal and Cerro Ventana volcano are two older domes in the surroundings which were active in the past (fig. 1). Studies indicate that these volcanoes are 1.64 Ma old based on $^{40}Ar/^{39}Ar$ dating of lithic blocks in the deposits on the slopes of the dome (Scolamacchia and Macias, 2015 chapter 1). However not much is known on these domes and more research is required to constrain their early activity. The volcanic activity of El Chichón is thought to have started between 276-55 ka (Layer et al. 2009, Duffield et al. 1984, Damon and Montesinos, 1978).

Duffield et al. (1984) described the volcano as a 'tuff cone surround by a ring of domes'. The dome is build-up of a pyroclastic sequence and deposited on top of each other in a chaotic way. The volcano lies on top of Jurassic to Miocene stratigraphy of carbonate, evaporate and sandstone deposits. These include Cretaceous marine limestones, claystones and sandstones from the Palaeocene to the Miocene (Canul et al. 1983).

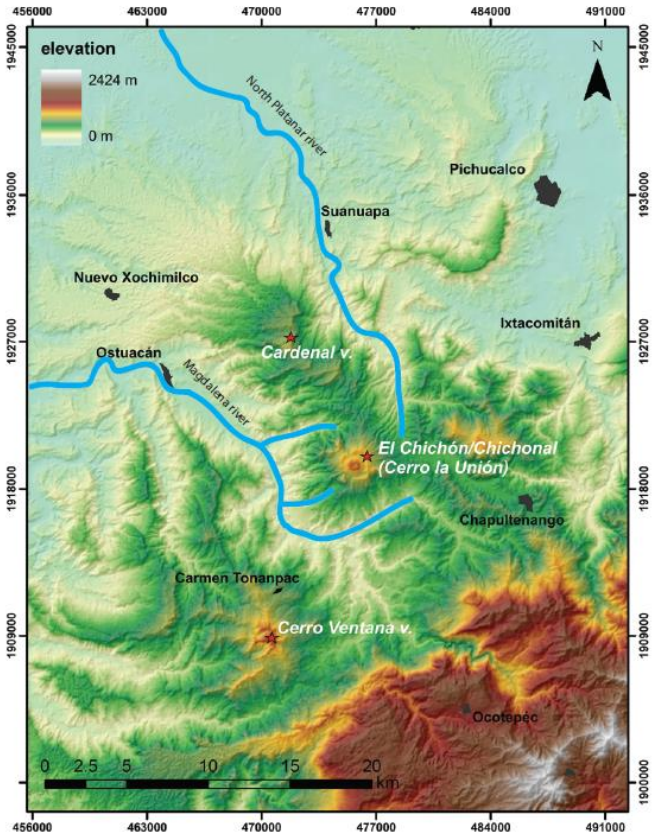

Figure 1. Adjusted elevation map of El Chichón area. In blue are the Magdalena and (North) Platanar River, stars show the past and present domes (Scolamacchia and Macias, 2015 chapter 3.1). Names in white are the volcanoes and in black the villages.

2.1 Origin of volcanic activity

Currently there are two theories which explain the origin of volcanic activity beneath El Chichón. The first theory states that the volcanism is related to subduction of the Cocos plate under the North American plate (Burbach et al. 1984, Mora et al. 2007) and second that it is caused by rifting (Nixon 1982, Arce et al. 2014). The CVA is located in a complex fault zone where the North American, Caribbean and Cocos plate interact with each other and is accompanied by volcanism. The volcanic activity of the CVA domes consist of mainly effusive eruptions accompanied by very explosive events which produce pyroclastic flows, pumice flows, block and ash fall. Research done on volcanic rock by Mora et al. (2007) show low concentration of P, Nb, Ti and Ta. There is an enrichment in LRE (Light Rare earth elements) and depletion in HRE (Heavy Rare earth elements), along with a minor Eu anomaly. All are indications of a subduction related process producing this type of volcanism, which is subducting of the Cocos plate beneath Central America. The second theory relates the volcanism to rifting. Kim et al. (2011) states that the Cocos plate is not present beneath the CVA and that the volcanism cannot be subduction related. The distinct high potassium and sulphur content of the volcanic products makes the first theory unlikely. Also there is a gap between the CAVA and CVA (Fig.

37) of ~150 km with no volcanic systems. It is more likely that the volcanism is related to rifting. El Chichón is located on the eastward extension of the Veracruz fault, which accommodate the complex movement of the three plates by sinistral transtension.

2.2 Eruption record

Not much is known on the early eruption history of El Chichón. Canul and Rocha (1981) were the first to make a reconstruction of the eruption history of the volcano, however no age was derived for the volcanic deposits. Tilling et al. (1984) found widespread pyroclastic flow and Plinian air-fall deposits in the proximity of the volcanic dome and used radiometric dating and pottery shards to constrain the age. Six units were found (A-F, fig. 2) and most of them were dated. Only unit A and E could not be dated. The 1982 eruption destroyed part of the dome, but implications were made that unit B was the last eruption that occurred before the 1982 eruption. In Unit E no charcoal was found. During the following years a more detailed eruption history was derived and the 1982 eruption was investigated in more detail (Macias et al., 1994, Macías et al., 1997, 1998). All these papers mainly focussed on the most recent event, the 1982 eruption. A more detailed eruption recorded was made by Espíndola et al. (2000), finding volcanic deposits of 12 eruptions from the last 8000 years. The eruption record derived by Tilling et al. (1984) was further improved and more units found. The age was constrained using charcoal remnants found in the deposits and paleosoils. Layer et al. (2009) analysed juvenile products of several domes and discussed the evolution of El Chichón in the early stages of formation. Their data suggests that the first activity started around 370 ka and did chemical analysis on these rocks. Nooren et al. (2009) recognized ten tephra layers in a drill core of beach ridges in the Grijalva-Usumacinta delta. their age was derived by radiometric dating of charcoal and pieces of wood along with an age-depth model using accumulation rates of sediments. Seven of these layers were related to the past eruptions. They correspond to units A-C and E-H described in Espíndola et al. (2000). These distal deposits show a strong correspondence with the proximal pumice air-fall deposits on the slopes of El Chichón. Huizinga (2013, unpub. MSc thesis) recognized several air-fall tephra layers in a drill core from the swamps in the Usumacinta-Grijalva delta (fig. 5). By radiometric dating of charcoal on different depth in the cores the age of the tephra is constrained. Of the nine identified tephra layers eight were connected to the eruption history units as described in Espíndola et al. (2000).

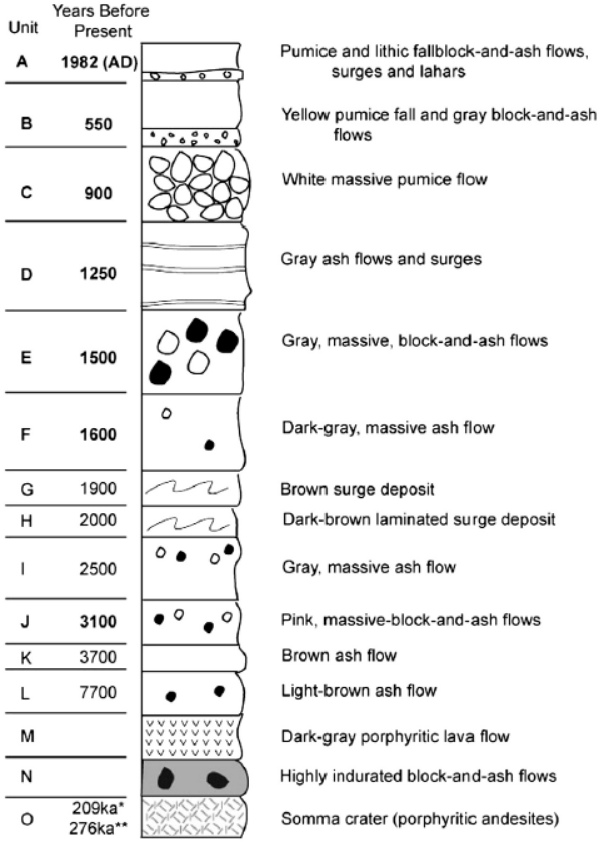

Figure 2. Simplified stratigraphic column from El Chichón's eruption history in Andrew et al. (2008, from Espíndola et al. 2000). Age and unit of the different eruptions are given in years BP. The Additional ages reported in unit O are from Duffield et al. (1984) and Damon and Montesinos (1978).

The 1982 eruption produced $2x10^9$ m^3 bulk deposit volume (Vogripa, 2015). The 550-700 BP eruptions (Unit B, C fig. 2) are suggested to be several times larger than 1982 eruption (Palais et al. 1992). Macias et al. (2003) analysed whole rock and pumice products from the 550 BP eruption near the soma and estimated $2.8x10^9$ m^3 bulk deposit volume.

2.3 Rock chemistry

The sources of data on whole rock chemistry available for El Chichón are from samples collected around the dome. Figure 3 shows the composition of tephra and whole rock data of El Chichón. Tepley et al. (2000) and Andrew et al. (2008) use phenocrysts from volcanic dome rock to investigate the volcanic system. There little information on tephra of this volcano. All data mainly discusses most recent eruptions (1982, 550 BP, Units A, B, table 1). In table one a summary is made from all papers that have analysed either whole rock and/or tephra data (fig. 3). The whole rock data goes back at least 8000 years or even to the Pleistocene (Arce et al. 2014), although they do not mention a specific age. The whole rock shows a pretty uniform composition (Macias et al. 2003, Luhr et al. 1984, Espíndola et al. 2000).

Table 1. Summary of authors that reported whole rock and/or tephra data of El Chichón.

Whole rock data	**Eruption**		**Tephra data**	**Eruption**
Luhr et al. 1984	1982		Luhr et al. 1984	1982
Rose et al. 1984	1982 and older but don't give age		Casadevall et al. 1984	1982
Espíndola et al. 2000	1982-8000 BP		Cochemé et al. 1983	1982
Macías et al. 2003	550 BP		Palais et al. 1992	1982
Andrews et al. 2008	3100 BP - 1982		Macías et al. 2003	550 BP
Layer et al. 2009	370 Ka-1982			
Arce et al. 2014	Pleistocene to 1982			

Besides pyroclastic flow and air-fall tephra deposits in proximity of the volcano, other sources of tephradata were found at more distal locations that possibly originate to El Chichón. From drill cores in the Usumacinta-Grijalva delta plain, air-fall tephra deposits with similir tephra composition as the volcanoclastic deposits from El Chichón were reported (Huizinga 2013, unpub. MSc thesis and Nooren et al., 2009). These distal tephra layers are most likely linked to El Chichón (fig. 4). However not all tephra layers were connected with great certainty. These distinct tephra deposits will be discussed later.

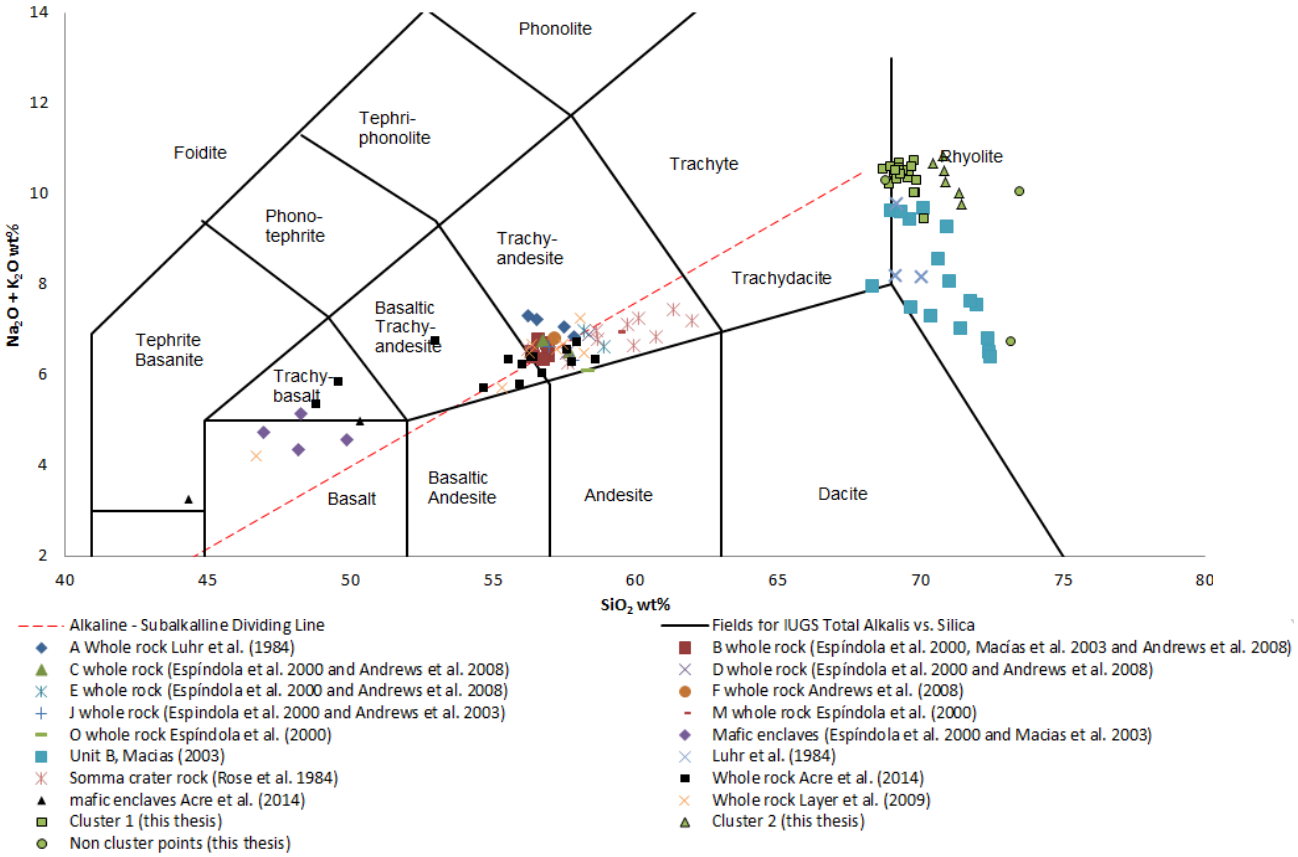

Figure 3. TAS diagram showing whole rock, tephra and mafic enclave chemistry of El Chichón rocks. Red line shows the subdivision between the alkaline and the sub alkaline rocks. Updated from Huizinga et al. (2013, unpub. MSc thesis).

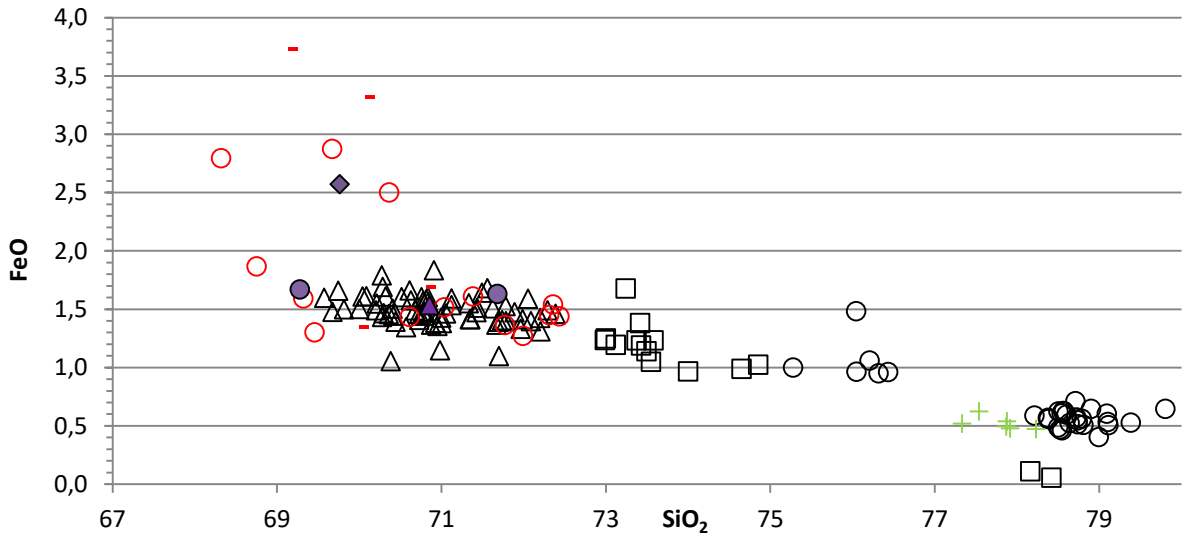

Figure 4. SiO_2-FeO composition plot showing all tephra data currently available from both the proximal and distal area in Tabasco, Mexico.

2.4 Nomenclature

In this thesis several definitions are used and need explanation. Sample names, coordinate numbers, cluster definitions and terrace names all have their own abbreviation.

The first nomenclature considers the groups derived in the thesis from Huizinga (2013, unpub. MSc thesis). Here three clusters were made on the basis of SiO_2 concentrations. Table 2 shows the details of clusters 1-3. In this thesis they are described as H_{C1}-H_{C3}, where the H stands for the author and C_1-C_3 for the cluster. This is to not confuse these clusters with the clusters defined in this thesis, which are described later. These will be mentioned as cluster 1, 2 or C_1, C_2.

Table 2. Cluster from Huizinga (2013, unpub. MSc thesis) mentioned in this work.

Name	SiO2 content (wt.%)	Definition in this work
Cluster 1	70-72.5	H_{C1}
Cluster 2	72.5-76	H_{C2}
Cluster 3	78-79	H_{C3}

Further the tephra gathered from the river terraces of the Magdalena and Platanar river (table 7) are named after the river accompanied by a number, for example samples from the Platanar get a P; S_{P1}, S_{M13}, etc. Tephra derived from matrix samples get an extra letter (m) to note that their derived from the matrix of the river terraces. Further GPS points are shown as waypoint numbers referring to Appendix B. Terraces are named after the height from the LIDAR images made during preliminary work. These images can be found in Appendix A (fig. A3, A11).

Figure 5. Lakes sampled during the 2015 fieldwork in the Chiapas and Tabasco province, Mexico. PP1 and Poztpetr are drill cores from earlier work (Nooren et al. 2009, Huizinga, 2013 unpub. MSc thesis).

2.5 Tephrochronology

Tephra is the collective word for large volume of ejected volcanic deposits and comes from the Greek word téfra meaning ash (Shipley and Sarna-Wojcicki, 1982). Tephra consist of several components, including juvenile parts, meaning that is molten or was molten at the time of the eruption. The major components of tephra are pumice, glass shards, lithic and crystalline fragments or crystalline minerals.

Pumice are large solidified rocks, composed of volcanic glass shards, crystals of different minerals and voids produced by gas bubbles which outgas after solidification. These rocks have a low density; 0.7-1.2 kg/m^3. Glass shards are very small, fine pumice shards which can travel large distance through the air. Their density is higher than the pumice; 2.35-2.45 kg/m^3. Lithic fragments in tephra are any rocks originating from the roof of sides of the volcano. They are solid rock fragments erupted from the crater because of the explosive force of the eruption. These rocks can vary from millimetre to meter size and usually have a density of 2.7-3.2 kg/m^3. The last group are crystal fragments which include minerals. These can be phenocrysts of any mineral that grew in the magma chamber and got incorporated in either pumice or erupted as particles. These minerals are coated by a rim of volcanic glass which solidifies after erupting. Their densities depend on the mineral properties, but generally are around 2.7-3.2 kg/m^3.

Lowe (2011) reviews the importance of tephrochronology and tephrastratigraphy; two powerful methods for linking and dating geological, climatic or archaeological sequences or eruptions. The age derived in the tephra can be linked to another location by comparing the unique fingerprints of the tephra layers. It is very useful to date layers and formations. For this thesis primarily the chemical fingerprints, mineral textures, compositions were used to identify tephra and its source. The method works because tephra is deposited over a very short time period of hours, days, months or sometimes years. Very fine ash cloud can travel through air and get deposited later. Zielinski et al. (1997) recorded glass shards from the 1982 eruption of El Chichón were deposited on Greenland one year after the eruption.

There are some aspects of tephrochronology that makes comparing chemical fingerprints hard. These can come from errors made in stratigraphy obtained during fieldwork (Lowe, 1986a). Second if one eruption had multiple chemical fingerprints, which are hard to recognise (Shane et al. 2008a). Similar to this is when tephra layers have comparable chemistries which makes it hard to individually describe or compare them (Brendryen et al. 2010). As already mentioned eruptions from El Chichón have a very uniform chemical fingerprint (Espíndola et al. 2000, Macías et al. 2003). Thus individual eruptions were distinguished by other lines of evidence. Fourth poor measuring causing bad analytical data that deviate from the original chemistry (Pearce et al., 2004b). Further processes that rework, alternate the chemical composition over time (Payne and Gehrels, 2010). These are the important errors which have to be accounted for using tephrochronology and fingerprinting.

3. Research strategy and techniques

3.1 Theory of river terrace formation

The theory of eruption related terrace formation in the Tabasco area is explained in this section. The importance of river terraces is one of the main focus points of this thesis.

In common river terraces, sediments are deposited after flooding or high river outputs. The sediments are deposited in the flood plains. The majority of the deposits are eroded and transported by the river to the delta plain. The sediments that remain form river terraces. In the case of the Magdalena and Platanar River, the hypothesis is that these river terraces were formed shortly after an eruption by massive hyperconcentrated and debris flows or perhaps by pyroclastic flows. This means that the river terraces mainly are composed of volcanoclastic sediments like pyroclastics, pumice, glass shard matrix, Andesites and Dacites with some degree of contamination.

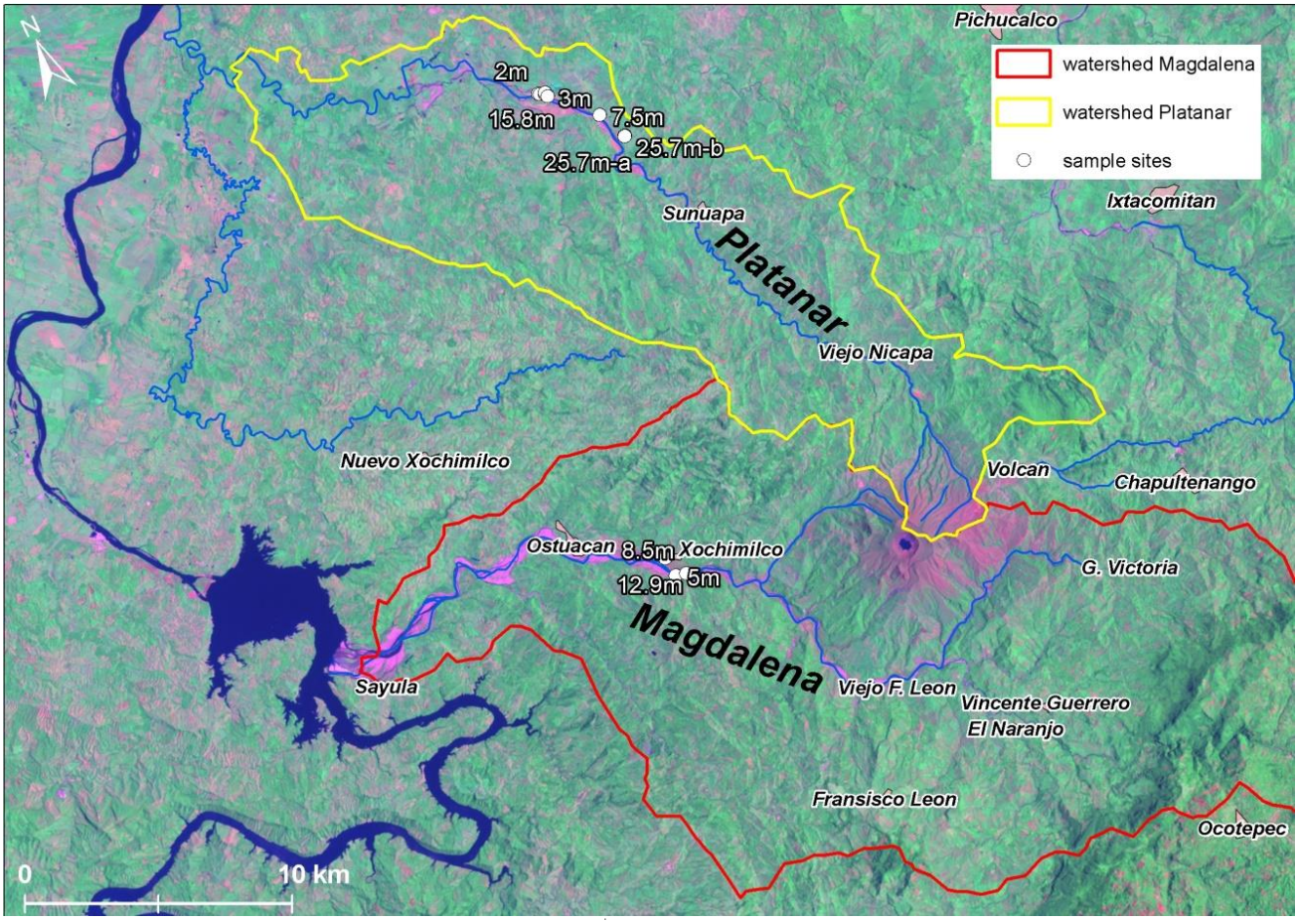

Figure 6. False colour image of the Platanar and Magdalena watershed area. White circles with notations are the visited terraces as described in the Fieldwork (Appendix A), names are nearby villages.

The theory is as follows and is illustrated by figure 7. The Magdalena and Platanar river transports most of the material erupted by El Chichón to the Usumacinta-Grijalva delta. If an eruption occurs there is so much new material available that during deposition it chokes the entire river (fig. 7.1). It is transported in the river valleys downstream in by a pyroclastic or debris flow, which fills the river valley. In the second stage the river settles again and cuts into volcanoclastic products (fig. 7.2). The remaining eruption materials form the event river terrace (T2). If then centuries later a consequent

eruption fills the valley again, but on top of the older volcanoclastics (fig. 7.3). The same process of river settling, erosion and incision by the river occurs. This way the second event river terrace will be formed. Figure 7.4-7.6 shows a third eruption with river terrace formation. In this way the eruptions are recorded as several terrace levels.

These event river terraces are young close to the river and older further away from the river. Further the thickness of river terraces decreases downstream and is dependent on several components. Namely downstream most of the sediments are already deposited by pyroclastic or debris flows and the thickness of deposition decreases. The volume, size of the river valley and the amount of sediments erupted by the volcano are important aspects. If the river valley becomes broader the thickness of the terrace will decrease. Also large eruption volumes give large event terraces which can be found further away from the source and forms higher terraces.

Do keep in mind that this only works in river valley in proximity of the volcano. The pyroclastic or debris flow has a certain range in which it deposits such huge amounts of rock (~ 30 km). Further downstream the thickness becomes less. Also if a floodplain is very broad the thickness of the terrace will vary. Sampling of these terraces has to be close to the volcano. This means also that laterally different terrace levels can form from the same eruption. It is thus important to describe the terrace in detail and report the locations of the terraces.

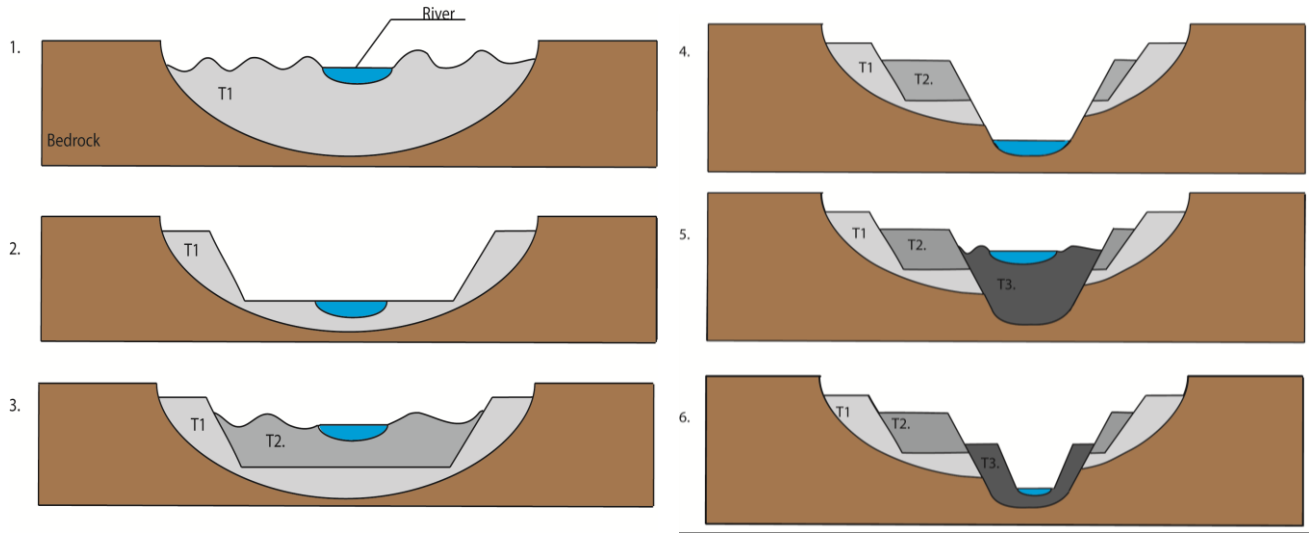

Figure 7. Schematic image of event river terrace evolution in the Magdalena and Platanar river valleys. T1-T3 represents eruption material from three events. The steps are explained in the text above.

3.2 Research strategy

Fieldwork was conducted in the river valley of the Magdalena and Platanar rivers. In total eight river terraces were found. From them pumice and matrix samples were taken. The terraces variate in thickness and multiple units were distinguished in the terraces based on textural and geomorphic features such as grain size, colour, cross bedding and type of clasts. For more details, see appendix A1. Afterwards the samples were prepared and measured by the EPMA for chemical composition analysis. The chemical fingerprint of the tephra was compared with the tephra database from deposits on the slopes of El Chichón and with the distal air-fall tephra from the drill cores of the Usumacinta-Grijalva delta plain. Close attention was paid to the geomorphic features of the river terraces and geographic framework present in the river valleys. Back scatter images of the glass shards, mineral assemblages, textural features in the glass shards were used to compare river terraces and further improve the eruption history of El Chichón.

All data was normalized to 100 wt.% to compare it to other tephra data from El Chichón. All deviations caused by the EPMA or samples were removed. Details on the accepted totals, analytical conditions, errors caused by the instrument are described section 4.

3.3 Field sampling

Preliminary to the fieldwork, research was conducted to distinguish possible river terraces. During the 2015 fieldwork research these river terraces and lakes were visited. In both tephra was found. Pumice and matrix was collected from river terraces of the Magdalena and Platanar River close to the volcano. From several lakes drill cores were taken for climate research of another master student (Smits, 2015 unpub. MSc thesis). In the drill cores several tephra layers were found and analysed.

3.3.1 River terraces

The first group of samples was collected from river terraces (fig. 8, 9). The sampling was done by handpicking pumice clasts and matrix in different units of the river terraces (Appendix E). The units and river terraces are described in appendix A. The locations of the terraces can be seen in figure 5. From each unit two pumice rocks were handpicked and some matrix at the same spot as the pumice clasts. The pumice clasts which were in best condition and of a size between 5 and 20 cm diameter were taken. Subdivision of the units is described in the field report (Appendix B).

Table 3. River terrace names, coordinate number and river as is described in Appendix A, B.

Terrace name	Coordinate number	River
5 m	545	Magdalena
8.5 m	546	Magdalena
12.9 m	548	Magdalena
2 m	616	Platanar
3 m	615	Platanar
7.5 m	586	Platanar
15.8 m	617	Platanar
25.7 m	587-588	Platanar

A. 5m terrace, Magdalena river

B. 8.5m terrace, Magdalena river

C. 12.9m terrace, Magdalena river.

D. 25.8m terrace, Platanar river.

E. 15.8 m terrace, Platanar River.

F. 2 and 3m terrace, Platanar River

Figure 8. Visited river terraces on the Platanar and Magdalena river. Older terraces were very weathered and overgrown with trees, bushes and other vegetation.

A.

B.

Figure 9. 7.5m terrace next to the Platanar river.

3.3.2 Lake Cantemual and Chicuacan ash layers

The other group of tephra was found in several small lakes in Chiapas and Tabasco (fig. 5). The lake sediments were sampled for climatic research by another master student at Utrecht University who studies the climate pattern during the Holocene in the Tabasco province (Smits, 2015 unpub. MSc thesis). In several of these cores ash layers were found. For the ash layers was no age obtained, but carbon dating of organic layers in the drill cores suggest that the tephra layers must have been of the last 5000 years (Smits, 2015 unpub. MSc thesis). The lake samples are mentioned as S48-55 and described in table 4.

Table 4. Description of tephra from lakes in Mexico (fig. 5). Age of lake samples from Smits (unpub. MSc thesis, 2015).

Sample number	Sample description	Tephra depth in drill core	Measured	Age
S48	Lake Cantemual (close to PP1)	193-194cm	No	1500 BP
S49	Lake Chicuacan	65-66cm	No	-
S50	Lake Chicuacan	5,5-6,5cm (including pumice clast)	Yes	1982
S51	Lake Chicuacan	5,5-6,5cm (including pumice clast)	No	1982
S52	Lake Chicuacan	59,5-60,5cm	Yes	550 BP
S53	Lake Cantemual (close to PP1)	154 cm	Yes	550 BP
S54	Mezcalapa river sand sample	*	Yes	1982
S55	Samaria River sand sample	*	Yes	1982

3.4 Sample description

Two types of glass tephra were measured, glass from the pumice clasts and matrix. By matrix is meant the matrix of the terrace units; fine grains. The matrix from terraces was collected, glass shards extracted and put into stubs (see 3.5, Appendix C). The pumice was cut and put on thin sections.

Matrix glass shards consist of grains with large amounts crystal fragments of minerals with glass rims. This made measuring their compositions difficult and some samples could not be measured. The crystal fragments include phenocrysts of plagioclase, hornblende, clinopyroxene and minor apatite and magnetite. The pumice clasts consist mainly of glass with large phenocryst minerals (fig. 11, 27). At smaller levels the glass contains microliths of orthoclase, plagioclase and pyroxene (fig. 10, 27). The samples have a vesicularity ranging from 10-60%, 5-25% minerals and the microliths vary from 2-20 µm, which mainly are plagioclase and orthoclase. The phenocrysts are much larger and vary between 50 and 500 µm. As can be seen in Appendix E as well as described in Appendix A, the pumice varies from very light grey to yellow. Some samples couldn't be measured because there was simply too much microliths in the glass to get a 25 μm^2 surface to measure (fig. 27).

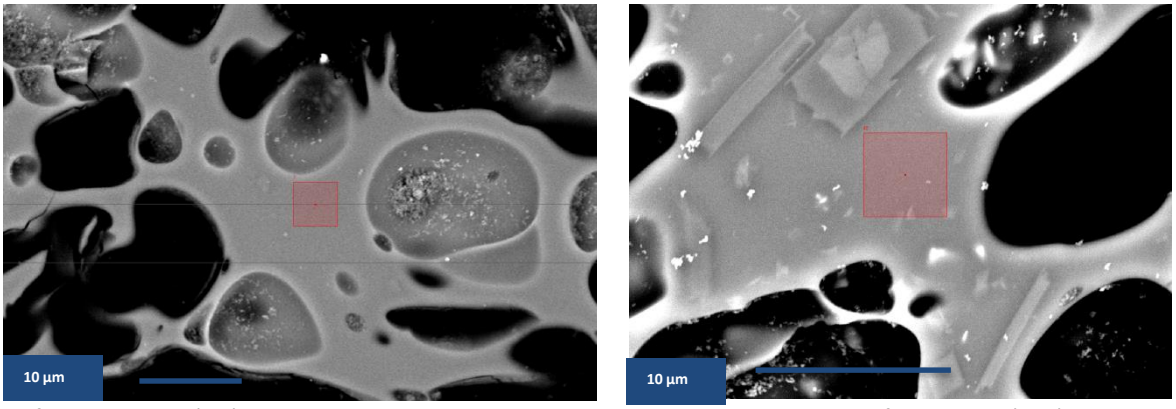

A. few microliths (S_{P7}) **B.** Sample with lot of microliths (S_{P10})

Figure 10. Backscatter image showing glass analysis with fresh surface (A) and contaminated surface with microliths (B, Appendix F).

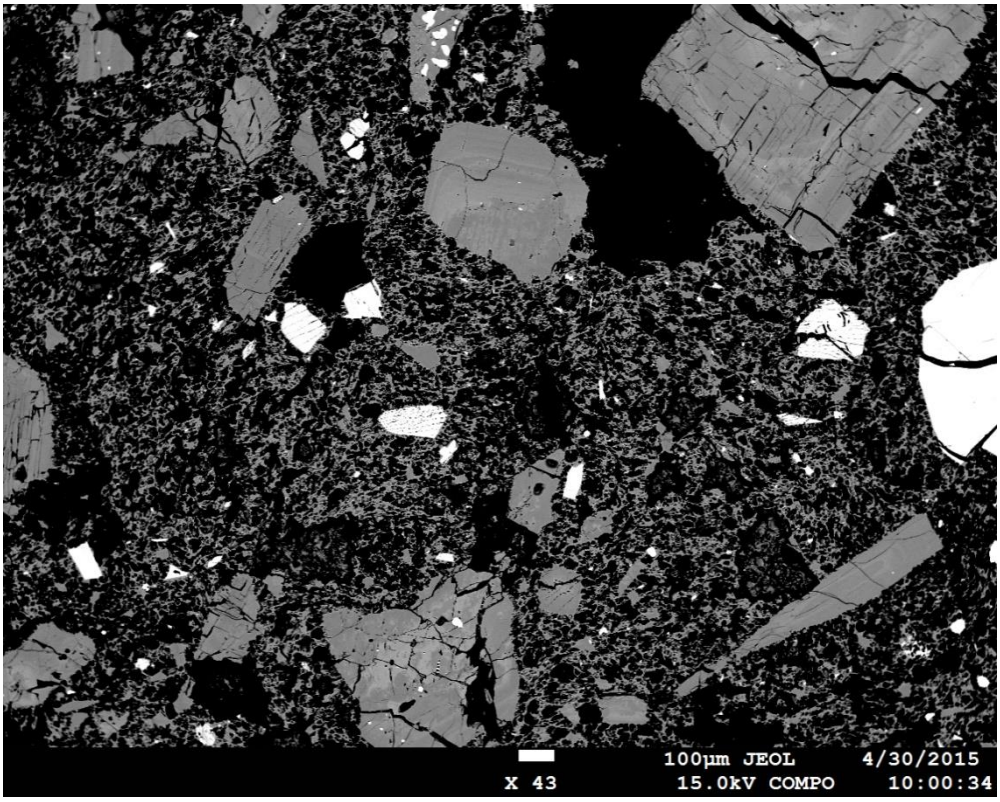

Figure 11. S_{P7} glass shard, network of glass shards between minerals, white bar is scale (Appendix F).

3.5 Sample preparation

3.5.1 Heavy liquid separation

From matrix samples the glass shards were extracted. This was done using heavy liquid separation method. Glass shards namely are less dens than quartz grains and other lithics present in the matrix. This property can be used to separate glass shards from denser grains. The method works as follows: the matrix is put into tubes filled with heavy liquid of 2500 kg/m^3. The tephra, which is lighter, flows upward while the heavier material sinks. The tephra and other light grains, like clay, are then separated from the heavier grains. Next remaining sample is poured into a new tube with a heavy liquid of a density slightly lower than the glass shards. The tephra sinks and the clay minerals and other light material will flow up and are removed. The remaining liquid contain only glass shards, after cleaning and drying they are ready to be measured. The tephra glass shards are put into stubs. One of the major advantages of this technique is that it can separate material based on density difference without affecting the grains, no chemical reaction occurs using this technique. This makes it very useful in tephrochronology.

3.5.2 Stub preparation

After the tephra is separated it can be put into stubs. Stubs are cylinders of plastic polymer with eight one inch holes (Appendix C, fig. C-1). Each of the holes is filled with glass shards of one unit and sealed with epoxy which is poured on top of the tephra. Lastly the surface is polished and carbon coated.

3.5.3 Thin sections

Most Earth science departments have their own thin section preparation lab. The thin sections created for this work were done by O. Stiekema from Utrecht University. From the pumice clasts a very thin slice is cut and glued to a glass plate. This surface is then polished in several steps until the

surface is flat and a thickness of 30 µm is obtained. In the last step the sample is carbon coated in order to enhance its conductivity under the microscope. This was done for both stubs and thin sections.

3.6 Electron Probe Micro Analysis (EPMA)

During six sessions days 55 samples were measured with the microprobe. Some samples appeared to be not containing any tephra and were not analysed. The samples were analysed for their major elements (table 5). During the sessions various totals were measured with very high or low totals. In general totals between 95-102 wt.% are considered good analysis. For lower and higher totals, the cause of the deviation was explained and considered if this measurement could be used or not. This is further explained in the data processing section. 2-4 standards were measured two times a day, one before measuring and one in the afternoon.

Each session day the standards were viewed to see any deviations in the elements that need to be accounted for. Major elements with high weight percentages require better standards in both accuracy and precision than elements with low weight percentages. SiO_2 for example is one of the major elements which had a ~70 wt.% in most samples, while TiO_2 has values lower than 1 wt.% (~ 0.26 wt.%). The standard deviation for SiO_2 needed to be much more accurate and precise than for TiO_2, because low measurement values are close to the detection limit of the instrument. A deviation from a small number is still very small. While very small differences in the standards for major elements will result in large differences in the results, since their weight percentages are high. Measurements which have accuracy and precision numbers that deviate less than 10% of the true value are accepted.

Table 5. EPMA analytical conditions.

Instrument:	JEOL JXA-8530F hyperprobe field emission Electron Probe Micro Analyser (Utrecht University)
Spot size:	WDS analysis: 5µm EDS analysis: 1µm
Beam current:	5nA
Voltage:	15kV
EDS counting time:	15-20sec.
Correction method:	CITZAF PRZ
Elements analysed:	Si, Na, P, Cl, Ti, K, Ca, S, Al, Mg, Fe and Mn
External standards:	VG568, VG2, NIST-SRM 620, VG A-99 (see table G-2, Appendix G.)

The samples were measured by Energy Disperse Spectroscopy and Wavelength Disperse Spectroscopy. EDS is a technique which gives rough measurements of the chemical composition in weight percentages. WDS is much more precise and has greater limits of detection for each element. The EPMA can measure from Beryllium up to Uranium, lighter elements such as Lithium, Helium and Hydrogen cannot be measured.

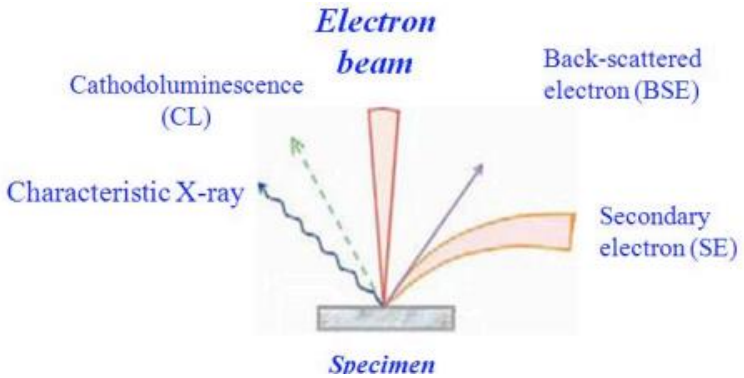

Figure 12. Electron beam hits the specimen thereby generating X-rays, secondary electron, back-scattered electrons and cathodeluminescence. From Chatterjee N. (2012).

The EPMA consists of several parts; stage, sample chamber, electron gun, WDS, EDS (fig. 13). Samples are mounted in a stage which is put in the sample chamber. This chamber is kept in permanent vacuum. An electron beam is put on the sample, exciting it which emits electrons of different wavelengths (fig. 12). These electrons are used to find the chemical composition and create images. Several spectrometers are used to absorb and measure the radiation. WDS and EDS are two ways of measuring the chemical composition of specimens. The wavelength and the energy of the generated x-rays are used with this technique.

3.6.1 WDS

Wavelength Disperse Spectroscopy is a technique that uses the wavelength generated by the specimen to measure weight percentages. As can be seen in figure 13 the x-rays measured by the WDS are first diffracted by an objective lens. Namely the sample emits x-rays with different wavelengths of different elements in the specimen that all have their own excitement state. Lighter elements emit long wavelengths and heavier elements emit short wavelengths containing more energy. Longer wavelengths are absorbed very easy by the surroundings. This makes it impossible to measure elements such as hydrogen, helium, lithium and oxygen. Other techniques like XRF need to be used to measure these light elements. Shorter wavelengths are easier to measure. To measure major element compositions, x-rays emitted by the glass shards are diffracted by the crystal, but only one certain wavelength at the time. This means only one element can be measured at the time. All other x-rays are absorbed, reflected or destructively removed and only the wavelength of the measured element falls on the spectrometer. To measure different elements, the crystal and spectrometer can move thereby change the angle of incidence.

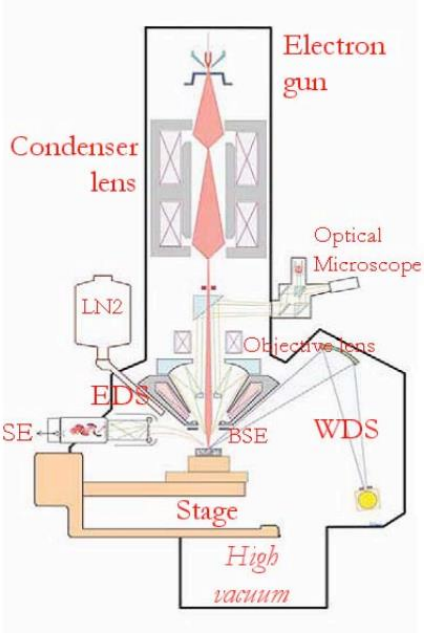

Figure 13. Overview image of EPMA showing major components. From Chatterjee N. (2012).

Using Bragg's law of diffraction these x-rays can be diffracted by changing the angle of incidence of the crystal. In this way only the x-rays of the elements are constructively diffracted and measured. All elements are measured one by one. By moving the stage of incidence and angle between the sample and the crystal each element can be measured.

The spectrometer usually is a gas flow detector (fig. 14) and works as follows: the detector consists of a rectangular shaped device filled with gas (usually a mixture of argon and methane), a window on which the X-ray fall and anode wire running in the centre. The X-rays go through the window and excite the electrons of the argon. The result is that a current is generated in the detector which is measured. Each element has their special potential ionization current and this way by using the amount of counts per second the weight percentage of each element is derived.

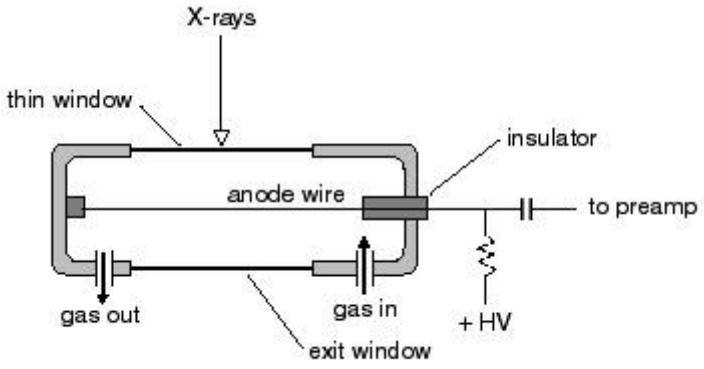

Figure 14. Schematic image of gas flow detector (after Goldstein et al. 1981). From Wittke, J.H. (2015).

3.6.2 EDS

Energy Disperse Spectroscopy is a similar technique as WDS. EDS consist of a semiconductor containing a detector crystal made of Si or Ge. These crystals have impurities in the crystal lattice, which makes it easier for electrons to move through the crystal. When X-rays hit the detector the

electron absorb them and produces a photoelectron with certain energy. This pushes a valence electron of the crystal on the conduction band. This interaction uses up some energy of the photoelectron and creates a small current. For Si the energy dissipated by the electron-hole pair is around 3.8-3.9 eV and X-rays having energy over 1 KeV produces many holes. Thus the energy of the absorbed X-ray is proportional to the total charge conducted. The higher the energy, the higher the charge. These charges are processed, amplified and the noise is filtered to find the element related to the X-ray. By measuring all wavelengths emitted on the detector the concentration of all elements can be found. EDS can count ~2000 per second, this means that 2000 X-rays can be measured per second. The EDS counts X-rays for 2 minutes and afterwards the energy level (measured from the charge strength) is shown in a spectrum. After measuring the data has to be processed, cleared of noise, amplified and then calibrated. From the spectrum the concentration of element can be shown in weight percentages. This is done for major elements only.

3.7 Analytical conditions

During microprobe analysis of tephra, the electron beam can change the composition of the glass by physical damage, volatilization or sodium migration through the tephra (Nielsen and Sigurdsson, 1981). This results in lower totals and low sodium concentrations in the measured area. The data point cannot be used. To achieve optimum conditions for measuring the glass, the finding of Froggatt (1982) were followed. They performed several analyses with various surface areas and beam currents. The count rate is dependent on the beam current and if the current is lowered the count rate is also less. This affects the counting statistics. This can be solved by increasing the counting time, but this leads to sodium loss. Eventually the optimal condition Froggatt (1982) found are; Beam current of 8 Nano amps, beam diameter of 10 µm and counting time of 3 times 10 seconds. Kuehn et al. (2011) found that the sodium has to be measured first in order to keep the accuracy and precision as best as possible. Further they state that the optical surface area has to be between 5-20 µm. However, in my case during the first session a surface area of 10 by 10 µm and 10 Nano amps beam current gave unacceptable results, the area of the glass was too small to measure. Therefor the surface area measured is put on 5 by 5 µm and with a beam current of 5 Nano amps (table 4, Kuehn et al. 2011). This gave better results.

3.8 Data processing

After measuring the data was fine-tuned and all bad data points were removed. The remaining measurements were averaged for each sample. Low totals, mineral contamination or potassium degassing can all affect the results and these measurements were removed. Their average with standard deviation of major elements are plotted against on and each other (fig. 26). In the figure two clusters are displayed.

In total 55 samples were collected from the Magdalena and Platanar river terraces (table 7). Of the 55 samples analysed, only 39 could be analysed. The other twelve samples were not analysed due to microliths of orthoclase and plagioclase in the tephra contaminating the measurements or there was no tephra found in the sample. In some samples the surface area of the glass was too small, a minimal 5 by 5 µm surface area is required for good analysis.

Measurements with totals of 95-102% were accepted as reliable data, however during several sessions days consistent low and high totals were derived. These samples were viewed individually to see if any data shows unusual concentrations. For instance, CaO weight percentage of 15%

(compared to the normal 1-2 wt.%), high or low totals or contamination by minerals samples were rejected (Appendix H2). Some samples have low totals that were explainable. During the first session day on 12-2-2015 consistent very low totals were derived (90-95%). During the second session day on 28-4-2015, measurements of sample 3 had unusual high totals (102-104%, Appendix H1). Lastly in the session on 2-6-2015, there were certain samples that showed consistent low totals (averages around 95%). The elements of the samples were plot against one and each other to see if they cluster, had contamination, or unusual compositions. As can be seen in table 7 two samples per unit were measured to check the consistency of the pumice in the outcrop. Later the matrix was compared with the pumice samples to check if there exist any difference between the pumice clasts and the matrix.

The measurements were normalized to 100 wt.%. It is important to note that comparing tephra data with each one and each other is very tricky when done incorrectly (Lowe, 2011). Many factors have to be accounted for, such as type of microprobe used, standards, normalized values, totals, plagioclase contamination. All these factors can change your chemical composition slightly and this will affect the outcome of your research.

4. Analytical Errors

There were several factors causing errors in the data. In this section each of them is explained and which samples were affected.

4.1 Errors of the instrument

When measuring major element compositions using EPMA there are many aspects that can affect the result. The instruments itself is one of them. For instance, beam current fluctuations or irregular radiation by the sample. Sample preparation, carbon coating, polishing is not properly performed. The calibration of the measured elements is incorrect and the spectral peak is not in range. Sodium and other volatile elements can evaporate and diffuse from the sample. Sample conditions, conductivity, old or weathered surfaces, water and volatiles that are not measured. All these factors and processes affect your results. The standards, quality of the measurements and other processes that could cause errors in your data are discussed here.

All these factors and processes were accounted for and eliminated as best possible. Any irregularities in data are explained. Accepted measurements are totals between 95-102 wt.%, with some exceptions where measurements had low totals, they were evaluated to see if they can be used. The low totals were mainly measured during the first session day and most of this data was rejected.

4.1.1 Secondary Standards

Secondary standards were measured to eliminate any errors caused by the instrument itself. Namely if beam current fluctuations or bad calibrations are present they are shown in your standards. Any fluctuation in beam current will change the result of all your elements while bad calibrations will only affect certain elements that were insufficient calibrated. Further there are two factors that need to be kept in mind, accuracy and precision. Accuracy is how close the measured value is to the real value and precision is how good the result can be reproduced (fig. 15).

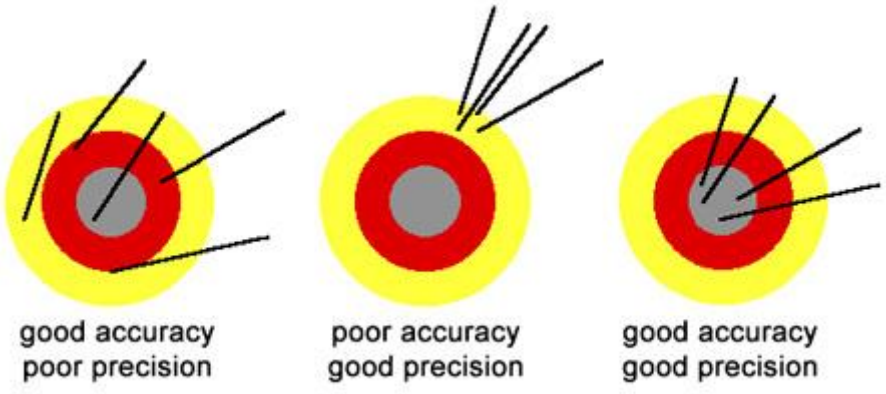

Figure 15. Visual description of precision and accuracy. From http://elchem.kaist.ac.kr/vt/chem-ed/data/acc-prec.htm.

Both errors were notated in percentages relative to the real value. Each element may have a different error depending on the weight percentage of the element. For example, the tephra samples consist mainly of glasses with high SiO_2, Al_2O_3 weight percentages and low MgO and CaO weight percentages. Small deviations in elements with low concentrations influence other elements less

than elements with high concentrations. In general sessions standards with an accuracy and precision error of 10% or lower were accepted values. Titanium-, Chlorine-, Phosphor-, Sulphur-, Magnesium- and Manganese-oxides were present in such low weight percentages that higher deviations in the standards were accepted. These elements were used for interpretation, taking their larger deviation in the standards into account. Na_2O is very volatile during measuring and this contributes to low totals and large values for the accuracy and precision error. To reduce this factor, Na_2O was measured first followed by SiO_2 and Al_2O_3.

The accuracy and precision derived by the standards measured on each day showed good results (table G-1, Appendix G). The best conditions were achieved on session 28-4-2015 and 30-4-2015 (Appendix G).

The accuracy derived from the standards showed good results. All measurement days showed good standard values for the accuracy and precision. Since potassium and sodium are very volatile and degas from the sample during measuring their error was much larger. This was seen on session days 12-2-2015 and 2-6-2015 in the VG-568 rhyolitic glass. Therefor most of the low totals were not caused by the instrument, but by the sample itself.

4.2 Water content

Water is present in the magma chamber of a volcano. The water is included in the mineral structure of rocks as hydroxyl group. After and before an eruption pumice, pyroclastic rocks, glass shard and mineral crystallize and include this water in the crystal structure. Light elements such as H, He and Li also cannot be measured by the microprobe. Simply because of the detection limit of the electron microprobe (section 3.6). When the glass shards are then measured with the EPMA this water is evaporated or not measured. The presence of water lowers the totals given by the EPMA. So high amounts of water give low totals.

Samples S_{M17}, S_{M18}, S_{P27}, S_{P28} and S_{P32} have got consistent low totals (~95 wt.%) and in the Back Scatter Images there appears no signs or any contamination of microliths in the measured spots (Appendix F) and no holes were seen. Also samples S_{P10}, SP_{12}, S_{Pm40} and S53 totals are a bit low (~96 wt.%). Further there is no increase in Al_2O_3 or CaO an indication of orthoclase contamination. As discussed earlier the standards do not show any low totals or elements that give a large error. This may be an indication that these samples contain higher percentages of water than other samples.

If low totals are consistent and limited to one sample than it is important to view the individual measured spots against one and each other. Consistent low totals in one sample of multiple measurements makes the presence of high amounts of water a suited explanation. It is important that this data clusters together, not that some elements will deviate too much. Else this data cannot be used.

4.3 Co-measurement of microliths in tephra analysis

Another source of error was contamination by microliths of plagioclase, pyroxene, hornblende or orthoclase in the samples (fig. 10 and 27, Appendix F). This made it tremendously hard to analyse the samples. During the sessions much time was spent on searching for the right area and many of these measurements gave unacceptable results. A clean surface was used for measurement spot, but still some results showed contamination of microlith minerals, which was not seen on the back scatter images (BSE). There were several contaminated measurements and some are plotted in figure 16.

Four samples are used to show the plagioclase contamination trend in the chemical content, these are sample S_{P32}, S_{Pm40}, S_{Pm46}, S50 and S51. In most samples the influence of plagioclase was strongest present, other minerals had much less influence on the results. Plagioclase and orthoclase were the most common microliths in these tephras. The best way to see the plagioclase contamination was by plotting Al_2O_3 and CaO against SiO_2. A straight line was drawn between the plagioclase and the data. To exclude any data affected by this trend and to interpret the data, the samples with the lowest Al_2O_3 and CaO values and highest SiO_2 content were used; the plagioclase namely increases the Al and Ca content relative to the other elements (contaminated data in Appendix H1). The effect of contamination was reduced significantly this way. For the other microlith minerals close attention was paid to the elements that deviated. Then the points were removed that were influenced by microliths.

A.

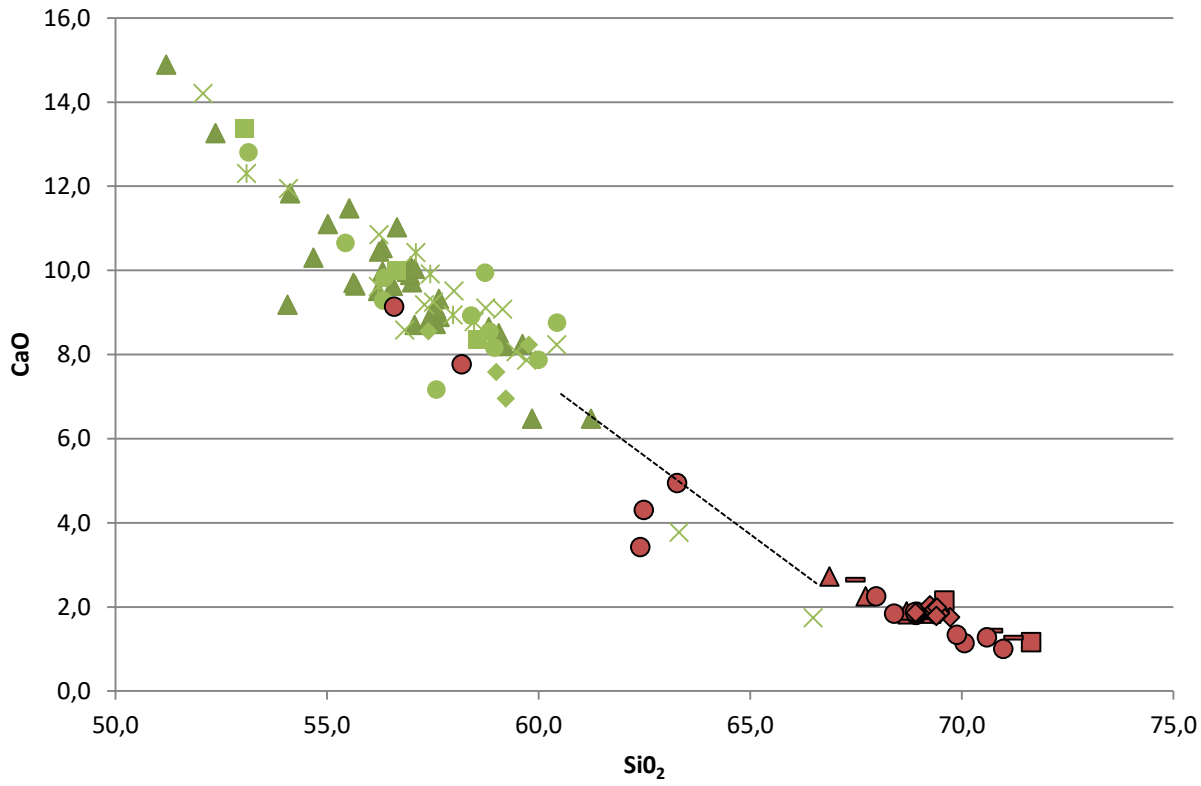

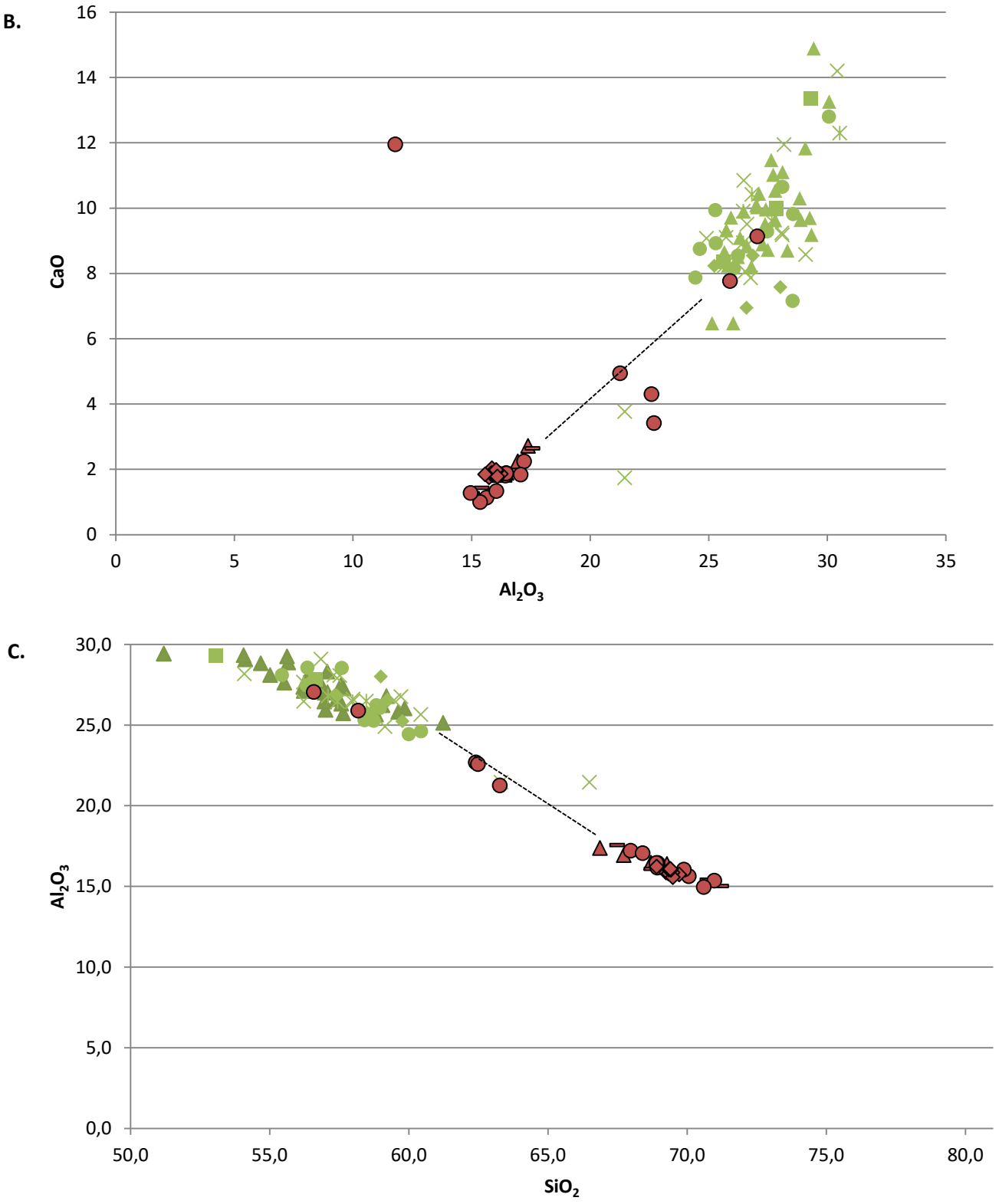

Figure 16. A-C. Samples with clear plagioclase contamination trend. Sample S_{P32}, S_{Pm40}, S_{Pm46}, S50 and plagioclase EDS of several terraces. **A)** SiO_2 against CaO is plot, **B)** Al_2O_3 against CaO is plot and **C)** SiO_2 against Al_2O_3 is plot.

5. Results

5.1 Terrace conditions

Three river terraces from the Magdalena River and five from the Platanar River were sampled (table 3, fig. 8 and 9). The terraces were generally pastures for cattle, with a 20-40 cm soil and vegetation. Under this soil the volcanoclastic deposits were found with some fresh cut sections at several locations (Appendix A).

Table 6. Overview of different terraces with their units (fig. 5, details in Appendix A).

Terrace	Amount of units	Overgrown	Condition terrace	Thickness (m)	Size pumice (cm)	Colour pumice (Grey/Yellow)
Magdalena						
5 m	4	No	Fresh cut	5	1-15	G
8.5 m	1	Little	Little weathered	3.5	0.5-5	G
12.9 m	2	No	Fresh cut	3.5	1-10	Y and G
Platanar						
2 m	1	Yes	Weathered	2	1-5	Y
3 m	1	Yes	Weathered	3	1-5	Y
7.5 m	4	No	Fresh cut	7.5	1-20	G and Y
15.8 m	1	Yes	Very weathered	1.5-3	0.1-1	G
25.7 m	1	Yes	Very weathered	2-3.5	0.1-1	G

Four units were defined in the 5 m terrace; unit A-D with a 5 m terrace thickness. It is the first terrace level next to the Magdalena River (fig. A3). The section was recently cut with only vegetation on the top of the terrace. There is a clear textural difference between the units. The unit D was poorly exposed, small angular clasts and conglomerate type of deposition. Unit C is much coarser with large clasts, grey and yellow pumice layers. On top are unit A and B which were much finer grained. Several lenses of grey pumice clasts are present.

At one terrace level higher 3.5 m of the 8.5 m river terrace was exposed. This terrace is overgrown with vegetation and the rocks were clearly weathered. In some places soil had developed. The texture and geomorphology is pretty uniform throughout with large dacite clasts and small weathered pumice. It has a strong resemblance with unit C of the 5 m terrace.

The third river terrace in the Magdalena is the 12.9 m terrace, consisting of unit A and B with 3.5 m exposed section. Unit A is the top layer which has a very yellow-brown colour and soil formation on the top. Unit B is the lower part of the terrace and has a grey to black colour. There were lenses of coarser grained clasts through both units and pumice clasts were found in these layers. The section was recently cut and shows a fresh surface.

In the Platanar River, the first terrace level is the 7.5 m terrace with a 7.5 m thickness. It consists of units A-D. The section shows much lateral variation, the first bottom meter of the section in not exposed and above it unit D. It consists of layers of yellow pumice on top of grey pumice layers. Unit C consisted of alternating layers of fine and coarse grained volcanoclastic material, with crossbedding in the finer layers. Unit B had a conglomerate appearance, with 1-20 cm clasts of dacites, grey and

yellow pumice. Unit A consists of layers of fine grained units of grey pumice and dacites. The terrace was covered with vegetation on top. There was much textural difference observed in this terrace indicating several episodes of high energetic transport processes.

Further downstream the two additional terraces next to the river were found; 2 and 3 m river terraces (fig, 5). These terraces were overgrown by vegetation and pumice with a weathered outer rim. Mainly yellow weathered pumice was found. The terrace had an oxidized brown colour on the outside. Both terraces had uniform fine grained textures, with pumice clasts spread throughout the terrace and localized in oxidized coarse grained layers.

At higher elevations the 15.8 terrace was found. It has a thickness of 2-3 m, large degree of weathering and overgrown entirely by vegetation. Soil had developed and much of the tephra was transformed into clays. No large pumice clasts were found and more pumice were weathered in to matrix.

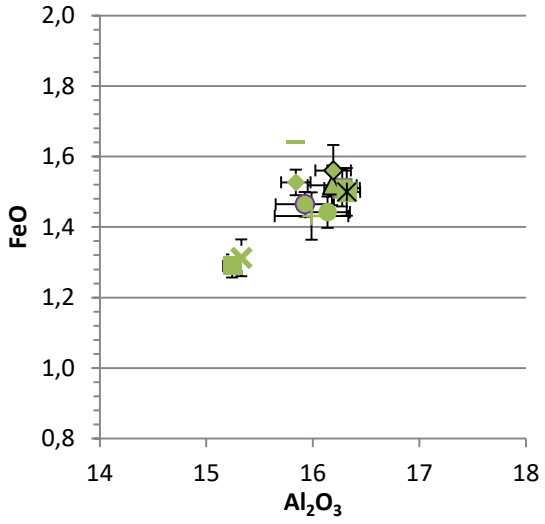

A.

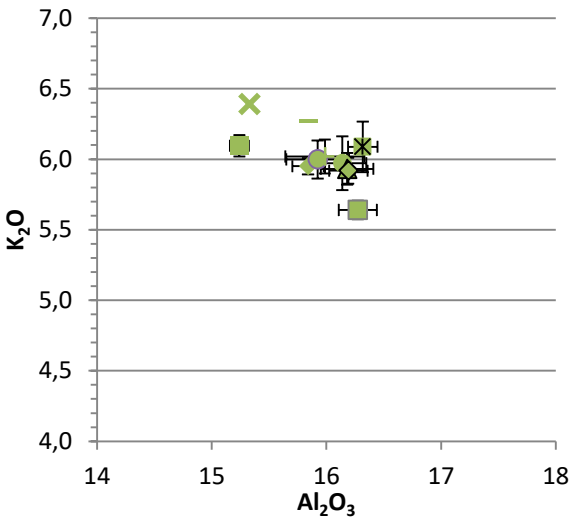

B.

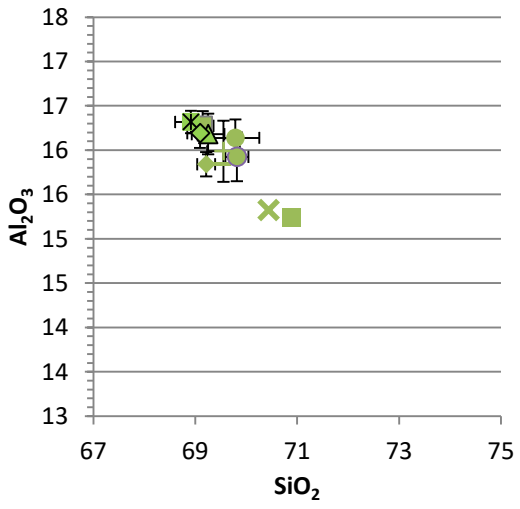

C.

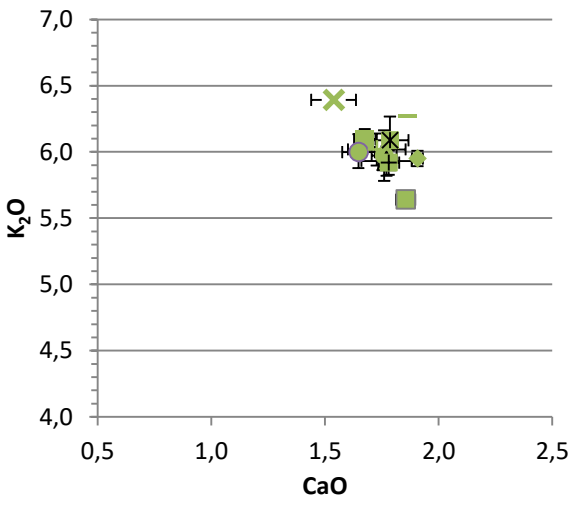

D.

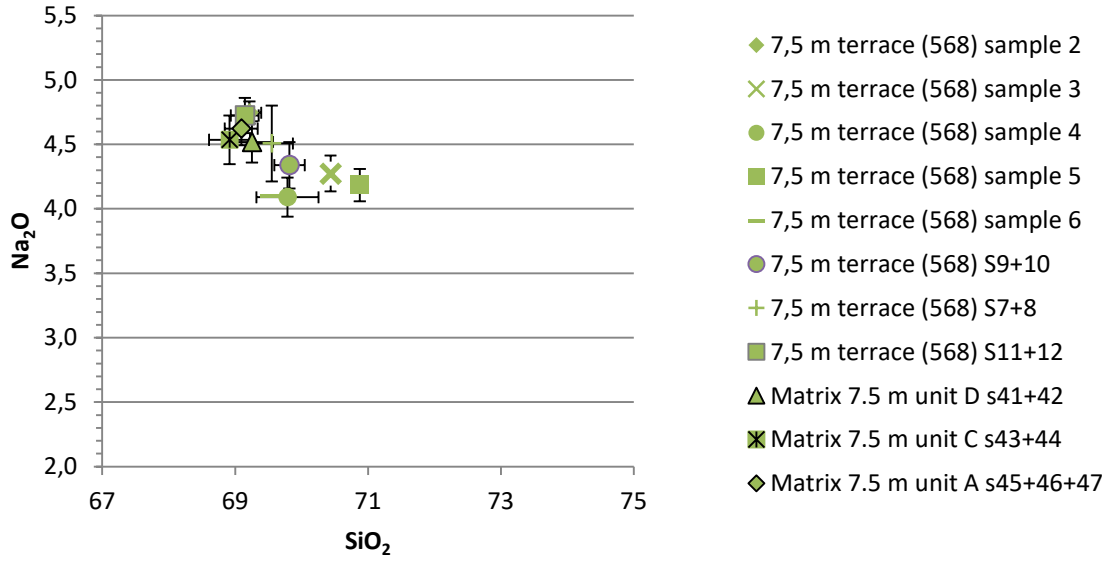

E.

Figure 17 A-E. Averaged samples from 7.5 m terrace. Standard deviation shown as bars. **A.** Aluminium against iron, **B.** Aluminium against potassium, **C.** Silica against aluminium, **D.** Calcium against potassium and **E.** Silica against sodium.

The last terrace was at an elevation of 25.7 m above the river it was overgrown entirely with vegetation and had a similar appearance as the 15.8 m terrace. The clasts were very weathered and the clasts collected were mostly dacites. The pumice clasts were crumbly and entirely weathered to fine matrix. No pumice samples were collected here. The section was weathered and brown oxidation layers were present.

5.2 Pumice and Matrix features

Geomorphic features found in river terraces are an important tool to identify event river terraces. Textures, size, conditions and degree of weathering can be important to compare them. Minerals inclusions, phenocrysts, microliths, weathering surfaces and other features determine the origin and relation of the river terraces to each other. Table 7 give a description of the measured samples. In general, 5-10 data points were analysed for every sample. In some cases, the samples contained too many microliths and could not be measured. Further a lot of data was rejected because of low totals, contamination of microliths and high water content. Most terraces include samples with microliths, but not all were measured.

5.2.1 7.5 m terrace pumice and matrix (586)

This terrace includes S_{P1}-S_{P12} and S_{Pm41}-S_{pm47} (fig. 18). Only S_{P1} was not measured because the tephra contained too much microliths (fig. 27). What is clear from figure 17 is that the majority of the samples cluster together. The chemical composition of the samples is very uniform. Some of these samples were combined, because they could chemically not be separated. Namely they were collected from the same place in the river terrace and their chemical composition was very similar. More details are given section 5.3. Furthermore, there were some samples that do not group. S_{P3} and S_{P5} show a slight difference with the other samples, they have different Al_2O_3, SiO_2, K_2O, FeO and Na_2O values. Also S_{P12} is somewhat low on K_2O, but the standards allow this (Appendix G).

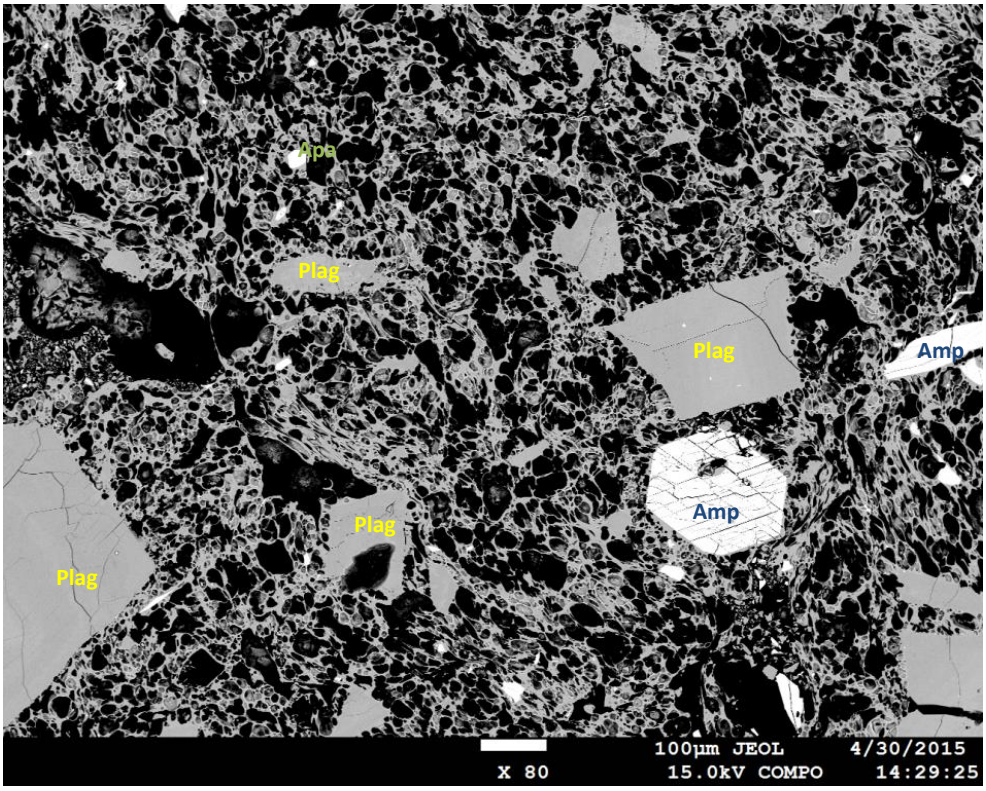

A. S_{P4}

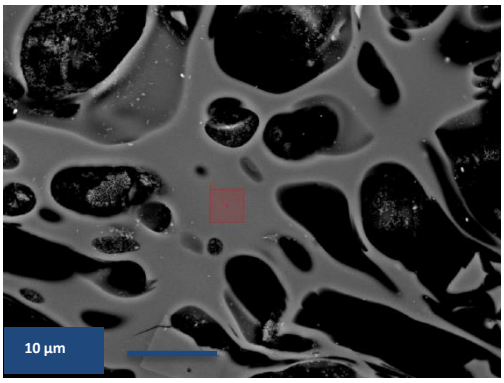

B. S_{P8}, Data point 9

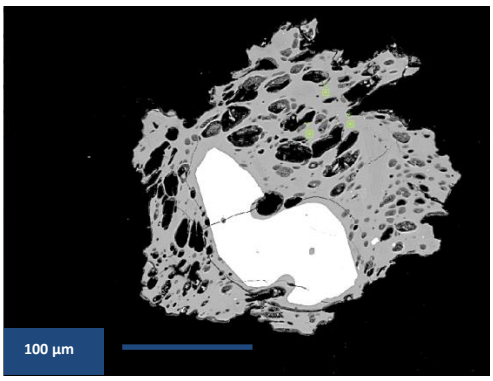

C. S_{Pm41}, data point 1-3 in green

Figure 18. BSE images from river terrace samples S_{P4} S_{P8} and S_{Pm41} tephra from the 7.5 m terrace. Derivations; Plag: plagioclase, Amp: amphibole, Apa: apatite.

From this terrace both glass shards from both pumice and matrix were measured. The matrix glass shards were 200-500 µm, with few microliths and fresh glass with no weathering patterns. The pumice surface is much larger than the matrix, consists of grey and yellow pumice, 30-60% vesicularity, 5-40% embedded plagioclase, pyroxene, amphibole, magnetite and apatite minerals. S_{P1}, S_{P8} and S_{P9} contain a lot of microliths. The pumice has a very uniform texture, mineral content and appearance. The glass shards from the matrix were made up large phenocryst minerals of plagioclase, pyroxene or amphibole enclosed in the glass.

5.2.5 5 m terrace (545)

This terrace includes S_{M13}-S_{M18} and S_{Mm34} from which S_{M14}, S_{M17} and S_{M18} were measured. In samples S_{m13}, $S_{m15\text{-}16}$ and S_{Mm34}, the tephra was recrystallized into clay minerals (Fig. F4-1 Appendix F3). The minerals were still present (fig. 19). This terrace is also described in Macias et al. (2004) and mentioned there as terrace 156. In the paper only a stratigraphy with lithology is made.

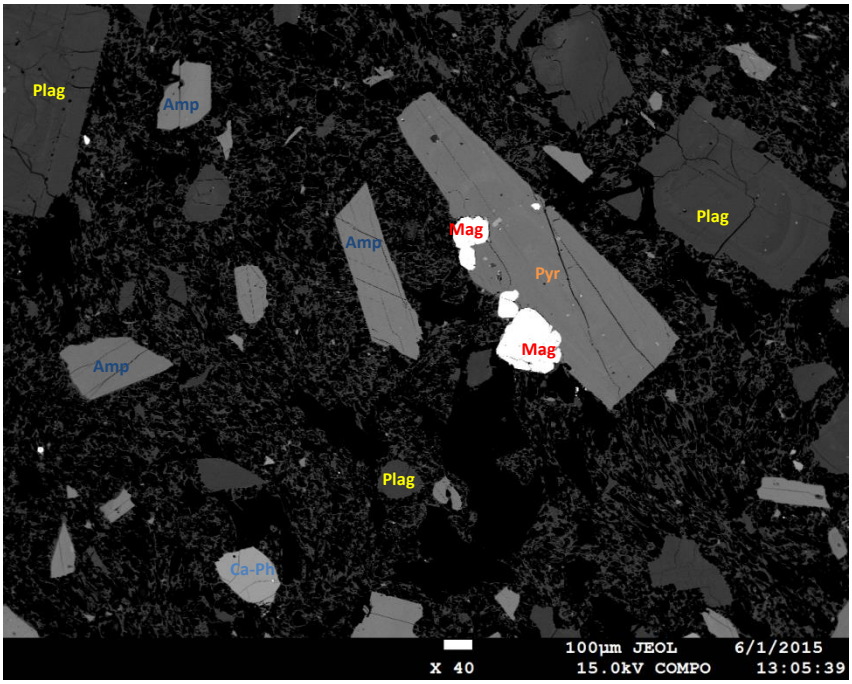

A. S_{M14}

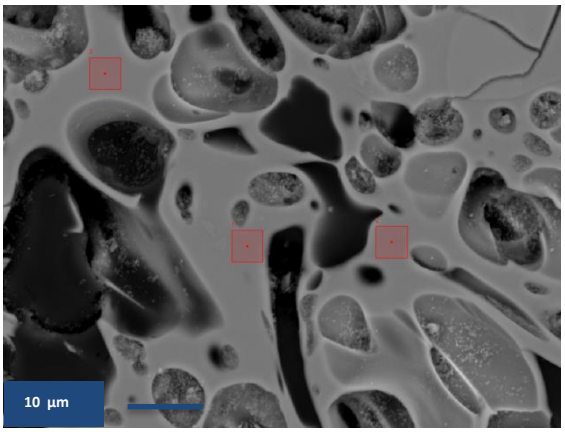

B. S_{M18} data points 1-3

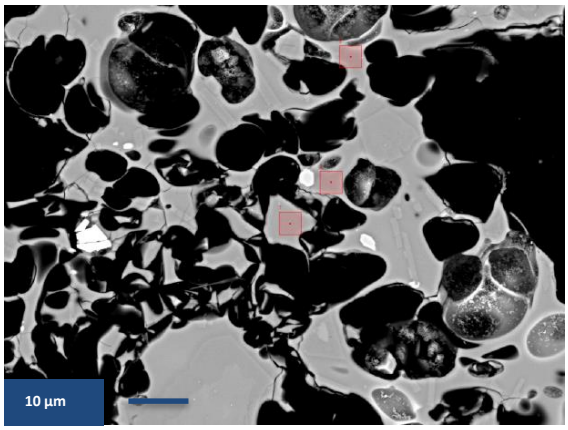

C. S_{M17} data points 7, 8, 9

Figure 19. BSE images from river terrace samples S_{M14} S_{M18} and S_{M17} representing tephra from the 5 m terrace. Derivations; Plag: plagioclase, Amp: amphibole, Pyr: pyroxene, Mag: magnetite, Ca-Ph: calcium phosphate.

The tephra texture and appearance is very similar to the tephra from the 7.5 m terrace. Only pumice clasts were measured from this terrace. The glass was made up of grey pumice with a vesicularity of 30-40% and 25% minerals of plagioclase, pyroxene, amphibole, magnetite and phosphate. Only small microliths of plagioclase and pyroxene were observed but not measured.

5.2.3 8.5 m terrace (546)

From this terrace three samples were collected and two were analysed; S_{M19} and S_{M20} (fig. 20). However, the measurements gave poor results. Low totals and contamination of microliths made most of the data unusable. S_{M19} is the only sample with good results, S_{M20} is based on one measurement and S_{Mm35} could not be measured. S_{M20} glass shards contain a lot of microliths that made it very difficult for analysis. The BSE image showed well preserved tephra with no indications for weathering, similar to the 5 m and 7.5 m terraces. The terrace had yellow and grey pumice and the glass shards had a vesicularity of 20-50% and 25% minerals of plagioclase, amphibole, pyroxene and magnetite.

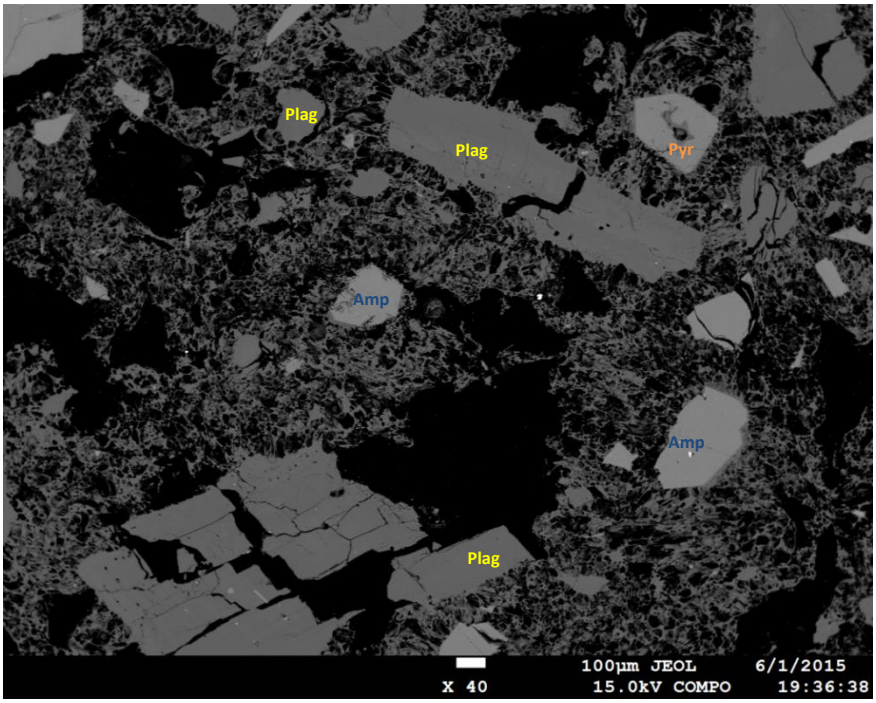

A. S_{M19}

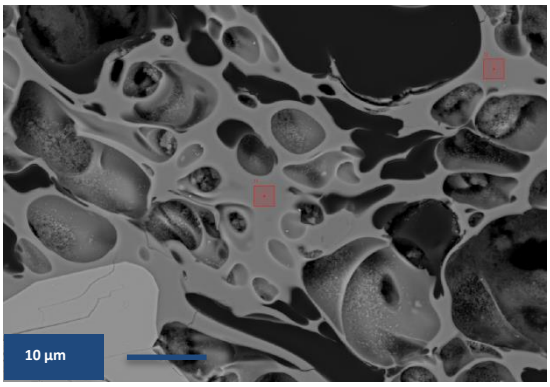

B. S_{M19} data point 11, 12

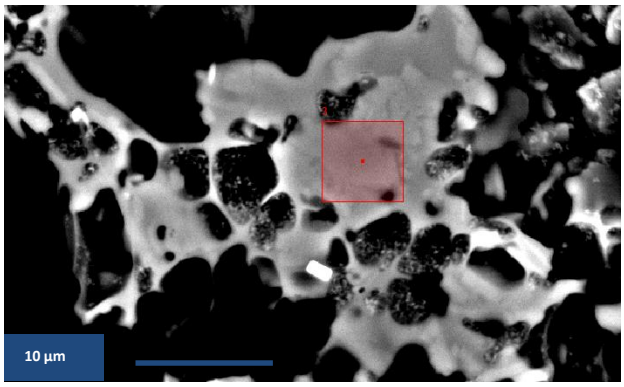

C. S_{M20} data point 3

Figure 20. BSE images from river terrace samples S_{M19} S_{M20} representing the tephra from the 8.5 m terrace. Derivations; Plag: plagioclase, Amp: amphibole and Pyr: pyroxene.

5.2.4 2 m and 3m terrace (615-616)

2 m terrace contained S_{P25-28} and S_{Pm33} and samples S_{P31-32}, S_{Pm39} were gathered from the 3 m terrace. Only S_{P25} was not measured, because this is a dacite clast. S_{Pm33} and S_{Pm39} were based on two or three measurements, samples $S_{P26-28,}$ S_{P31-32} on 5-8 measurements. S_{P31} does show somewhat low CaO, high K_2O values in the plot, but is not exceptionally deviating. The standard deviation S_{P31} is high.

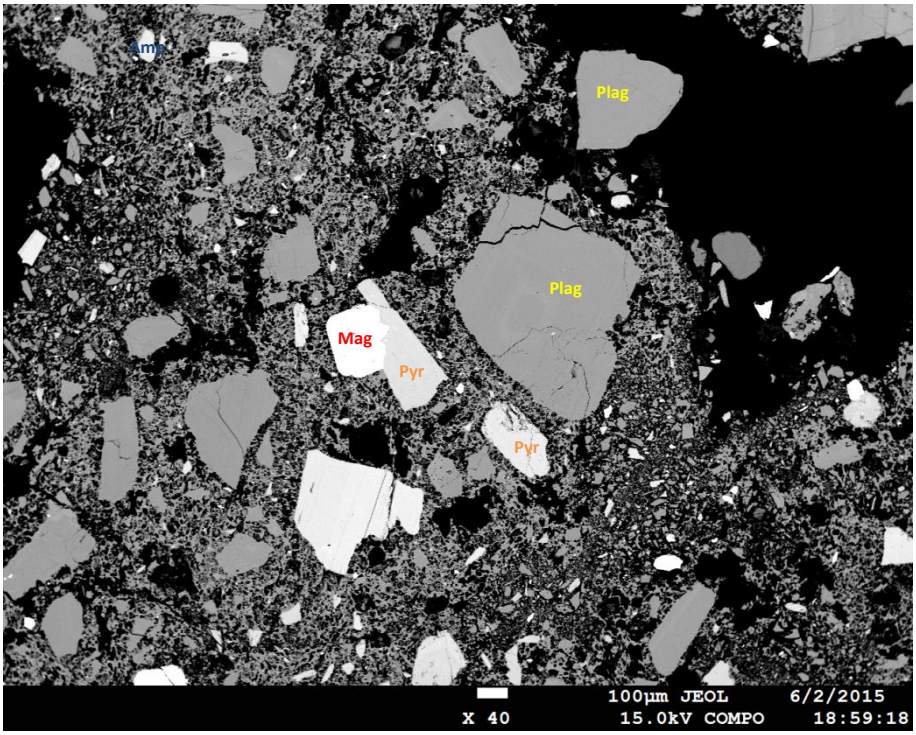

A. S_{P31}

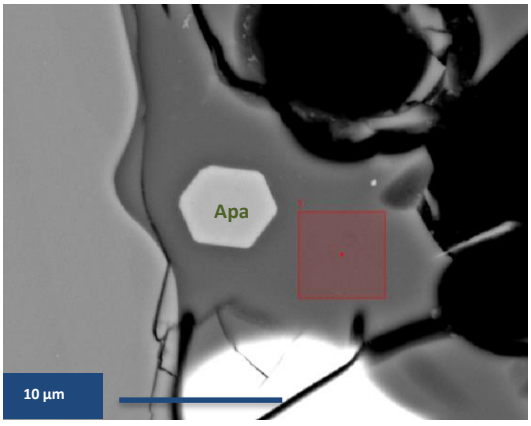

B. S_{P28}, data point 5

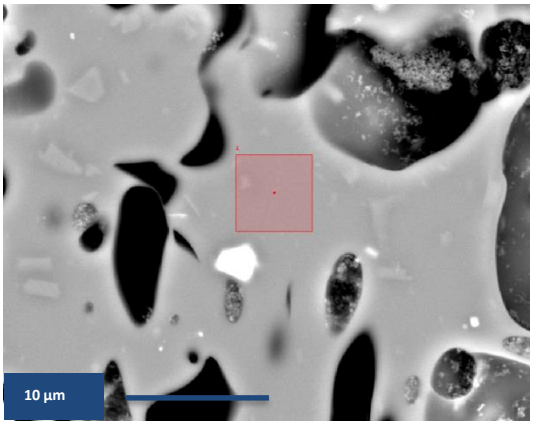

C. S_{P26} data point 4

Figure 21. BSE images from river terrace samples S_{P26} S_{P28} and S_{P31} representing tephra from the 2 and 3 m terrace. Derivations; Plag: plagioclase, Amp: amphibole and Pyr: Pyroxene, Mag: magnetite, Apa: apatite.

The texture of the tephra pumice of both terraces is similar and is in good condition. The pumice from the 2 m terrace consists of grey and yellow pumice with 30-50% vesicularity, 20-30% minerals of plagioclase, amphibole, pyroxene and magnetite. In the tephra a clear apatite phenocryst (fig. 21 B) and quite some microliths were found.

Mineral compositions were similar in both terraces except there was a higher density phenocrysts minerals of plagioclase, pyroxene, magnetite and apatite in the 2 m terrace. The glass shards have a vesicularity of 30% and 35% phenocryst minerals. Tephra from samples S_{P26} and S_{P27} showed cracks and was not well connected as the 8.5 m and 7.5 m terraces. Also large microliths were found in the tephra.

5.2.5 12.9 m terrace

Samples S_{M21-24} and S_{Mm36} were made from the clasts and matrix of this terrace. None of the samples were suited for measuring. S_{M21-24} appeared to be dacites and the glass in S_{Mm36} was recrystallized entirely. From this terrace no measurements were derived.

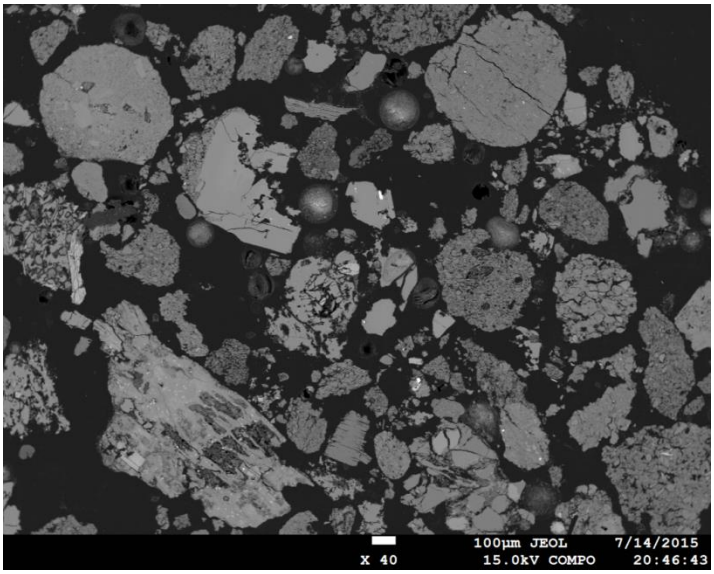

A. S_{Mm36}

Figure 22. BSE images from sample S_{Mm36} of 12.9 m river terrace.

5.2.6 15.8 m terrace

Samples S_{P29-30} and S_{Pm40} were made from pumice of this terrace. Pumice samples S_{P29-30} are a bit different in appearance (fig. 23). S_{P29} consists more of individual clasts, however this is probably due to the cutting process from the thin section preparation. In both samples strong weathering patterns were seen, which made measuring impossible. The edges of the glass shards showed crystallization of new minerals and cracks were found throughout the glass. Few amphiboles, magnetite and apatite microliths were observed. Although plagioclase and pyroxene were not measured, observations suggest the present of these minerals in the samples. In general, the phenocrysts (amphibole, plagioclase and pyroxene) were smaller than ones in the more recent terraces, but had a similar shape and appearance. This is most likely a weathering effect; older samples are altered more than younger terraces.

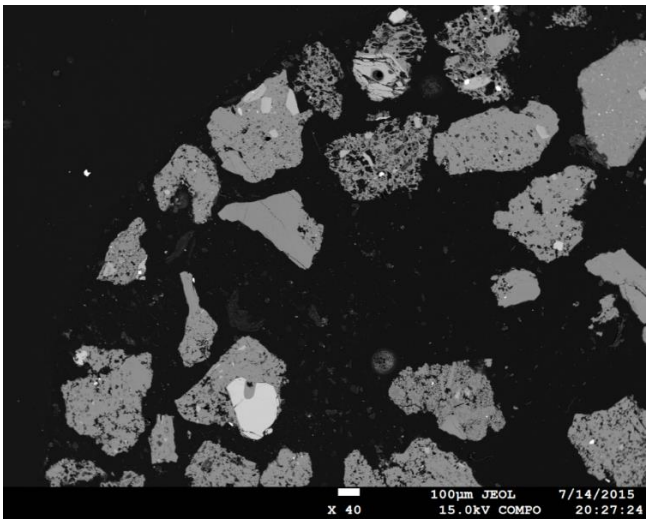

A. S_{Pm40}

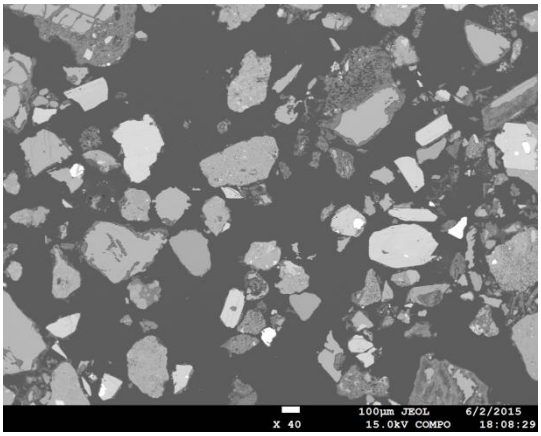

B. S_{P29}

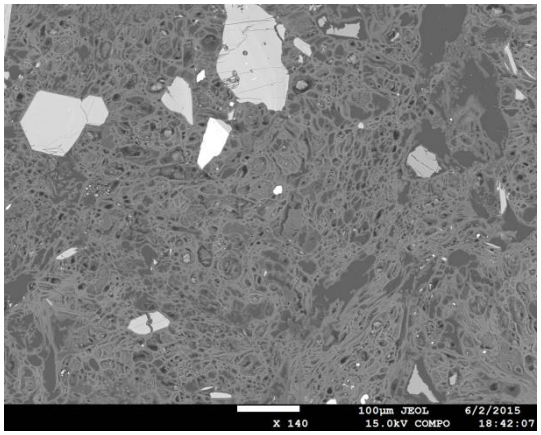

C. S_{P30}

Figure 23. BSE images from sample S_{P29-30} and S_{Pm40} of 15.8 m river terrace. Strong alteration present in all samples.

This results in smaller phenocrysts and alteration of tephra. Glass shards from S_{Pm40} were analysed. The glass shards are 300 µm size and contain plagioclase, pyroxene and amphibole phenocrysts. The glass shards appeared to be broken and some weathering on the edges was observed.

5.2.7 25.7 m terrace

This is the oldest terrace measured in this thesis. Since no pumice clasts were found only matrix could be analysed. Samples $S_{Pm37-38}$ were analysed. S_{Pm37} was hard to measure, because most tephra was strongly weathered. Three spots were analysed, but all were contaminated. S_{Pm38} however the tephra was in better condition. Of the 12 spots 6 could be used. The grains were variating from 100 to 500 µm and the glass shards usually were 200 µm.

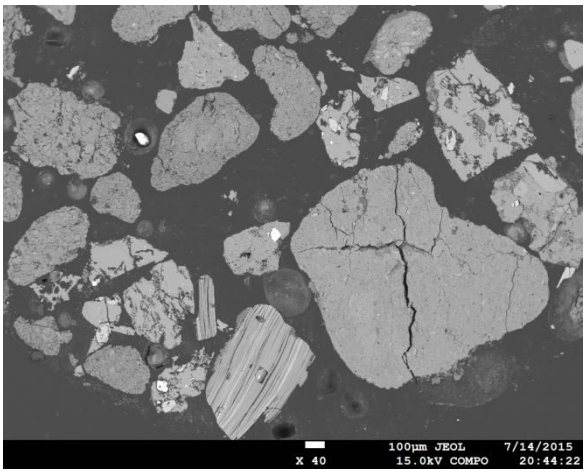

A. S_{Pm37}

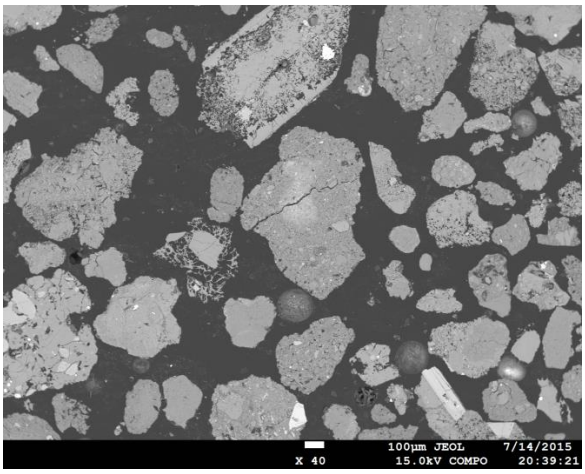

B. S_{Pm38}

Figure 24. BSE images from $S_{Pm37-38}$ of 25.7 m river terrace.

In conclusion the tephra of the river terraces textures and appearances variate little. The 2 m, 3 m, 7.5 m, 5 m and 8.5 m all contained very well preserved tephra. In the terraces further away from the river; 12.9 m, 15.8 m and 25.7 m, the tephra was weathered and broken. Also in general the amount of microliths was similar in all terraces except for the S_{P1}, S_{P8} and S_{P9}, S_{M20} in the 7.5 m and 8.5 m terrace. It remains unclear why these samples contain so much microliths. The vesicularity and phenocryst mineral content is similar. The tephra in the pumice is larger than in the matrix glass shards.

River	Terrace level	GPS number	Unit	Sample number	Sample description	Height sample	Tephra measured	Cluster
P	7.5 m	586	A	S_{P1}	Grey pumice, lot of microliths	7 m	No	-
P	7.5 m	586	A	S_{P2}	Grey pumice	7 m	Yes	C_1
P	7.5 m	586	B	S_{P3}	Large yellow pumice	5 m	Yes	C_2
P	7.5 m	586	B	S_{P4}	Large yellow pumice	5 m	Yes	C_1
P	7.5 m	586	C	S_{P5}	Grey pumice	4.5 m	Yes	C_2
P	7.5 m	586	C	S_{P6}	Grey pumice	4.5 m	Yes	C_1
P	7.5 m	586	D1	S_{P7}	Yellow pumice	3 m	Yes	C_1
P	7.5 m	586	D1	S_{P8}	Yellow pumice	3 m	Yes	C_1
P	7.5 m	586	D2	S_{P9}	Grey pumice	2 m	Yes	C_1
P	7.5 m	586	D2	S_{P10}	Grey pumice	2 m	Yes	C_1
P	7.5 m	586	D3	S_{P11}	Yellow pumice	1.5 m	Yes	C_1
P	7.5 m	586	D3	S_{P12}	Yellow pumice	1.5 m	Yes	C_1
M	5 m	545	A	S_{M13}	Dacite	2.7 m	No	-
M	5 m	545	A	S_{M14}	Grey pumice	2.7 m	Yes	C_1
M	5 m	545	B	S_{M15}	Dacite	2 m	No	-
M	5 m	545	B	S_{M16}	Dacite	2 m	No	-
M	5 m	545	C	S_{M17}	Large grey pumice	1.5 m	Yes	C_2
M	5 m	545	C	S_{M18}	Large grey pumice	1.5 m	Yes	C_1
M	8.5 m	546	-	S_{M19}	Grey pumice	Middle part	Yes	C_1
M	8.5 m	546	-	S_{M20}	Grey pumice	Middle part	Yes	Other
M	12.9 m	548	A	S_{M21}	Dacite	Top layer	No	-
M	12.9 m	548	A	S_{M22}	Dacite	Top layer	No	-
M	12.9 m	548	B	S_{M23}	Dacite	Lower part	No	-
M	12.9 m	548	B	S_{M24}	Dacite	Lower part	No	-
P	2 m	616	-	S_{P25}	Dacite	Lower part	No	-
P	2 m	616	-	S_{P26}	Grey pumice	Lower part	Yes	C_2
P	2 m	616	-	S_{P27}	Yellow pumice	2 m	Yes	C_2
P	2 m	616	-	S_{P28}	Yellow pumice	2 m	Yes	C_2
P	15.8 m	617	-	S_{P29}	Weathered grey pumice, 'crumble pumice'	Top part	No	-
P	15.8 m	617	-	S_{P30}	Weathered grey pumice, 'crumble pumice'	Top part	No	-
P	3 m	615	-	S_{P31}	Yellow weathered pumice	Top part	Yes	C_1
P	3 m	615	-	S_{P32}	Yellow weathered pumice	Top part	Yes	C_1
					Matrix samples			
P	3 m	616	-	S_{Pm33}	Mainly yellow particles	Lower part	Yes	C_1
M	5 m	545	B	S_{Mm34}	Grey, black and few yellow particles	Middle part	No	-
M	8.5 m	546	-	S_{Mm35}	Yellow, grey and black particles	Middle part	No	-
M	12.9 m	548	B		Fine grained grey particles	Lower part	No	-
P	25.7 m	587	-	S_{Pm37}	Grey particles	Lower part	No	-
P	25.7 m	588	-	S_{Pm38}	Grey particles	Lower part	Yes	C_2
P	2 m	616	-	S_{Pm39}	Mainly black and little grey particles	Top part	Yes	C_1
P	15.8 m	617	-	S_{Pm40}	Grey particles	Top part	Yes	C_1

P	7.5 m	586	D	S_{Pm41}	Grey and black particles	2.5 m	Yes	C_1
P	7.5 m	586	D	S_{Pm42}	Yellow, grey and black particles	3.5 m	Yes	C_1
P	7.5 m	586	C	S_{Pm43}	Yellow and black particles	4 m	Yes	C_1
P	7.5 m	586	C	S_{Pm44}	Grey and black particles	4.5 m	Yes	C_1
P	7.5 m	586	B	S_{Pm45}	Grey and black particles	5 m	Yes	C_1
P	7.5 m	586	A	S_{Pm46}	Black and grey particles	5.5 m	Yes	C_1
P	7.5 m	586	A	S_{Pm47}	Mainly black and some grey and yellow particles	6 m	Yes	C_1

Table 7. Samples description, location, unit and height in the section. Texture of the samples is described in Appendix A. Units were derived in the field based on texture and depositional environment. GPS number refers to the coordinates which can be seen in Appendix B. P: Platanar, M: Magdalena.

5.3 Sample pairs

In the table 8 the samples are described that cannot be separated by their chemical composition. The sampling was done in pairs, which means two pumice samples from every unit in the river terrace. This was done only for the pumice. Textures observed in river terraces indicated that several depositional events created these terraces. In order to get the fingerprint of the terrace multiple samples were needed to avoid contamination by non-juvenile rocks and check homogeneity of the terrace. In this way the hypothesis of event related terrace formation is checked. If there is variation present it must be explained.

For example, the 7.5m terrace multiple pumice samples on different heights were taken, because it was a very thick, layered and chaotic deposit. The terrace consists of four units with very different geomorphologies. One pumice sample would not be a good representation of this terrace. There were several samples pairs that were chemically very similar and for convenient reasons they are paired in the compositional plots (fig. 26). The sample pairs can be seen in table 8.

Table 8. Pumice and matrix samples from 7.5m terrace which cannot be chemically separated.

Samples	**Note**
7.5 m terrace pumice and matrix	
S_{P7-} S_{P8}	S_{P7} High sodium content
S_{P9-} S_{P10}	-
S_{P11-} S_{P12}	-
S_{Pm41}- S_{Pm42}	S_{Pm42} high potassium content
S_{Pm43}- S_{Pm44}	S_{Pm44} high sodium, S_{Pm43} high potassium
S_{Pm46} - S_{Pm47}	-
2 m terrace	
S_{P26} – S_{P28}	S_{P28} large standard deviation

5.4: Clusters

5.4.1 Cluster 1 and 2

After removing all data with low totals, contamination by microliths and earlier mentioned errors the data of the individual samples was averaged and shown with their standard deviation (fig. 26). What is clearly seen on figure 26 is that the composition of the terraces is very uniform. Not only the chemically composition of samples from individual terraces is very uniform but also from different terraces. The data is combined into three groups, cluster 1, cluster 2 and others.

When all the samples are plotted for their six major element oxides; SiO_2, Al_2O_3, K_2O, Na_2O, CaO and FeO, two clear clusters are defined; cluster 1 and 2. In table 9 the range for the elements is given. The two clusters are very close to each other and for K_2O, Na_2O and CaO they overlap.

Table 9. Element weight percentages of two clusters with range.

Cluster	SiO_2 (value + range wt.%)	Al_2O_3 (value + range wt.%)	K_2O (value + range wt.%)	CaO (value + range wt.%)	Na_2O (value + range wt.%)	FeO (value + range wt.%)
1	69.2 ± 1	16.2 ± 0.5	6 ± 0.5	1.8 ± 0.3	4.5 ± 0.4	1.5 ± 0.1
2	71 ± 0.5	15.2 ± 0.3	6 ± 0.5	1.5 ± 0.2	4.25 ± 0.25	1.3 ± 0.1

Cluster	MgO (value + range wt.%)	TiO_2 (value + range wt.%)	Cl (value + range wt.%)
1	0.2 ± 0.05	0.26 ± 0.06	0.22 ± 0.04
2	0.16 ± 0.04	0.22 ± 0.07	0.23 ± 0.05

The first cluster consists of samples from several terraces; S_{P2}, S_{P4}, S_{P6}-S_{P12}, S_{Pm41}-S_{Pm47}, S_{M14}, S_{M18}, S_{M19}, S_{P31}-S_{Pm33}, S_{Pm39} and S_{Pm40}. They all fit into cluster one nicely except for S_{P31}. S_{P31} falls on the edge of the cluster. This sample has a large standard deviation from averaging all data points, low AlO_3 and CaO weight percentages. For the other elements it fits with the first cluster, therefor it is group with cluster 1.

The second cluster consist of less samples and overlaps with cluster one for K_2O, Na_2O and CaO. The other elements are clearly different. S_{P3}, S_{P5}, S_{M17}, S_{P26}, S_{P27}, S_{P28} and S_{Pm38} are part of cluster 2. Cluster 2 has lower Al_2O_3 and FeO, higher SiO_2 weight percentages. S_{M17} however deviates for K_2O and CaO than cluster 2. The cluster defined with small compositional variance between C_1 and C_2. The terraces show a uniform composition in general.

5.4.1: Other samples

Sample S_{M20} is one of the samples that do not fall into either cluster. It is probably due to plagioclase contamination and that it consists of only one measurement. It lies closest to cluster 1 and since sample S_{M19} fall into cluster 1 (sample pair), sample S_{M20} probably falls into the same cluster.

The second group are the samples derived from the lake sediments. They glass shards all have a cluster 1 chemical composition. Sample 52 is the only sample that has a bit high FeO value to fall entirely in cluster 1.

If we zoom out and view the results per terrace, both clusters can be present in one terrace. Cluster 2 samples are from the 5 m (S_{M17}) terrace of the Magdalena River and 2 m ($S_{P26\text{-}P28}$), 7.5 m (S_{P3}, S_{P5}) and 25.7 m terrace (S_{Pm38}) of the Platanar River. If we then compare the geomorphology of the units where the samples were collected from, there is a similarity found. Namely all samples were

collected from a layer of coarse grained, conglomerate type unit. The 5 m and 7.5 m terraces show this very good (fig. 25). The 2 m river terrace was a bit overgrown and oxidation affected the section, with coarse grained lenses consisting entirely of pumice and dacite clasts. In the 25.7 m terrace all pumice was altered to matrix, thus this could not be observed. Cluster 1 samples were also collected in these terraces. The matrix from the 2 m terrace is part of cluster 1.

Cluster 1 is present in all terraces. The only samples that not fit in the two clusters were from the 8.5 m terrace (S_{M20}) and lake samples (S52). In table 7 all samples are shown with their clusters.

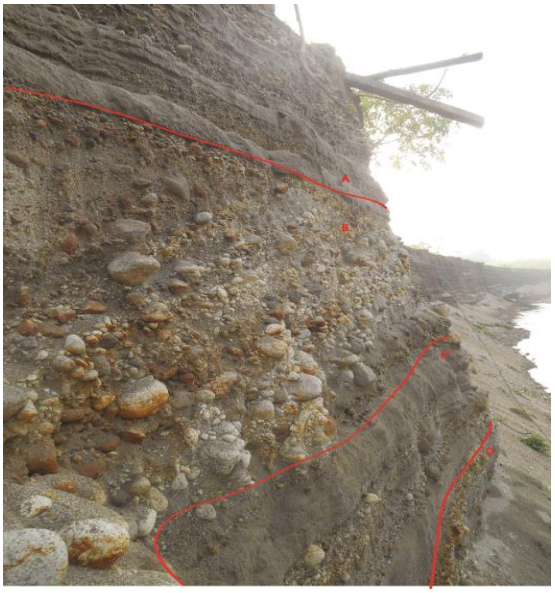

A. 7.5 m terrace, S_{P3}, S_{P5} from unit B

B. 5 m terrace, S_{M17} from unit C.

C. 2 m terrace, $S_{P26\text{-}P28}$

Figure 25. Locations of pumice sample with 2 clusters. Cluster two is present in similar deposits which were deposited during a highly energetic event.

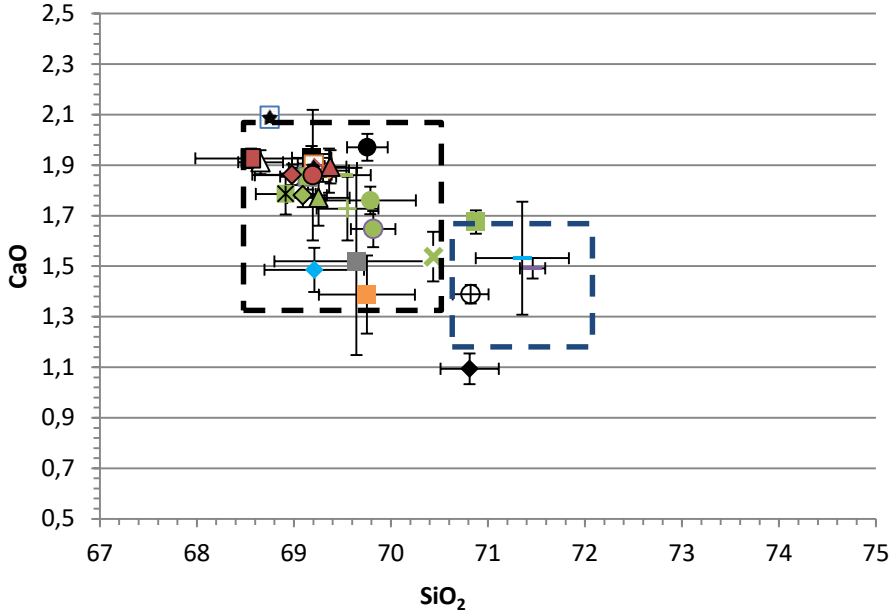
2,5
2,3
2,1
1,9
1,7
1,5
1,3
1,1
0,9
0,7
0,5
CaO
67
68
69
70
71
72
73
74
75
SiO2

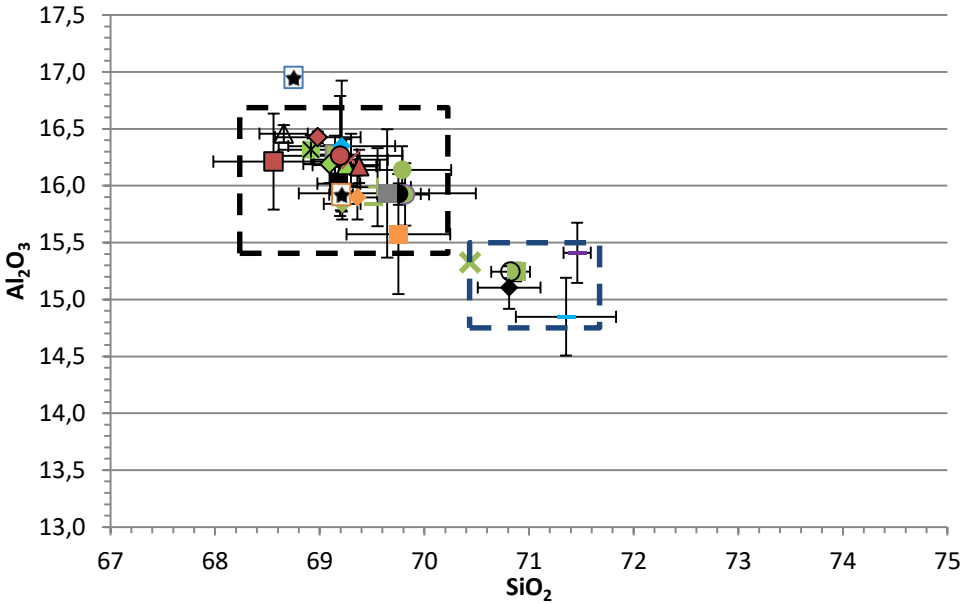
17,5
17,0
16,5
16,0
15,5
15,0
14,5
14,0
13,5
13,0
Al2O3
67
68
69
70
71
72
73
74
75
SiO2

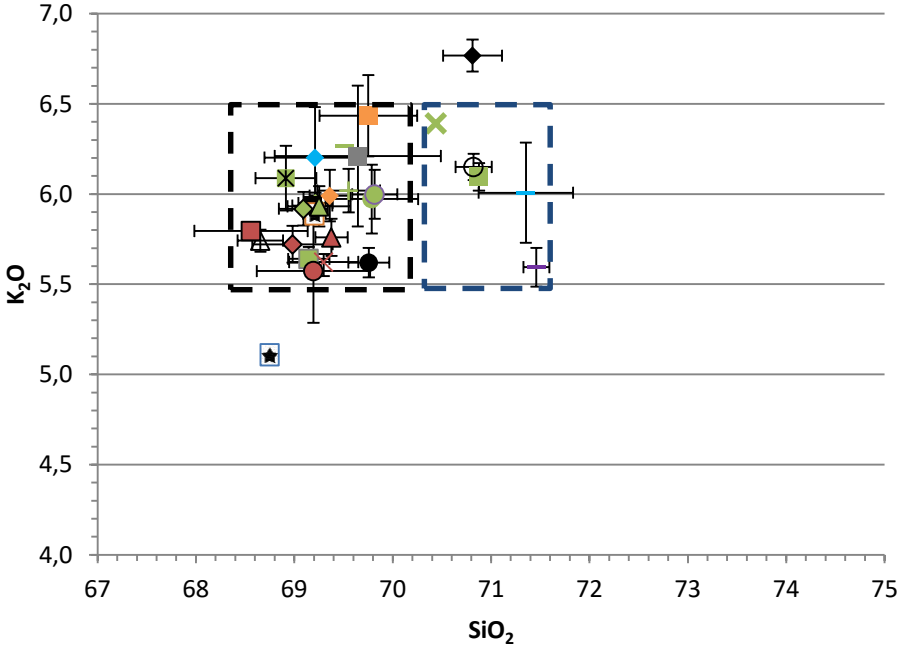
7,0
6,5
6,0
5,5
5,0
4,5
4,0
K2O
67
68
69
70
71
72
73
74
75
SiO2

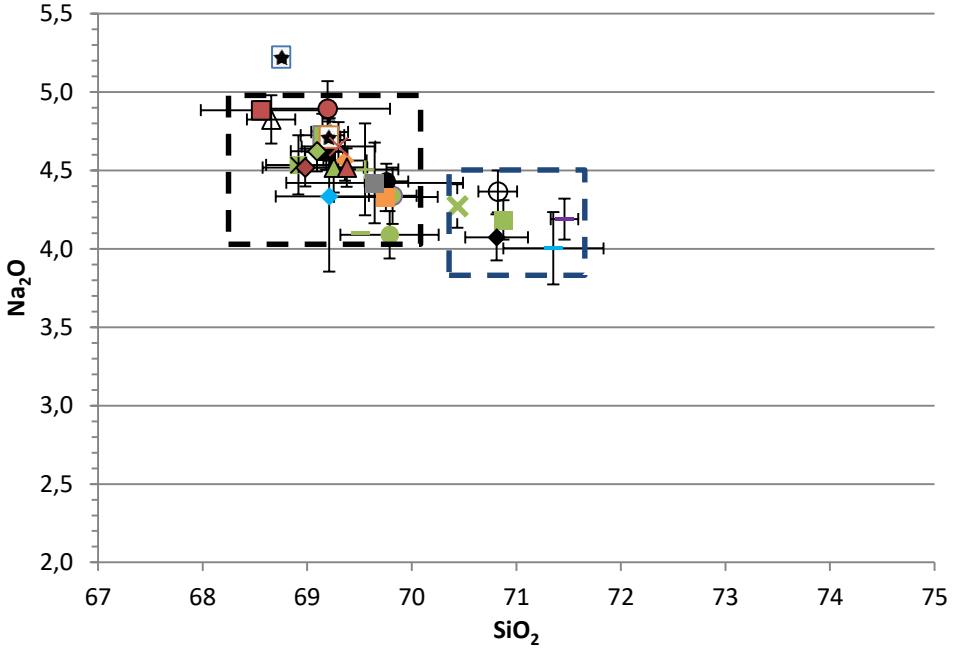
5,5
5,0
4,5
4,0
3,5
3,0
2,5
2,0
Na2O
67
68
69
70
71
72
73
74
75
SiO2

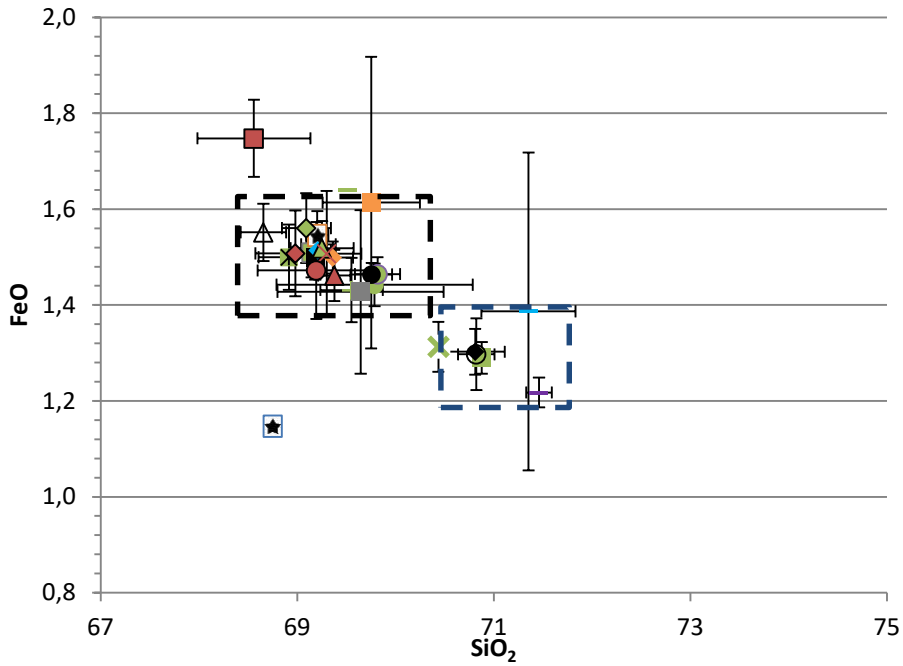
2,0
1,8
1,6
1,4
1,2
1,0
0,8
FeO
67
69
71
73
75
SiO2

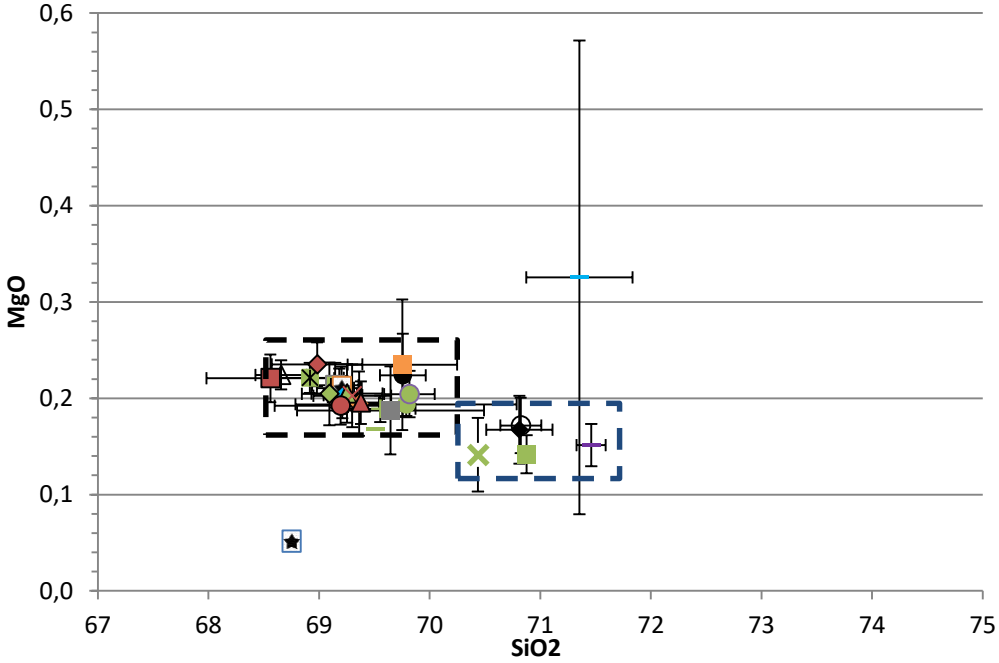
0,6
0,5
0,4
0,3
0,2
0,1
0,0
MgO
67
68
69
70
71
72
73
74
75
SiO2

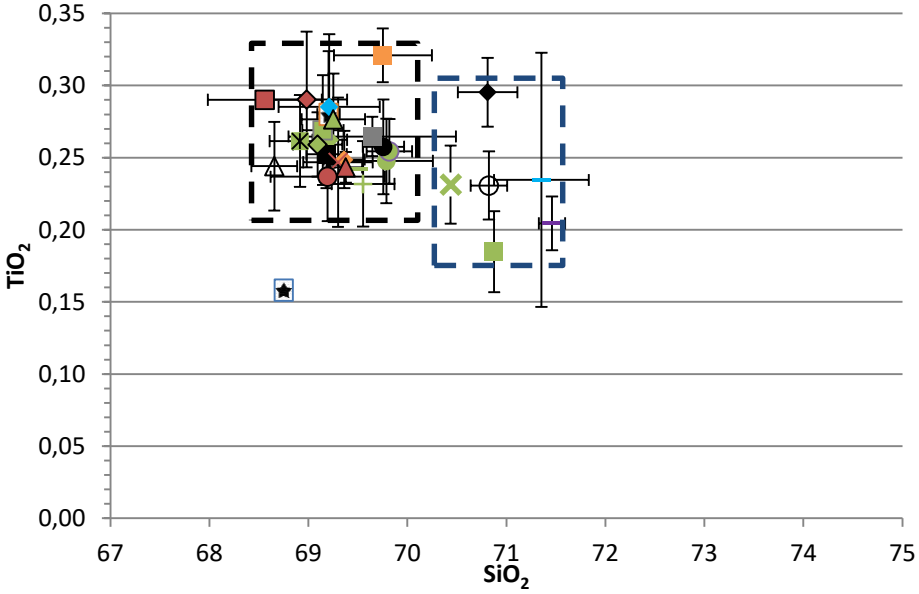
0,35
0,30
0,25
0,20
0,15
0,10
0,05
0,00
TiO2
67
68
69
70
71
72
73
74
75
SiO2

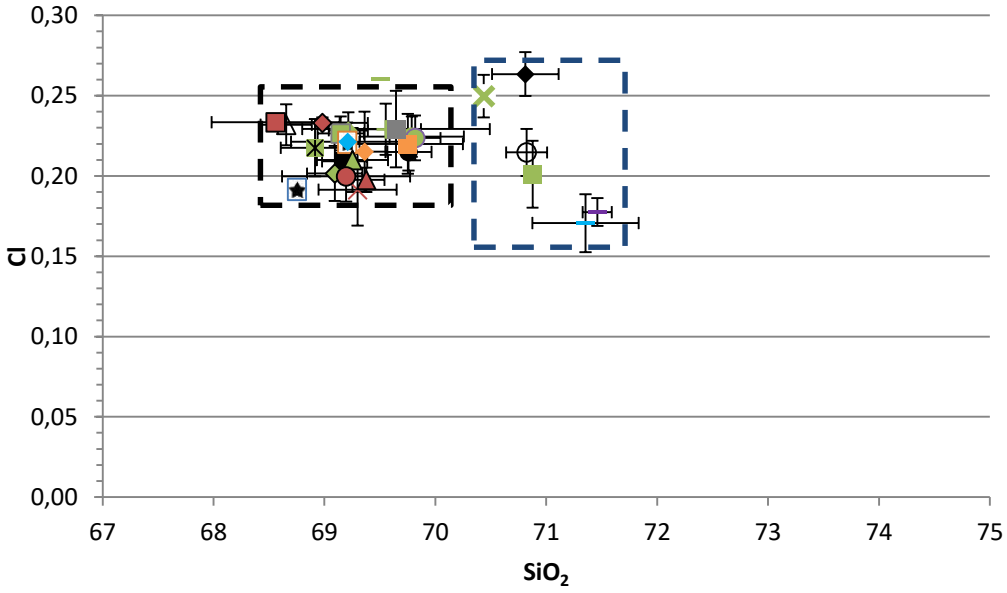
0,30
0,25
0,20
0,15
0,10
0,05
0,00
Cl
67
68
69
70
71
72
73
74
75
SiO2

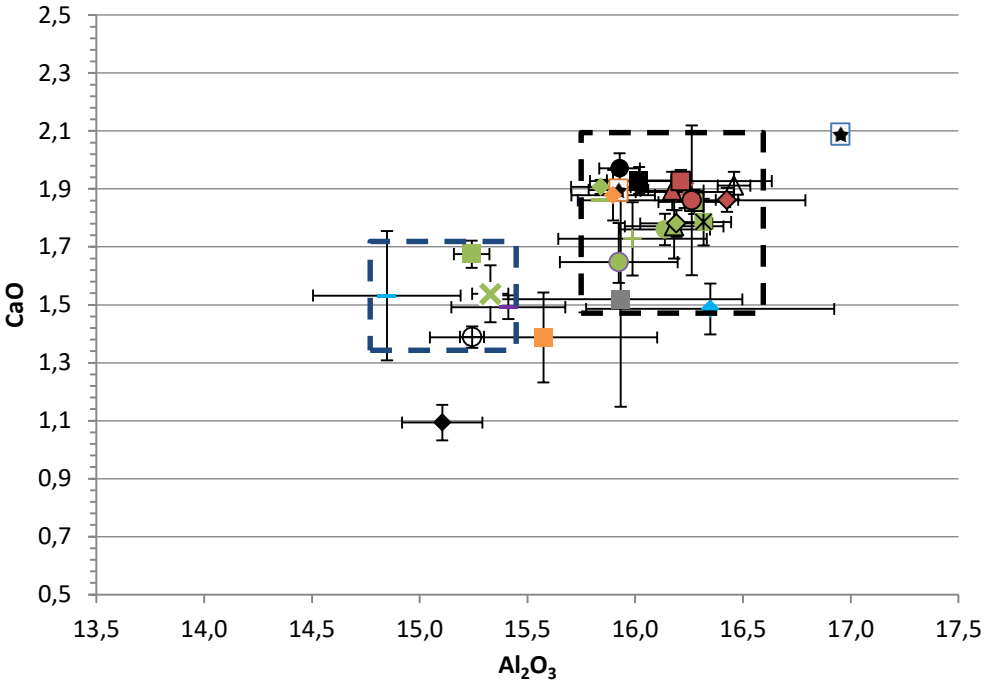

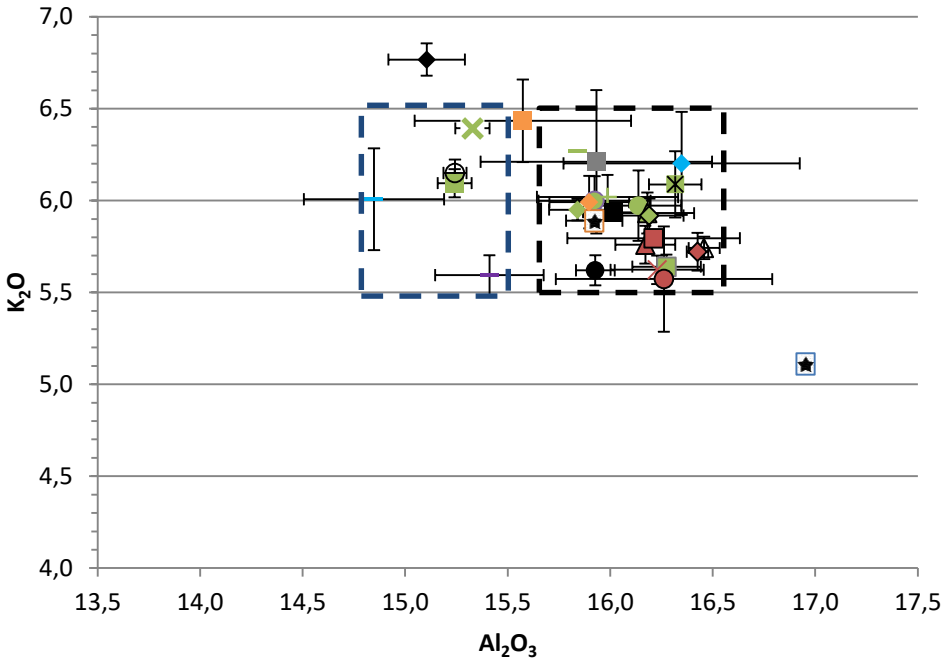

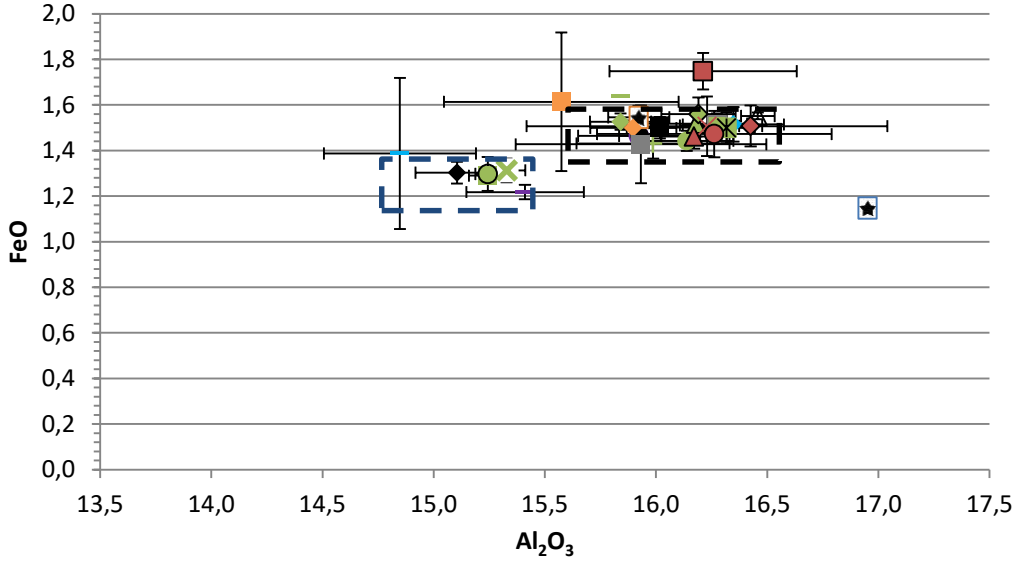

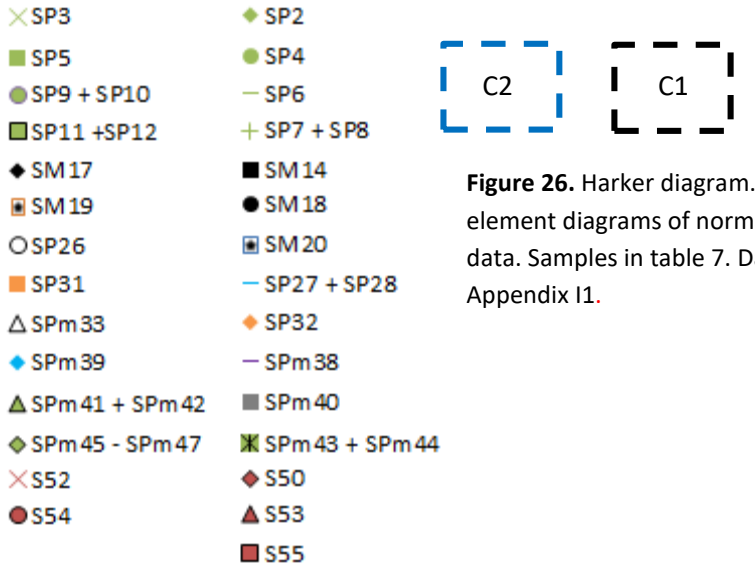

Figure 26. Harker diagram. Major element diagrams of normalized data. Samples in table 7. Data in Appendix I1.

5.5 Microliths and Phenocryst minerals

An effort was made to find characteristics of the enclosed minerals. Plagioclase is most abundant minerals, then hornblende, pyroxene, k-feldspar and magnetite, apatite, sphene are present in minor amounts. Further a lot of orthoclase was seen as microliths. The majority of the minerals was measured by EDS, with few WDS measurements (see appendix K). The average composition of the enclosed minerals was calculated, size and textural features were described. Large minerals shown on the BSC images were randomly picked to for EDS measurement based on the colour difference seen on the EPMA.

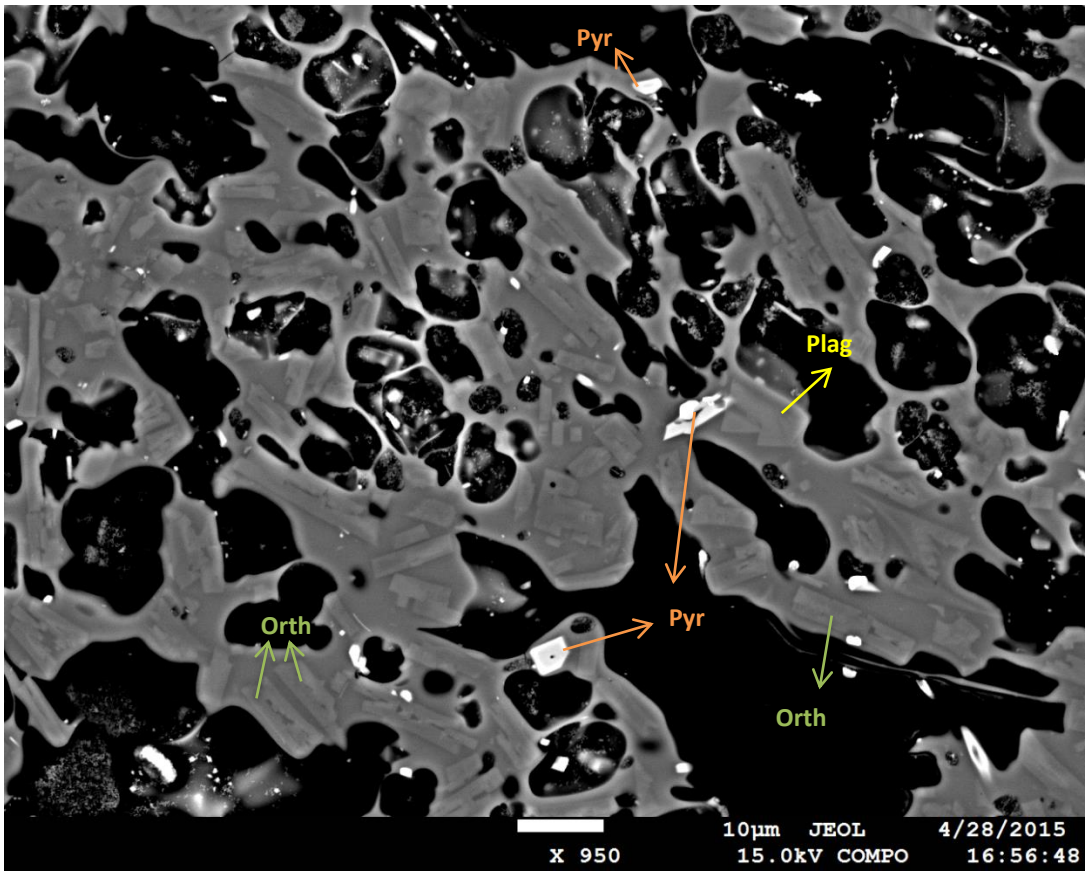

A. S_{P1} showing microliths of pyroxene (white spots) shown in orange, orthoclase in green and plagioclase (grey elongated rectangles) in yellow.

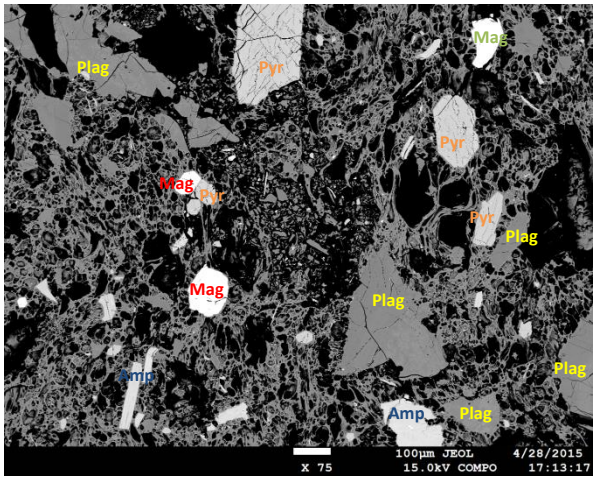

B. S_{P3}.

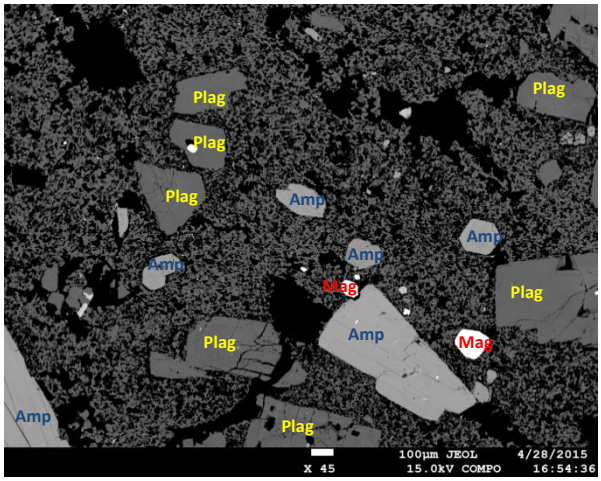

C. S_{P1}.

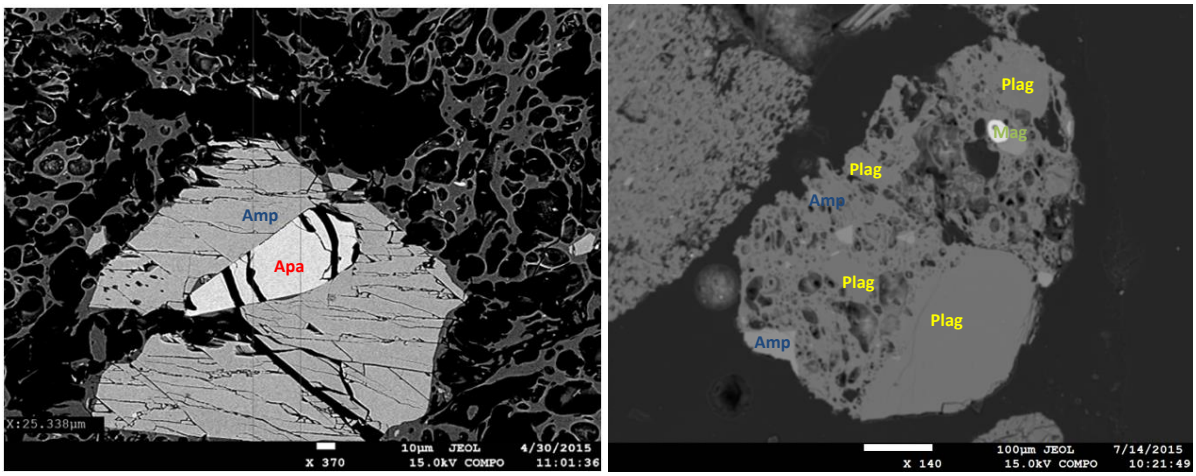

C. S_{P7}. **D.** S_{Pm33} grain 1.

Figure 27. Large phenocrysts in pumice samples with colour code and name; Plagioclase (plag), Amphibole (mainly hornblende, amp), clinopyroxene (pyr), magnetite (Ti rich, mag) and apatite (apa). **C.** The apatite is enclosed inside the amphibole; the apatite has overgrown the amphibole. **D.** Matrix grain showing phenocrysts minerals plagioclase, amphibole and Ti-magnetite.

5.5.1 Plagioclase

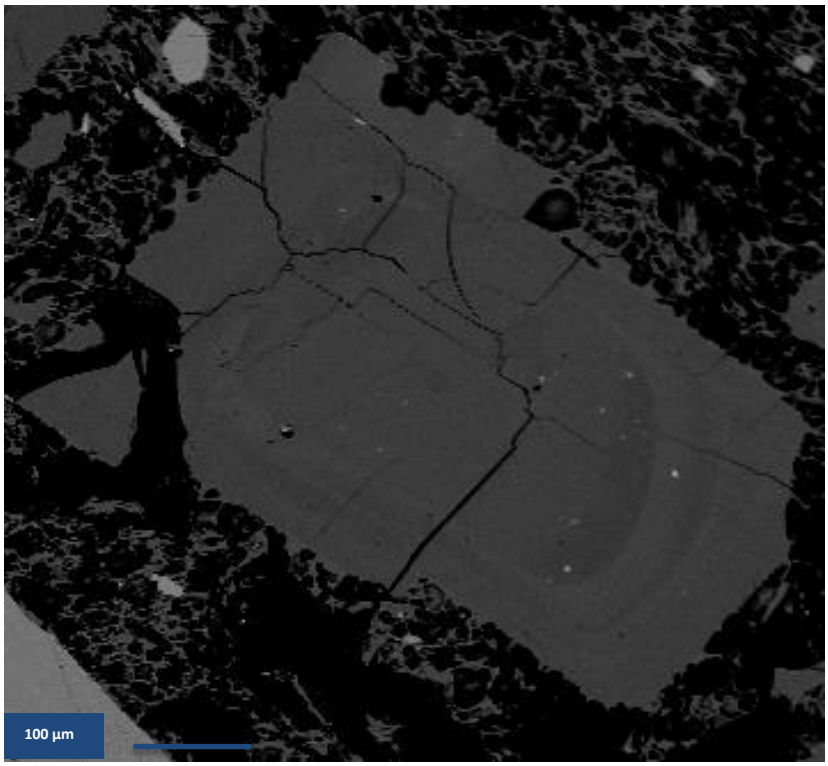

Figure 28. Zonation in plagioclase phenocryst in pumice sample S_{M14}.

Plagioclase is the dominant mineral in the glasses and is present as 10-700 µm phenocrysts and as 2-20 µm microliths in the glass. They are elongated to cubic shaped and sometimes contain cracks (fig. 28). The ternary diagram shows a relative potassium poor average plagioclase (fig. 30). From the plot the average plagioclase is calculated; $Ab_{0.53}$ $An_{0.44}$ $Or_{0.03}$, structural formula; $(Na_{0.52}$ $Ca_{0.43}$ $K_{0.03})$ $(Al_{1.41}$ $Si_{2.59})$ O_8. The plagioclase in cluster 1 and 2 samples are very similar, although cluster 1 has more potassium rich plagioclases (S_{P1}, S_{PM33}). The purple points in table 10 are minerals analysed in samples from small lakes in the surroundings of El Chichón in the tabasco area. They show a large variation,

with pure albite and anorthite (fig. 29). Some zonation is observed in the plagioclases (S_{P7}, appendix F3). For the ternary diagram the ratio K, Na and Ca was calculated from the samples, which are listed in appendix K.

Table 10. Legend for plagioclase, pyroxene and amphibole ternary diagram.

Colour tags in figures 29-32	Samples
◆ Cluster 1	2, 4, 6-12, 14, 18, 19, 31-33, 39-47
◆ Cluster 2	3, 5, 17, 26-28, 38
◆ Others	20, 48-55

Although most plagioclase plots around 0.6 An-Ab, S50, 52-53 are more Calcium rich. The plagioclase from terraces samples is very uniform with an average 0.55-0.6 An-Ab ratio. The 7.5 m terrace shows a larger variety, ranging from 0.35-0.65 An-Ab with no clear difference between matrix and pumice. The terrace samples from the Magdalena river (5 m, 8.5 m, and 12.9 m) show slightly lower An-Ab ratios than the Platanar river terraces. In general, the plagioclase composition is very uniform in all measured terraces. It must be reported that although not all phenocryst minerals of the different terrace were analysed. The plagioclase phenocrysts in the terraces have a similar textures and show zonation (Appendix F).

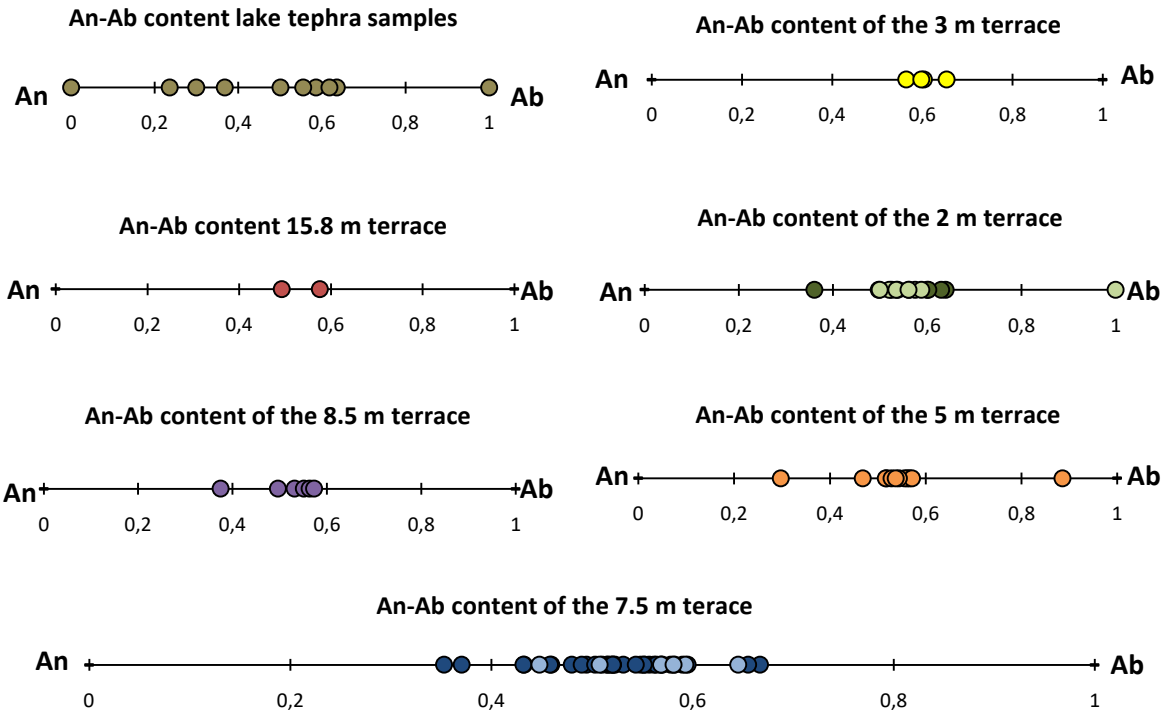

Figure 29. Anorthite-Albite content of river terraces. Every terrace is marked with a different colour, for the 2 m and 7.5 m both matrix and pumice samples were analysed. The light colours in these plots show matrix: 7.5m terrace dark blue: pumice, light blue: matrix, 2 m terrace green: pumice, light green: matrix.

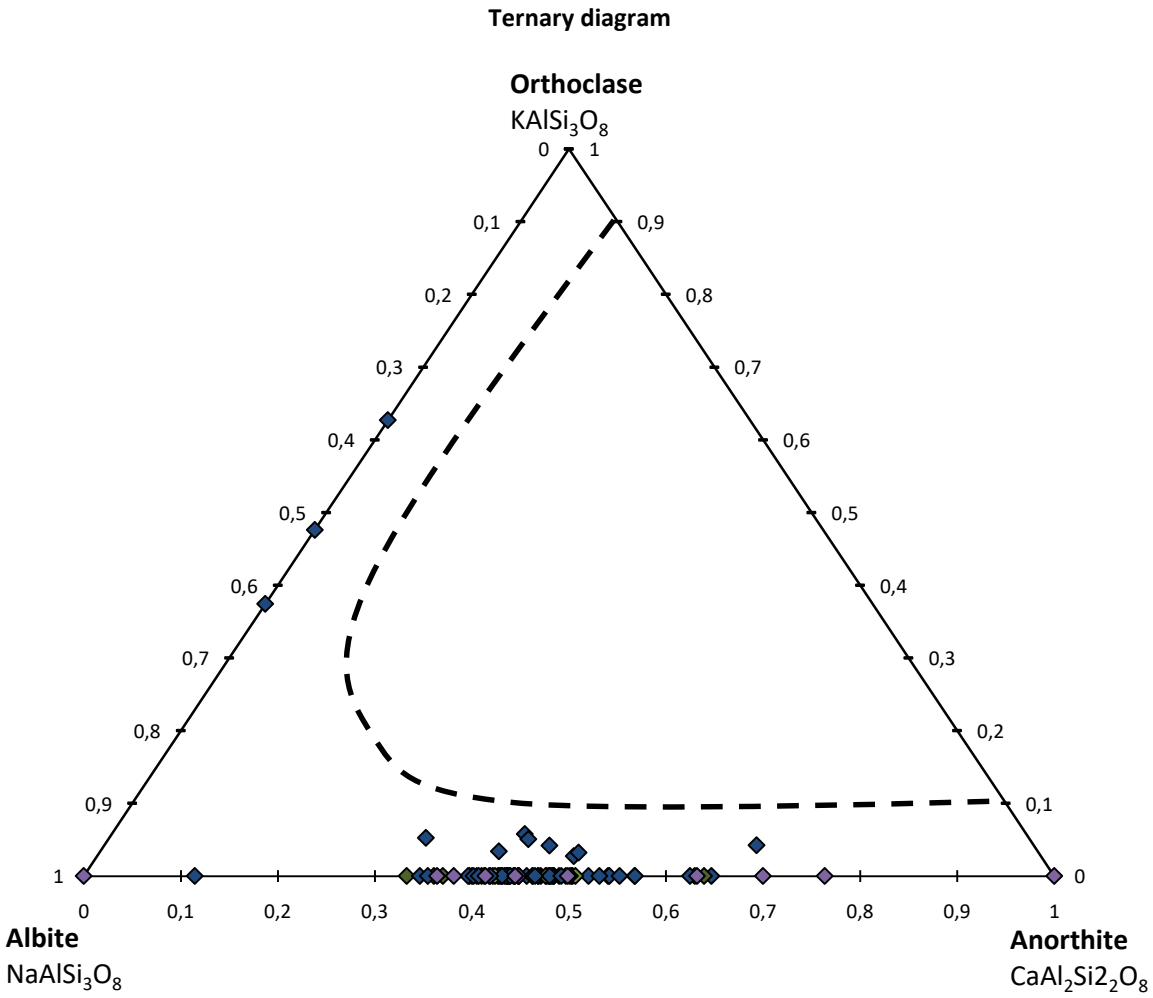

Figure 30. Ternary diagram for plagioclase with Albite, Anorthite and Orthoclase endmembers. Data from Appendix I2 and for symbols see table 6.

5.5.2 Orthoclase

The majority of the microliths is orthoclase (fig. 27A) and too small to measure. Some EDS show the presence of more potassium rich plagioclases, but no orthoclase microliths were analysed. On the microlith scale, the samples were flocked with orthoclase minerals. It has an elongated, rectangular to blocky shape and 1-15 µm size.

5.5.3 Amphibole

The amphiboles in the tephra mainly consist of (Mg-)Hornblendes with an occasional K-rich amphibole, elongated rectangular shape. The majority plots in the Mg-Hornblende field, with some samples in the Tschermaki compositional field (fig. 31). The average amphibole composition is $(Na_{0.67}$ $K_{0.35})$ $Ca_{1.87}$ $(Mg_{2.63}$ $Fe_{2.24}$ $Al_{1.00})$ $(Si_{6.74}$ $Al_{1.29})$ O_{24}, assuming little water in the amphibole. The Al content is a bit too high and the Na and K are a bit low. The Mg/(Mg+Fe) varies between 0.4 and 0.6 and the Si varies between 6 and 7.3. All three clusters plot in the same range for Si and Mg/(Mg+Fe). The amphiboles are on average smaller than the plagioclase and vary 10-400 µm. Although no microliths of hornblende were measured, they were observed with similar sizes as the plagioclase but in lesser amounts.

Further from comparing individual terraces there is not much variation in the Mg ratio, but for the Si there is quite some variation (Appendix K). The 5 m terrace shows a Si ratio of 7, while the lake samples and the 2 m show average Si ratios of 6.5. The 7.5 m terrace shows a large variation from 6.2-7.2 Si.

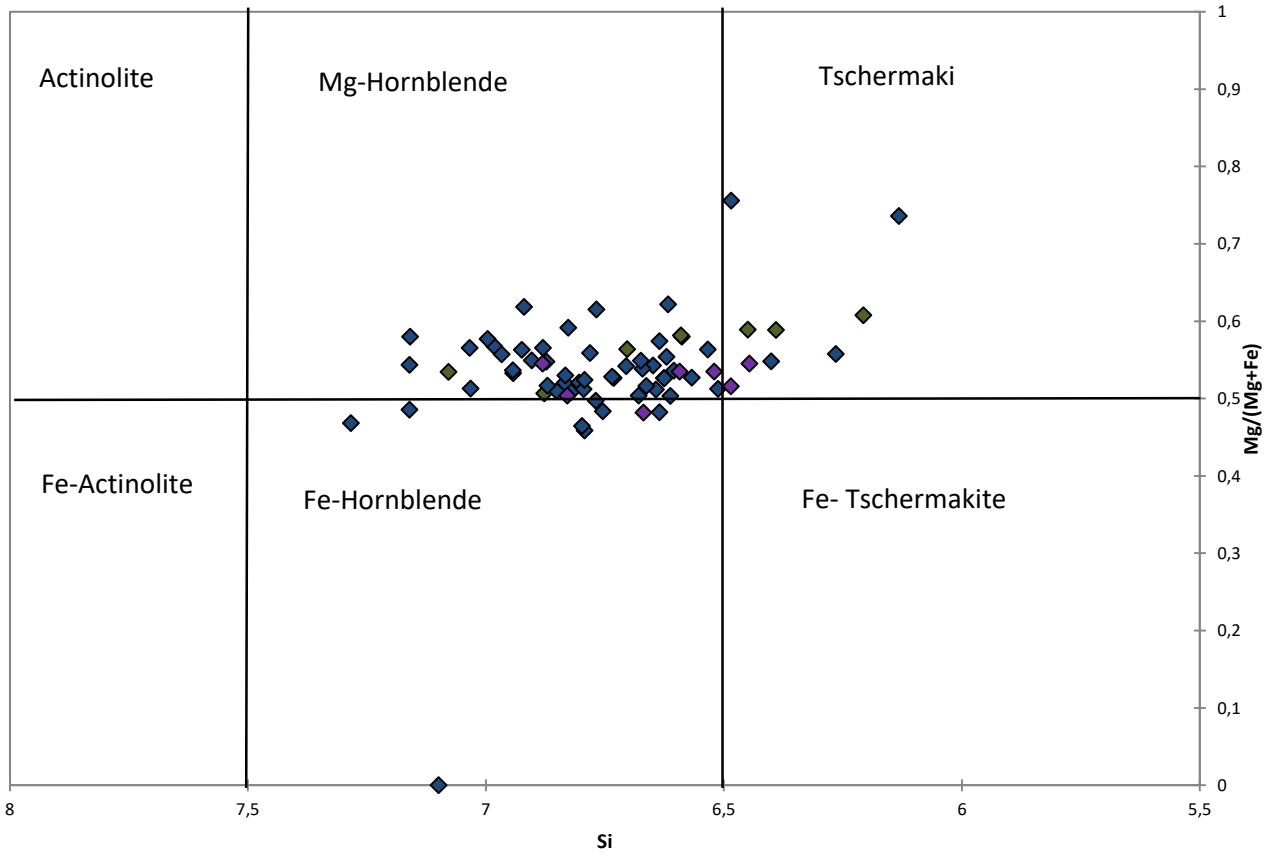

Figure 31. Endmember compositional diagram for Hornblende with Fe and Mg endmembers. Stoichiometry of Si, Mg and Fe from EDS data on axis. Data from appendix K and symbols from table 6.

5.5.4 Pyroxene

The pyroxenes consist mainly of euhedral Diopside and Augite (fig. 32). Two Hedenbergites were measured. The minerals were present as large phenocrysts and occasionally as smaller microliths in the tephra (fig. 27). The pyroxene phenocrysts were smaller than the amphibole and plagioclase phenocrysts and range from 10-200 µm. The pyroxene microliths were the same size as the plagioclase and amphibole microliths. Similar to the plagioclase minerals, the pyroxenes show no real compositional difference between terrace samples. They all show a very uniform Diopside composition.

5.5.5 Minor minerals

Apatite, magnetite and sphene are present as small phenocrysts and microliths (fig. 20, 21). Several clear apatite microliths and phenocrysts were analysed which show a clear hexagram (fig. 21). These minerals are smaller than the major phenocryst minerals. The magnetite was 50-100 µm, while the apatite and sphene were much smaller (5-50 µm). The magnetite had 7 wt.% TiO_2 and some apatite minerals include ZrO_2.

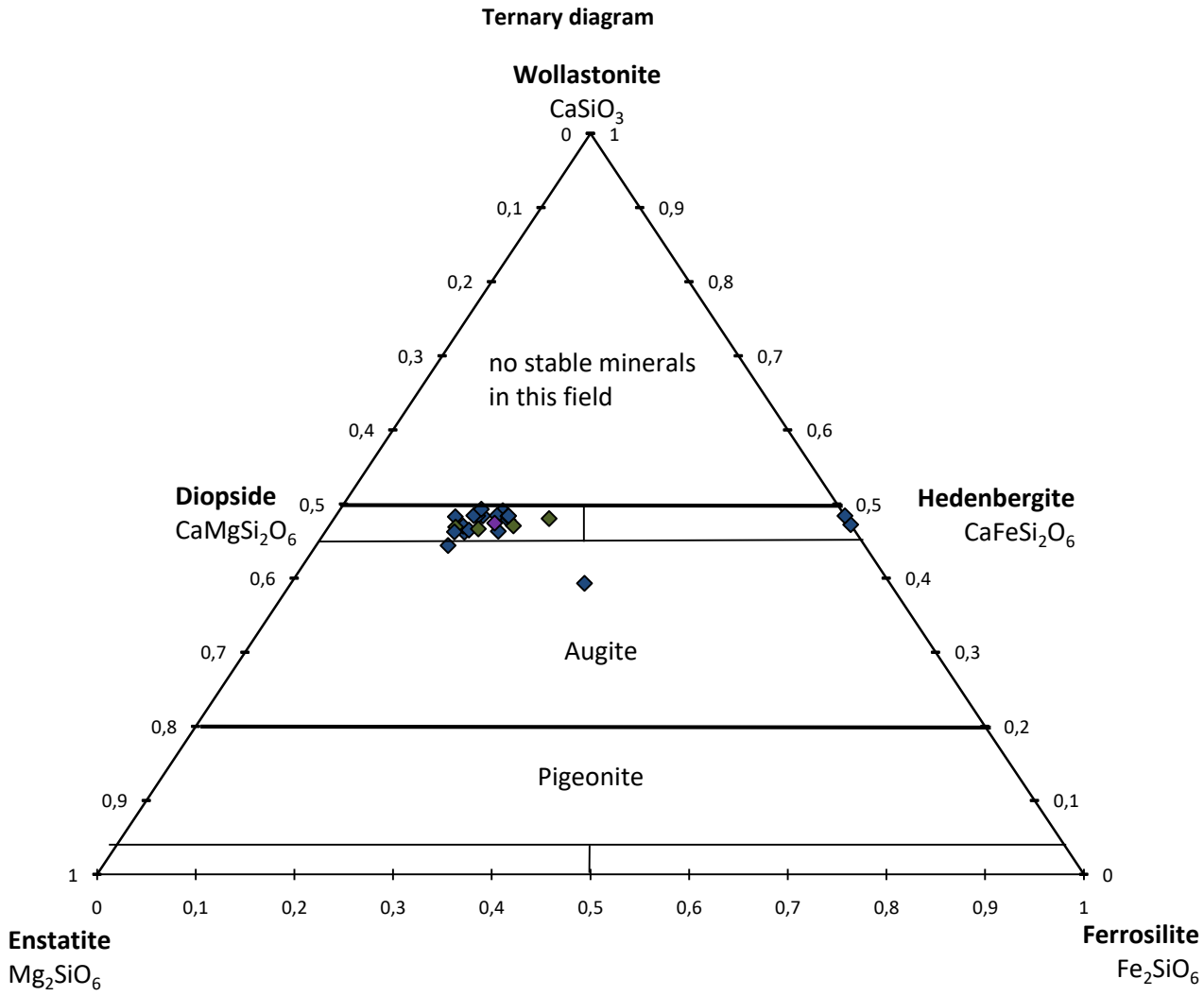

Figure 32. Ternary diagram for pyroxene with Enstatite, Ferrosilite, Hedenbergite, Diopside and Wollastonite endmembers. Data from appendix K and symbols from table 6.

6. Discussion

An attempt was made to link the river terrace of the Magdalena and Platanar River to the eruptions of El Chichón. The proximal tephra is compared to the distal tephra to find the origin of the clusters derived in the MSc thesis of Huizinga (2013, unpub. MSc thesis).

6.1 Field evidence of eruption related river terraces

The hypothesis is that river terraces of the Magdalena and Platanar formed after or during an eruption (section 3.1). The deposits consist of pyroclastic rocks, tephra and minor amounts of accidental lithic rocks that are transported by several debris flows with large amounts of rocks (Appendix A, D-1). After an eruption there is a massive amount of new material deposited in the river valleys. The huge amount of new material chokes the river. Then during a period of heavy rainfall large volcanic debris flows transport the eruption material to form large massive river terraces. The thickness of the river terraces decreases as the debris flow transports the deposits downstream.

This idea of eruption related terraces was derived from height elevation maps made preliminary to the fieldwork. The idea was to look for the chemical signature of El Chichón from deposits closer to the volcano. Since the dome structure and surroundings (within 3 km of the dome) have a very complex stratigraphy and different eruptions are difficult to distinguish (Espíndola et al. 2000). Other locations were searched to find chemical signatures of El Chichón eruptions. In the river beds of the Magdalena and Platanar the LIDAR maps (Appendix A for explanation) showed that many river terraces have constant thicknesses (fig. A-3, A-11, Appendix A). The river terraces were very easily identified and show constant thickness on several locations along the river (fig. A-11). This raised the idea that these terraces were formed by several massive hyperconcentrated or pyroclastic flows. These massive flows form shortly after an eruption. Arguments for this are described in the next sections.

6.1.1 LIDAR images

The first argument already mentioned is the LIDAR images. During the preliminary work close attention was paid to the geophysical and geographical character of the river valleys. The Platanar and Magdalena River were searched for multiple river terraces of similar thickness (6.5-8.5 m terraces, fig. A-11). In the river beds several terrace levels were found. In several locations the same terrace level was found (fig. A-11), indicating a large event that deposited these volcanoclastic sediments. Using LIDAR images with GIS software several river terraces were found.

6.1.2 1982 Ostuacán flooding

There are also several reports of massive hyperconcentrated flows formed shortly after the 1982 eruption of El Chichón (Duffield, 2001, Macias et al. 2004). Macias et al. (2004) reported two debris flow of volcanoclastic material flooding the village of Ostuacán in May 1982. One month after the eruption an enormous amount of pyroclastic sediments build-up a natural dam 4 km downstream the river. On May 26 1982 this dam failed causing multiple debris flows containing pyroclastics and tephra to flow downstream. The transport variated from debris flows to hyperconcentrated flows. The flow reached as far as the big lakes northwest of Ostuacán (fig. D-1,2, A-2). The hot hyperconcentrated or debris flow formed shortly after the eruption and created multiple river terraces in the Magdalena River of similar heights. The terraces contain 1982 volcanic products,

including tephra. They made several stratigraphic sections across the Magdalena River and one terrace is analysed in this work. Stratigraphic section 156 is the same as the 5 m river terrace (Macias et al., 2004). Tephra of this terrace was analysed and was used to identify volcanoclastic deposits in other river terraces. Although this river terrace was not formed from a primary pyroclastic flow, it was still formed shortly after the eruption, which makes it reasonable to assume that tephra from the river terrace was fresh, juvenile and not altered much before deposition. The depositional features and textures of section 156 were also found in other river terraces in the Magdalena and Platanar River. Characteristics of these hyperconcentrated and debris flows are coarse sand to gravel sized clasts, lack of imbrication, thick and coarse units in stratification with the debris flows showing inverse grading. Analysed terraces in this thesis show similar characteristics (section 5, Appendix A). In a more general way stratigraphic section 156 was formed after one massive event, from a debris flow containing massive amounts of material.

6.1.3 Depositional environment river terraces

As described above the 5 m river terrace was used to describe the unique stratigraphy of river terraces formed by hyperconcentrated and debris flows. In the other river terraces close attention was paid to the environment which the rocks were deposited. The 5 m river terrace is composed of four distinct units which were interpreted as debris and hyperconcentrated flow deposits. Two units had a very different texture representing these flows; the first had a conglomerate texture with immense grain size variation (debris flow) and the other unit was finer grained with smaller pumice clasts (hyperconcentrated flow). The same stratigraphy was seen in the other river terraces.

Table 11. Visited river terraces with measured samples.

	River terraces	Measured samples	River	Deposition environment	Flow deposit
1	7.5 m terrace pumice and matrix	S_{P2}- S_{P12}, S_{Pm41}- S_{Pm47}	Platanar	High energy, catastrophic deposition	Hyperconcentrated and debris
2	5 m terrace (Macias et al. 2004)	S_{M14}, S_{M17}, S_{M18}	Magdalena	High energy, catastrophic deposition	Hyperconcentrated and debris
3	8.5 m terrace	S_{M19} – S_{M20}	Magdalena	*	Debris
4	2 m terrace	S_{P26} – S_{P28}, S_{P33}	Platanar	High energy, catastrophic deposition	Hyperconcentrated and debris
5	3 m terrace	S_{P31} – S_{P32}	Platanar	High energy, catastrophic deposition	*
6	15.8 m terrace	S_{Pm40}	Platanar	*	*
7	25.7 m terrace	S_{Pm38}	Platanar	*	*
8	12.9 m terrace	-	Magdalena	High energy, catastrophic deposition	Hyperconcentrated and debris

*Could not be observed, because the surface was not fresh cut, weathered or overgrown by vegetation.

Further the 7.5 m terrace shows this stratigraphy very clearly. This terrace is well exposed, fresh cut and 7.5 m thick. Multiple coarse grained, conglomerate and fine sand grained units were observed. Yellow and grey pumice layers intercalated with fine grained layers containing pumice clasts, similar to the 5 m terrace, but much thicker and more lenses with coarse grained volcanic sediments. Further crossbedding was observed in the fine grained layers of the 7.5m terrace. This could be a short period of less chaotic, calm deposition. The terrace was the result of several intervals or episodes of debris and hyperconcentrated flows. Inverse grading was seen in unit C and D. The terrace lower part mainly consists of grey pumice, while the upper part the pumice is yellow. This

could represent the several phases of the 1982 eruption. The 1982 eruption occurred in two phases with ten eruptive episodes (De la Cruz-Reyna, 2009, Macias et al. 1997).

The 12.9 m, 2 m and 3 m river terraces also showed this stratigraphy. They all have similar features that indicate high energy depositional environment, unsorted conglomerate type depositions with fine grained deposits on top of it containing pumice clasts, inverse grading. In the 15.8 m and 25.7 m this was not seen, because these terraces were too weathered and overgrown. The pumice in these terraces was altered and crumbled into matrix. However, no indications were found that these older terraces were formed otherwise. Assumed is that the 15.8 m and 25.7 m terrace were formed in a similar way as the other terraces.

In summary all geomorphic features indicate high energetic event formed terraces in the Magdalena and Platanar river valley. After the eruption volcanoclastic deposits choke the river until, during a period of heavy rainfall the material is transported downstream in a large debris flow. The tephra and pyroclastic material forms event terraces. Documentation of dam break breach (Macias et al., 2004), geomorphic features in the river terraces and LIDAR images support this. River terraces were formed shortly after the eruption by one or several massive flows with large amounts of volcanic sediments. Another way could be as described in Macias et al. (2004); material is transported by hot hyperconcentrated or debris flows as a consequence of natural dam failure. Further the river terraces closest to the river were best preserved, with fresh pumice clasts and glass shards. The terraces further away from the river are more eroded, contain smaller pumice clasts and are overgrown. The next step is to find the age of these terraces in order to link them to an eruption of El Chichón.

6.1.4 River terrace ages

From geographical and geomorphic features and LIDAR maps along with carbon dating of charcoal an attempt is made to find the age of the river terraces. In the 7.5 m a piece of charcoal was found (fig. 8, A-11). Analysis of the charcoal in the middle part of the section showed that the river terrace was deposited in recent time, meaning 1982 eruption products (courtesy of C.A.M. Nooren).

The other age constraint is from LIDAR images made before and 2 years after the 1982 eruption. In Smid (2015, unpub BSc thesis) LIDAR images were used to calculate the amount of produced volcanoclastic material by the 1982 eruption. Both the Platanar and Magdalena River were analysed. What is very clear from these images (fig. 33) is that the 7.5 m river terrace is part of the 1982 volcanic deposits. Just as earlier confirmed by the charcoal. Further the 2 m and 3 m terrace of the Platanar river appear to lie outside the area where 1982 volcanic sediments were deposited. From river terraces of the Magdalena river, the 5 m and 8.5 m originate from the 1982 eruption, something not expected from preliminary research and geomorphic appearance of both terraces. Although they both have indications implying event related terraces; the 8.5 m consists of poorly imbricated, conglomerate texture, debris flow deposits in which no hyperconcentrated flow deposits were observed (Appendix A). However strong weathering and poor exposure made it difficult to distinguish hyperconcentrated flow deposits. It is most likely that this terrace is made up from only debris flows, with no hyperconcentrated flow deposits or this deposit is covered with vegetation and not visible. Nevertheless, this terrace is concluded to be formed from deposits of the 1982 eruption.

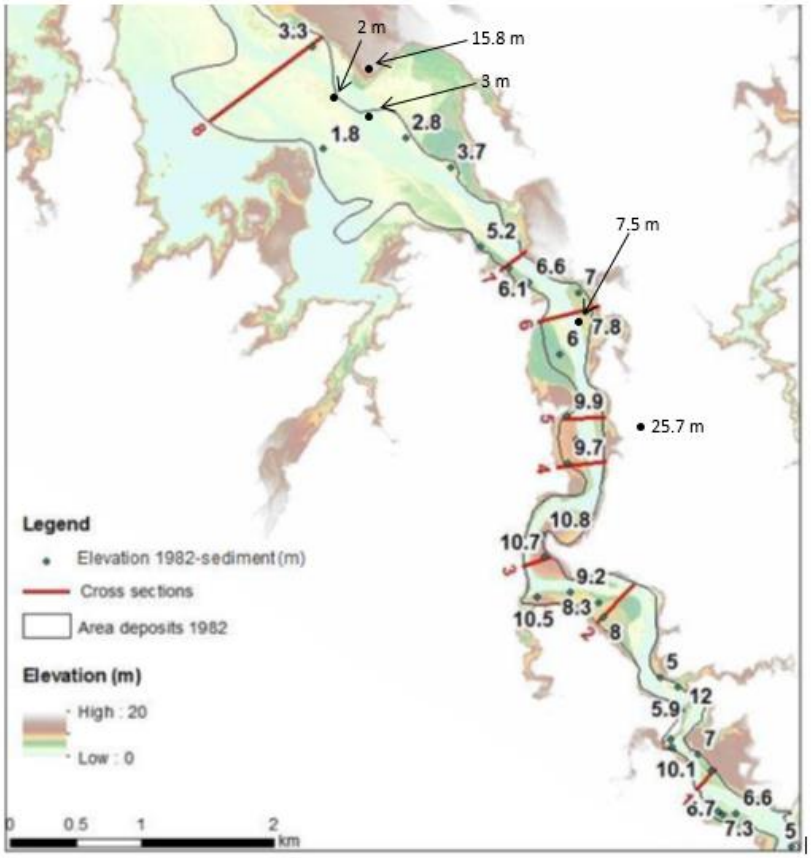

A.

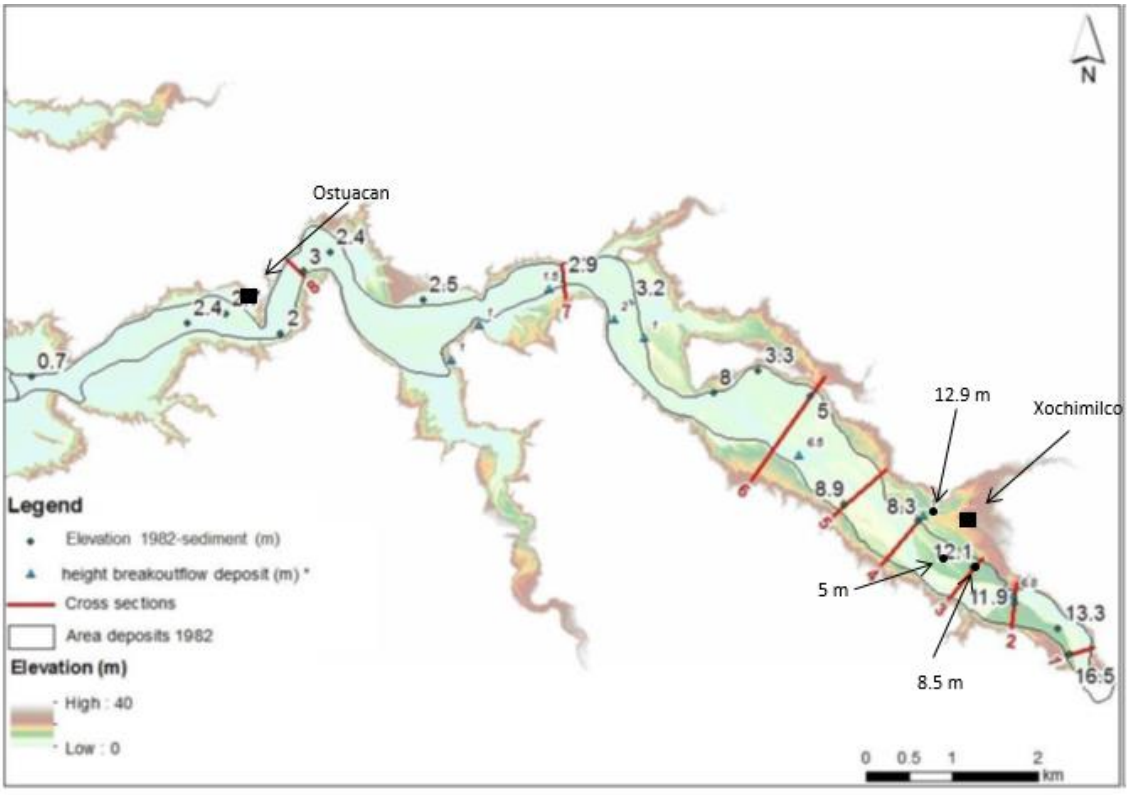

B.

Figure 33. LIDAR image of 1984, Area deposits of the 1982 eruption in the Platanar and Magdalena River. Arrows point to the area in which the river terraces are located. **A.** Platanar River with distributed 1982 deposits. **B.** Magdalena with distributed 1982 deposits. From Smid (2015 unpub. BSc thesis).

Platanar river terraces

From the four river terraces sampled at the Platanar river only two consist of 1982 eruption products. From the 7.5 m terrace an age was derived (fig. 33A). Since for the other terraces no age could be obtained by carbon dating or LIDAR images, it must be inferred from other lines of evidence.

The 2 m terrace is the other terrace made up from 1982 volcanoclastic rocks. The 2 m terrace is on the edge of the depositional area of the 1982 eruption (fig. 33A). The terrace had similar textures as the 7.5 m terrace but is much thinner. The river valley is much wider in this part of the river, which means that the debris flows will spread out and create smaller terraces. The 3 m terrace is very close to the 2 m terrace but this terrace has a different appearance. The 2 m river terrace shows mainly debris flow deposits and small layers of fine sands which might be hyperconcentrated flow deposits, although this could not be concluded. The 3 m terrace is much different; oxidised, weathered and smaller pumice clasts. Further there is a tree on top of the 3 m terrace which is at least older than 50 years (interpretation from C.A.M. Nooren and W. Hoek), which means that it was not formed after the 1982 eruption. The tephra was in good condition and not weathered as was observed in the 15.8 m and 25.7 m terraces. It remains unclear to which eruption this terrace is linked. The 15.8 m and 25.7 m terrace are more distant from the river and no age constraint was found. It is most likely linked to an older eruption.

Magdalena river terraces

From three terraces on the Magdalena River two are reported from the work of Smid (2015, unpublished thesis) to be deposits from the 1982 eruption; The 5 m and 8.5 m river terrace (fig. 33B). Further the 5 m terrace is also reported by Macias et al. (2004) as hyperconcentrated and debris flow deposits from the dam breach shortly after the 1982 eruption. The 8.5 m is also part of these deposits. However, the textures of both terraces are different. While the 8.5 m is weathered, made up of debris flow deposits with clasts up to 20 cm. The 5 m terrace has fine grained, hyperconcentrated flow deposits, with inverse grading. However, the 8.5 m is abandoned by the river, while the 5 m lies close to the active river bed. The 8.5 was strongly affected by vegetation, improving the weathering rate. While the 5 m terrace erosion by the river terrace created fresh cut surfaces.

The other theory is that the 1982 brought an enormous amount of new material to the river valley that it flooded the older terraces with a layer of volcanoclastic deposits. After the event the river cuts into the valley again and removes most material. The result is that some of the 1982 volcanoclastics will be on top of older volcanic products. However, no evidence for this theory is found and it is more likely that both terraces were derived from the 1982 volcanic products and that incision by the river and abandonment by the river created to river terraces. Another explanation is that the two terraces are the result of two pulses of the 1982 eruption, creating these two terraces

The 12.9 m terrace is not part of the 1982 eruption deposits, but not dated. It must have formed after an older eruption. Perhaps the 550 BP eruption, however no evidence for this hypothesis. It is unclear what the age of this terrace is, but assumed by its location and terrace level that it originates from the 550 BP eruption.

In summary it is very difficult to link river terraces to eruptions without age constraints. Different river terraces can be formed from the same eruption, meaning that not every different terrace level

necessarily represents one different eruption. The 1982 eruption formed the 2 m and 7.5 m terraces on the Platanar River and the 5 m and 8.5 m terraces on the Magdalena River. More research is required to link the other terraces to El Chichón eruptions.

6.2 Uniform chemistry of river terraces

Individual eruptions can be distinguished by their characteristic chemical fingerprint. This can be a very powerful tool linking river terraces to eruptions or separate them from each other if no age constraint was found. However, El Chichón eruption products have a very similar chemical fingerprint (this work, Macias et al. 2003, Espíndola et al. 2000). To distinguish different events, mineral assemblages, amount of weathering, tephra condition become very important tools.

As already is shown in table 8, most sample pairs were linked and cannot be distinguished from one and another by chemistry. They are essentially the same. This includes both matrix and pumice samples. Evidence comes from the 7.5 m terrace, which contains samples S_{P1}-S_{P12}, S_{Pm41}-S_{Pm47} (table 8, 7). Figure 17 shows these samples and they cluster perfectly together except for samples S_{P3}, S_{P5}, S_{P6}. However, their totals were very high (102-104 wt.%, Appendix H2), which causes this difference. S_{P6} was based on one point, because other S_{P6} measurements had plagioclase contamination and couldn't be used. The uniformity of the 7.5 m terrace supports the event related river terraces hypothesis. Namely you would expect differences in chemistry if the terrace would consist of multiple eruptions or was contaminated by other rocks. Since the El Chichón is very uniform, closer attention was paid to the condition of the tephra and mineral assemblages. This was in consensus with the compositional uniformity of the glass shards.

If we then consider all the terraces; their composition is very uniform as well. Most of the samples fall into cluster 1, with few exceptions. Some tephra samples deviate either by contamination, low totals or few amounts of reliable measurements. This can be seen in figure 26 and in table 9. Clusters 1 and 2 are very uniform for almost all elements. The range of the clusters is less than 10% of their noted values (0.5 range for K_2O value of 6 wt.%). Only CaO and TiO_2 show a slightly larger range, between 2.1 and 1.3 wt.%, but expected as the error in the standards is larger.

This uniformity is present in both matrix and pumice. Most samples plot in cluster 1 with mainly the 2 m and some 7.5 m samples plotting in cluster 2.

What is expected is the fact that all the terraces show a very uniform chemical signature that confirms the current knowledge on the uniform fingerprint of El Chichón eruptions. They either fall in cluster 1 or 2. Only the glass shard chemical composition of the 12.9 m terrace is not known, for no pumice was sampled. The older river terrace did not contain any pumice, because they were altered and crumbled into matrix by weathering. The uniform tephra composition of samples from individual terraces suggests that they were formed during or after one eruption, but more information is required to separate different events.

The mineral assemblages of the river terraces are very similar (section 5). The plagioclase composition has a 0.5-0.6 An-Ab ratio with the largest variation in the 7.5 m terrace. The pyroxene and hornblende shows this as well. In several plagioclases zonation was found. The condition of the tephra was different for the older terraces. The 12.9 m, 15.8 m and 25.7 m all contained glass shards

with reaction rims, include weathering minerals or were entirely transformed into a new phase. Also pumice sizes were smaller in the older terraces.

6.3 Comparison between distal and proximal tephra

Tephra from river terraces is compared with the tephra from the slopes of El Chichón. Then the proximal tephra (river terraces) is compared with the distal tephra (swamp drill core Usumacinta-Grijalva delta plain). Figure 34 shows several compositional plots made from this tephra data. This proximal tephra is very uniform (section 5, 6.2). The chemical composition was separated into three clusters; cluster 1,2 and other points (or non-cluster points, fig. 26). The last group consist of points that not fall into either cluster either due to contamination, bad measurements or were derived from the lakes of Mexico (section 3.3.2 and 5.4.1).

As earlier mentioned, several authors researched glass shards in ash from El Chichón. Its products are characterised by a high potassium content, abundant plagioclase, amphibole, augite and minor amounts of magnetite, biotite, sphene and apatite (Espíndola et al. 2000). Also some orthoclase present as small minerals were reported (Huizinga, 2013, unpub. MSc thesis). El Chichón was quite active in the Holocene and the products erupted during different events show a homogeneous chemical composition (Macias et al. 2007, Acre et al. 2013). The chemical composition of the volcanics of El Chichón is similar to products from the Chiapanecan Volcanic Arc (CVA, Capaul, 1987). The magmas are of trachandesitic composition and Plinian eruptions with high plumes containing large amounts of ash and volatiles characterize the eruptive behaviour of this volcano. Crustal assimilation, partial melting of the mantle, fractional crystallization and magma mixing are the processes forming these magmas (Macias et al. 2007).

The data from Huizinga (2013, unpublished MSc thesis) are from glass shards derived from a peat core in the swamps of the Tabasco delta plains, where the Grijalva and Usumacinta river flow into the Gulf of Mexico. Twelve tephra layers from this core and one other tephra layer from the same area (pozpetr core, Nooren et al. 2009) were analysed. Three clusters were defined based on SiO_2 content, which varies from 69-80 wt.%. These clusters from Huizinga (2013, unpub. MSc thesis) are referred to as H_{C1}, H_{C2} and H_{C3}.

Comparing river terrace samples with H_{C1-3} shows that my data points correlate well with H_{C1} for almost all elements (fig. 34). Only K_2O and Na_2O show slight deviations. The Na_2O-SiO_2 plot shows a clear degassing trend, the Na_2O goes down as the SiO_2 goes up. Quite a lot of samples from Huizinga's database have low Na_2O values. The Na_2O is 0.5-2.5 wt.% lower. Also the K_2O trend is 0.5 wt.% lower than the river terrace samples.

Macias et al. (2003) analysed glass inclusions in pumice from sites within a radius of 10 km of the El Chichón 1982 crater. They sampled unit B (Espíndola et al., 2000) in several areas. Unit B represent the deposits from the 550 BP eruption, above this unit a paleosoil was reported indicating influence of vegetation. The glass shards fit with H_{C1}, cluster 1 and 2 for most elements, but Al_2O_3 is higher (~0.5 wt.%), Na_2O is lower (~ 0.5-2.5 wt.%) and K_2O is lower (1 wt.%). The Al_2O_3 probably is higher because of plagioclase microliths in the pumice glass enhancing the Al_2O_3 and CaO slightly. The Na_2O trend is the same as observed in the data from Huizinga (2013, unpub. MSc thesis). However, the low K_2O value, which is more than 1 wt.% lower than cluster 1 and 2, cannot be explained by plagioclase contamination.

Palais et al. (1992) analysed tephra layers found in ice cores from Greenland and the South pole and based on the chemical composition and age found indicate that these glass shards are from the 550 BP eruption. Their chemical composition is quite similar to the composition of Macias et al. (2003) and cluster 1 and 2, except for a lower Al_2O_3 weight percentage (15.5 wt.%). Further CaO is higher by almost 0.5 wt.% and FeO slightly higher, this is probably due to some plagioclase contamination in their analysed samples.

Luhr et al. (1984) analysed pumice clasts from the 1982 eruption, two glass shards were analysed. The first analysis falls perfect in cluster 1 and the other point is similar to the measurements of Macias et al. (2003). Al_2O_3 content is similar to the measurements of Macias et al. (2003), Na_2O is 1.5 wt.% lower than cluster 1 and K_2O is lower by 1 wt.%.

Casadevall et al. (1984) studied the change in chemical composition of sediments from the lake inside the El Chichón crater, they found that the glass shards were enriched in CaO, MgO, FeO and TiO_2 and depleted in K_2O. One glass shard is measured (fig. 34).

The tephra from the drill core of Nooren et al. (2009) all fit with cluster 3 of Huizinga (2013, unpub. MSc thesis). The source of this cluster is yet to be discovered, the current idea is that it is from an older event of El Chichón or from a Los Chocoyos eruption (Huizinga 2013, unpub. MSC thesis, Nooren et al. 2009).

The plagioclase composition in glass shards and pumice shows similar values as plagioclase from the distal drill core in the Tabasco delta plain. Further the zonation of plagioclase is reported by several authors (Espíndola et al. 2000, Macías et al. 2003, Andrew et al. 2008, Huizinga, 2013 unpub. MSc thesis, this work), which was also observed in S_{m14} (fig. 28). The Diopside composition of Pyroxenes are similar to the enclosed phenocrysts reported by Luhr et al. (1984), Cochemé et al. (1982) and Huizinga, (2013 unpub. MSc thesis). Only the Amphibole group derived in this thesis is different than Huizinga, (2013 unpub. MSc thesis). Using the nomenclature reported in Leake et al. (1997), Huizinga reported hornblendes with low potassium and sodium values, however in this thesis most hornblendes had Na+K values larger than 0.5. Further the terrace samples contain more Mg relatively to Fe compared to the minerals from the distal part.

In conclusion all the data suggest that the tephra from the Magdalena and Platanar River originate from El Chichón (fig. 34). The uniformity of terrace samples all overlap with the samples of El Chichón from other data sources (Macias et al. 2003, Palais et al. 2003, Luhr et al. 1984, Casadevall et al. 1984 Cochemé et al. 1983). Cluster 1 and 2 fit well with H_{C1}, but H_{C2} has higher SiO_2 values. The other elements show a strong correspondence with data from the slopes of El Chichón, except for K_2O and Na_2O. The Al_2O_3 content is not much different (1 wt.% for Macias et al. 2003), which is probably due to the influence of plagioclase. There appears to be much Na_2O loss in the tephra data of $H_{C1\text{-}3}$ (Huizinga, 2013 unpub. MSc thesis), which enhances the SiO_2 content. The second argument is that mineral assemblages are very similar. Only the river terrace tephra contains more Na and K rich minerals. As discussed in section 5.5 the pumice contains similar plagioclase, amphibole, pyroxene with minor apatite, magnetite and sphene minerals as the swamp core tephra and the tephra from the slopes of El Chichón (Huizinga, 2013 unpub. MSc thesis).

Since there are no indications that the glass shards are from another source than El Chichón, as well as evidence supporting event related river terraces (section 6.1). The conclusion is that the tephra

from the river terraces originate from El Chichón. Further from the distal tephra only H_{C1} fits well with the tephra from El Chichón. H_{C2} has similar values as cluster 2, but deviates for SiO_2, K_2O and Na_2O. This difference is explained in section 6.6.

However, the high SiO_2 cluster (H_{C3}) does not fit with any of the analysed tephra data. It has different SiO_2, Al_2O_3, MgO, FeO^t and K_2O values. Also the tephra from another drill core in the Usumacinta-Grijalva delta plain plots in the area of H_{C3} (Nooren et al. 2009). The origin of this tephra is discussed later. In the next section the K_2O difference is discussed with possible explanations.

6.4 K_2O trend

On basis of geomorphological evidence found in the field (appendix A) and the chemical composition of tephra it is concluded that tephra is from El Chichón. The samples of the 1982 and 550 BP described here correlate well with each other for almost all elements. However, in the K_2O plot there is a clear difference between samples from this thesis (mainly 1982 eruption), Huizinga (2013, unpub. MSc thesis, 1982 and older eruptions) and Macias et al. (2003, 550 BP eruption). Figure 35 highlights the K_2O and Na_2O differences.

The samples from Huizinga (2013, unpub. MSc thesis) are lower in K_2O (0.6 wt.%), lower in Na_2O (0.5-2 wt.%), higher in SiO_2 (~2%) and P_2O_5 might be lower although the deviation falls within the error range. Samples from PP1 core were collected in the swamps in the Usumacinta-Grijalva delta, about 25 km from the Gulf of Mexico coast. Tephra consist of a network with bubbles, wholes and phenocrysts of plagioclase, Mg-hornblende, clinopyroxene, apatite and magnetite. This tephra is reported as fall out, juvenile tephra that had travelled through air and deposited into the swamp. The date of these layers is known from C^{14} dating of the layers and all but one could be linked to the units described in Espíndola et al. (2000). Samples 1-5, 7 and some data points of samples 10, 11 and 12 fall into cluster 1 from this thesis (H_{C1}, Huizinga 2013, unpub. MSc thesis).

The samples from Macias et al (2003) show a wider range of chemistry variety for pretty much every element, K_2O is lower (~1.5 wt.%), Na_2O is lower (0.5-2.5 wt.%) and Al_2O_3 is higher (~1 wt.%). Samples from unit B (Espíndola et al. 2000) were collected from 119 sections within proximity of El Chichón (~15 km). Much of the sampling sites lie close to the river and the glass analysed came from the lower, middle and upper part of unit B tephra layer.

Since all data originate from El Chichón the K_2O difference has to be explained. What causes the 10-30% (6, 5.5, 4.7 wt.%) difference in K_2O between the samples of this work, Macias et al. (2003) and Huizinga (2013, unpub. MSc thesis)? How come there is a difference between the 1982 pumice found in the river terraces of the Magdalena and Platanar rivers and the volcanic glass in the peat core near the coast? Why is there a difference between the 1982 and 550 BP samples? Several explanations were proposed.

6.4.1 Compositional difference between microprobes

The first explanation is that the difference is caused by alkali migration under beam irradiation of the microprobe. Fluctuations in beam current resulting in bad measurements that affect the Na_2O and K_2O content. Further rough surface areas affect totals of the samples. Contamination by microliths can affect the chemical composition of the measurements.

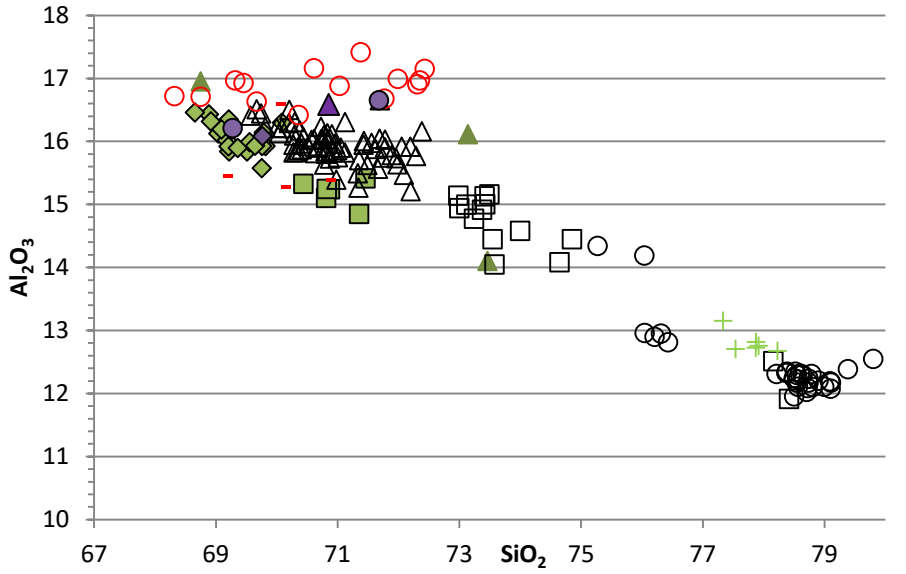
18
17
16
15
14
13
12
11
10
Al_2O_3
67
69
71
73
SiO_2
75
77
79

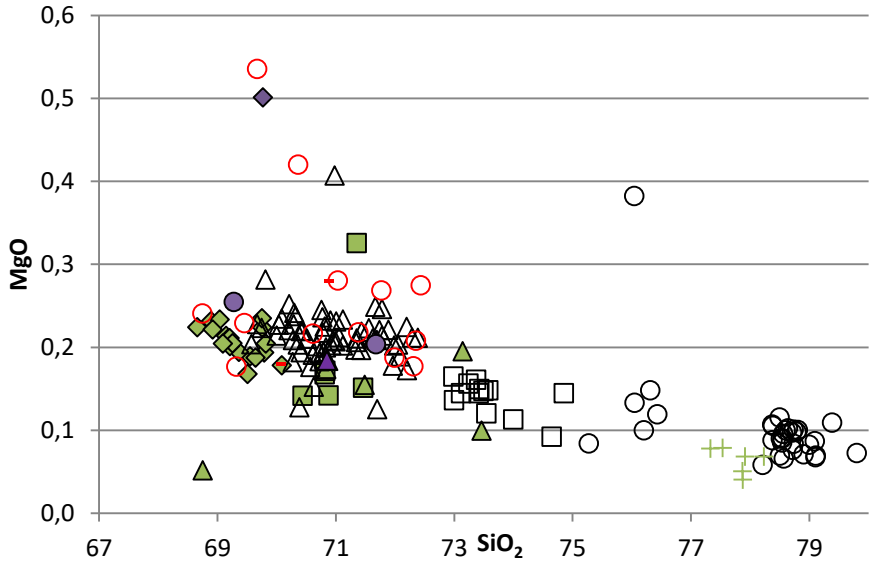
0,6
0,5
0,4
0,3
0,2
0,1
0,0
MgO
67
69
71
73
SiO_2
75
77
79

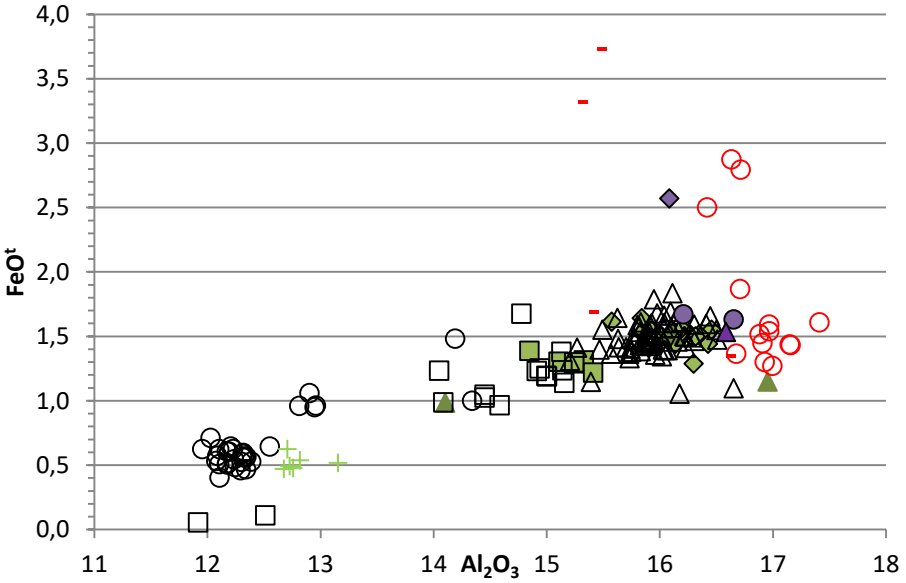
4,0
3,5
3,0
2,5
2,0
1,5
1,0
0,5
0,0
FeO^t
11
12
13
14
Al_2O_3
15
16
17
18

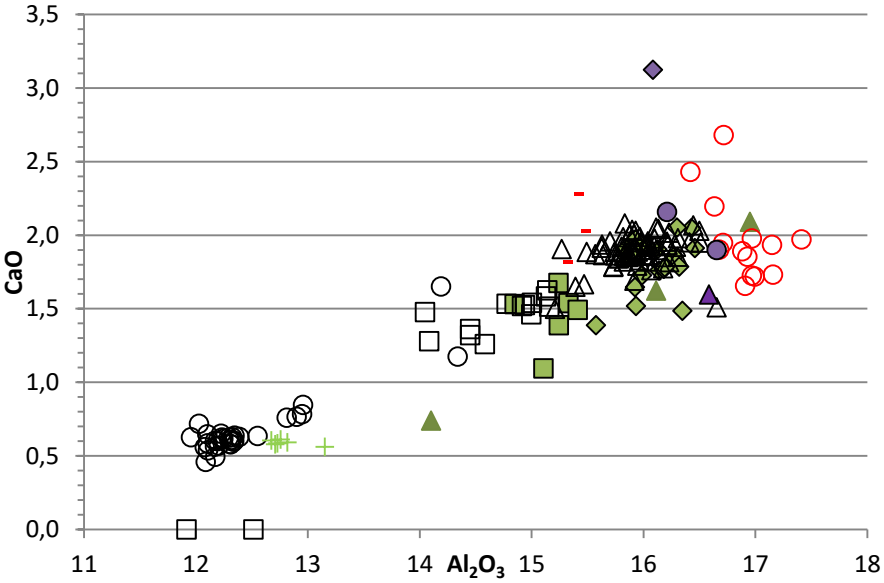
3,5
3,0
2,5
2,0
1,5
1,0
0,5
0,0
CaO
11
12
13
14
Al_2O_3
15
16
17
18

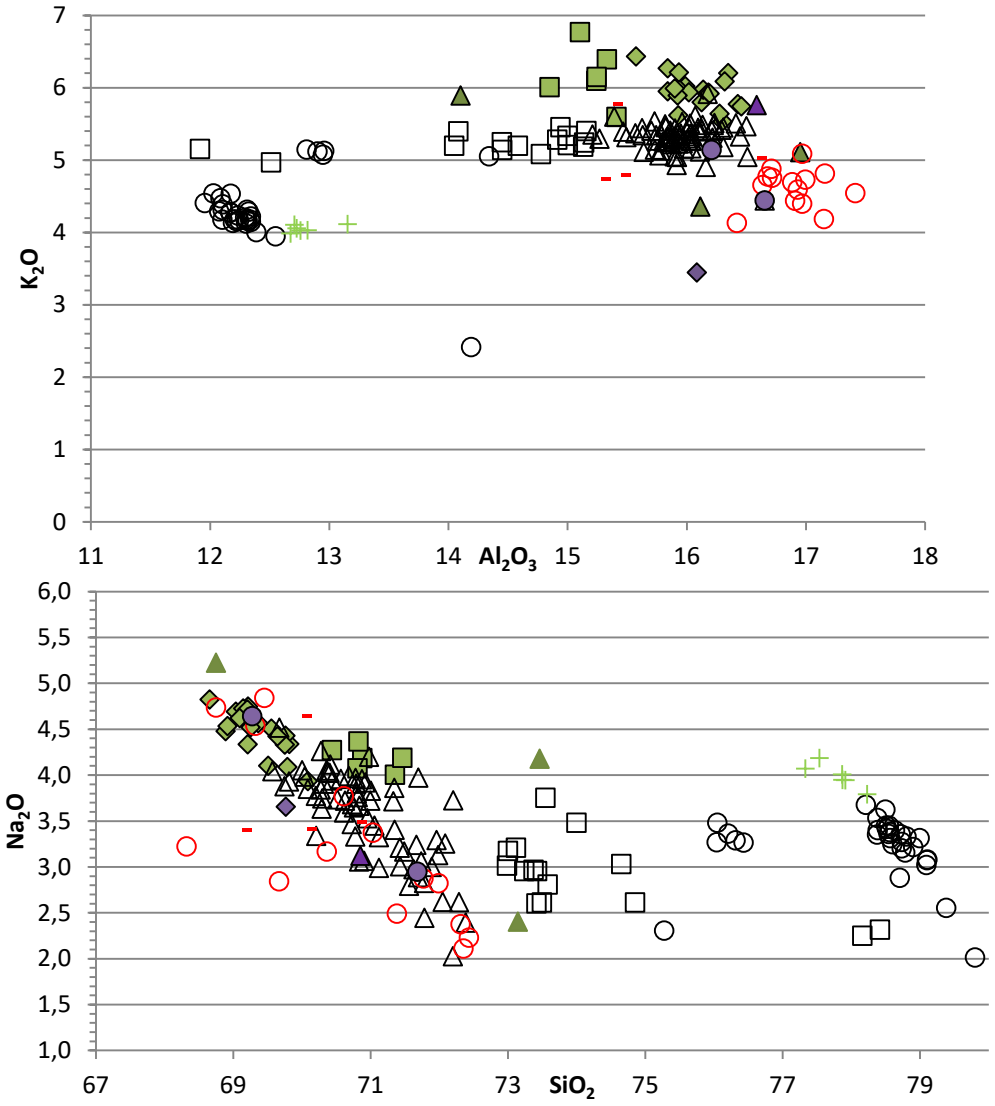

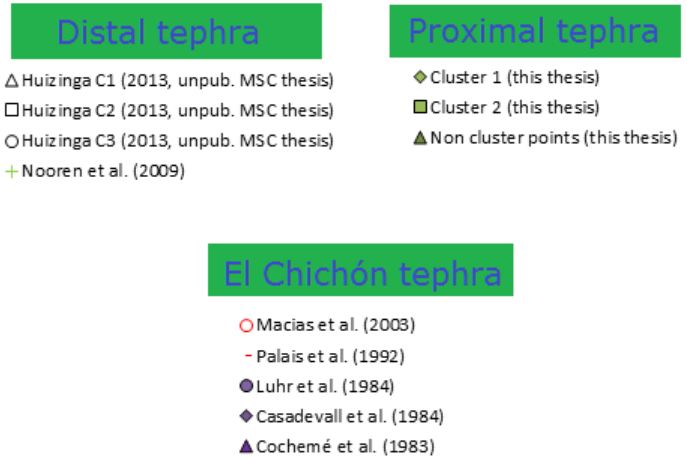

Figure 34. Compositional plots of proximal, distal glass shards and glass shards from the slopes of El Chichón (Cluster 1, 2 and non-cluster points, $H_{C1\text{-}3}$). SiO_2, Al_2O_3, K_2O, FeO^t, CaO, MgO, Na_2O are plotted against each other.

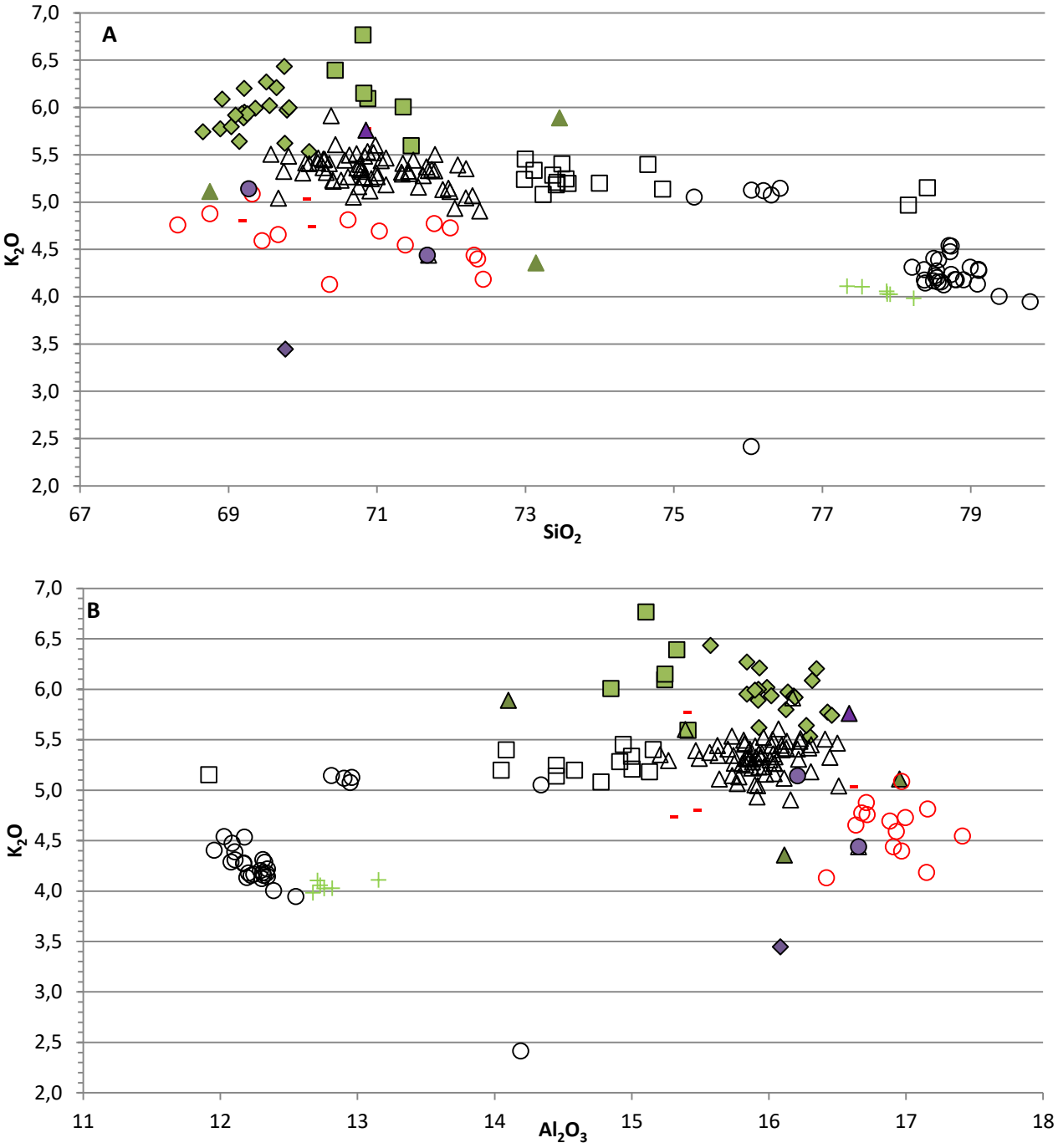

Figure 35. K_2O-SiO_2 and Al_2O_3 plot showing only the El Chichón data. Clear difference can be seen in the potassium. C_1-H_{C1} difference is 0.6 wt.% on average, C_1-550BP difference is 1.5 wt.% on average.

Plagioclase contamination for example increases the Al_2O_3 and CaO relatively to other elements. Lastly large deviation in standards can affect your data. Careful attention was paid to the elements that are first affected by these processes. Most factors were eliminated as good as possible. As mentioned earlier SiO_2, K_2O and Na_2O are the elements with the largest difference.

In order to validate these earlier mentioned factors, the performance of the two instruments was compared. Namely the SiO_2, Na_2O and K_2O difference could be the result of measuring with different instruments. Although this shouldn't occur and all precautions were taken to produce reproducible results that are instrument independent it cannot be entirely eliminated. Therefor one sample analysed in Huizinga (unpub. MSc thesis, 2013) was reanalysed by the microprobe used in this work. Normally it should give the same geochemical tephra composition for both instruments within the error of the standards.

I measured sample 193. This is a piece of pumice found in PP1 drill core in the beach ridge of the Usumacinta-Grijalva delta plain (Huizinga, 2013, unpub. MSc thesis). This pumice was already measured by Huizinga with a different microprobe and I measured it again to find if there are any differences present between the two instruments. The sample was both times carbon coated and the conditions were the same. Further the sample consists of one large glass piece and the measured points were close to each other. Special attention was paid to the point selection, because any earlier measured spot results in low sodium concentrations, these are seen as holes already created during the EPMA session of Huizinga et al. (unpub. MSc thesis, 2013).

Further one additional sample was compared. S53 was found in Cantemual lake (section 3.3.2, fig. 5). This is a small lake close to the coast and where PP1 core was drilled. The pumice was found in a small tephra horizon and dated on 550BP by an age-depth model (Smits, 2015 unpub. MSc thesis). The same tephra was also found in the PP1 core in the Usumacinta-Grijalva delta as part of H_{C1}. S53 is compared to the average of the measured 550BP tephra samples from Huizinga (2013, unpub. MSc thesis).

Lastly one standard was compared. Standard VG-568, a rhyolite glass was compared to evaluate the performance of the instruments. For this work Jeol JXA 8530F and Jeol JXA 8600 was used to measure the tephra from the PP1 core (Huizinga, 2013, unpub. MSc thesis).

The results show a clear difference in geochemical composition (fig. 36, table 12). The two instruments give a different result for sample 193. The SiO_2 content is 2 wt.% higher for the Jeol JXA 8600, while most other elements have lower values.

Most elements are within the range given by the standards. However, some elements show differences; the Al_2O_3 content is 0.5 wt.% higher, Na_2O 0.6-1 wt.% higher, K_2O 0.4 wt.% higher and CaO 0.1 wt.% higher for the Jeol 8530F. Thus the instrument used to measure distal tephra from the PP1 core, gives higher SiO_2 values and lower values for Al_2O_3, Na_2O, K_2O and CaO.

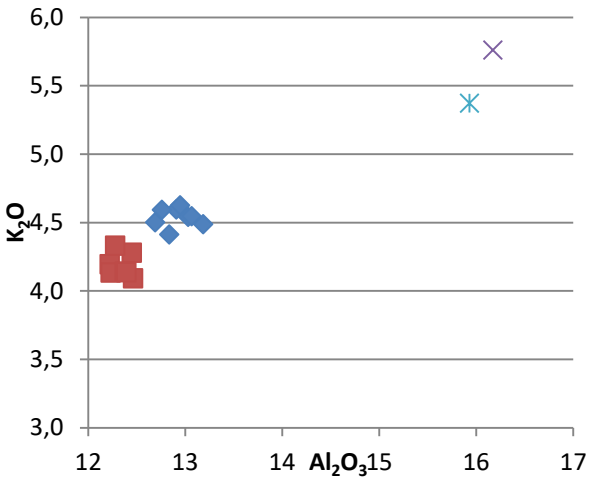
6,0
5,5
5,0
4,5
4,0
3,5
3,0
K2O
12
13
14
Al2O3
15
16
17

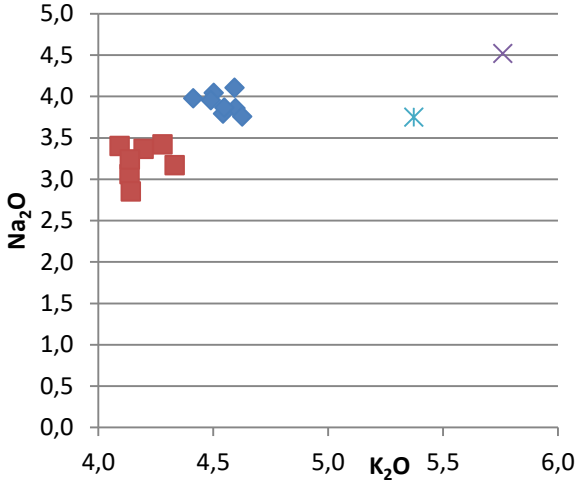
5,0
4,5
4,0
3,5
3,0
2,5
2,0
1,5
1,0
0,5
0,0
Na2O
4,0
4,5
5,0
K2O
5,5
6,0

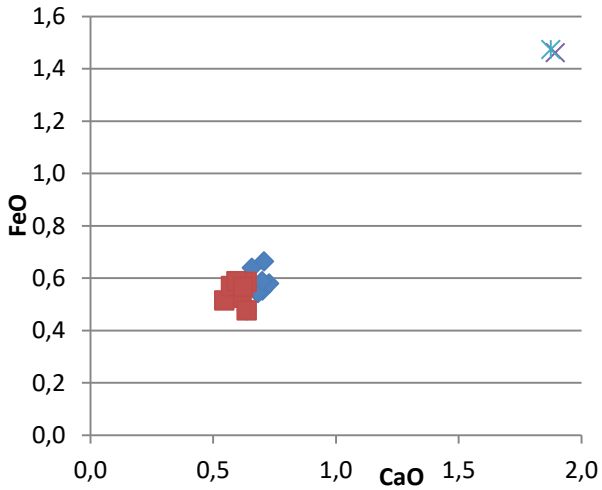
1,6
1,4
1,2
1,0
0,8
0,6
0,4
0,2
0,0
FeO
0,0
0,5
1,0
CaO
1,5
2,0

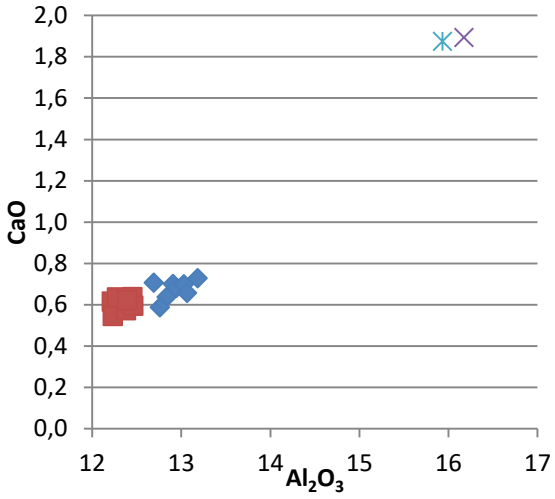
2,0
1,8
1,6
1,4
1,2
1,0
0,8
0,6
0,4
0,2
0,0
CaO
12
13
14
Al2O3
15
16
17

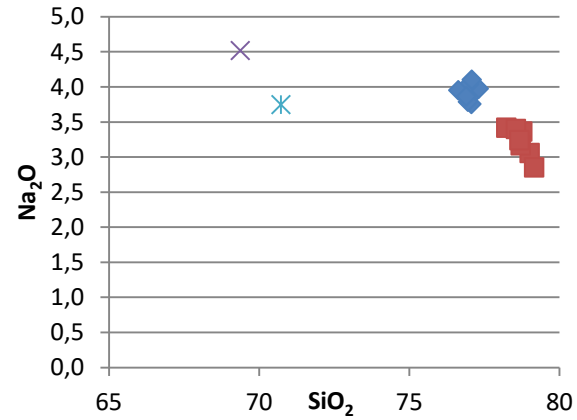
5,0
4,5
4,0
3,5
3,0
2,5
2,0
1,5
1,0
0,5
0,0
Na2O
65
70
SiO2
75
80

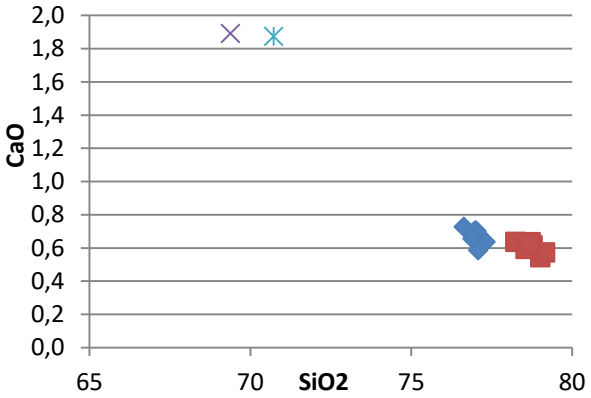
2,0
1,8
1,6
1,4
1,2
1,0
0,8
0,6
0,4
0,2
0,0
CaO
65
70
SiO2
75
80

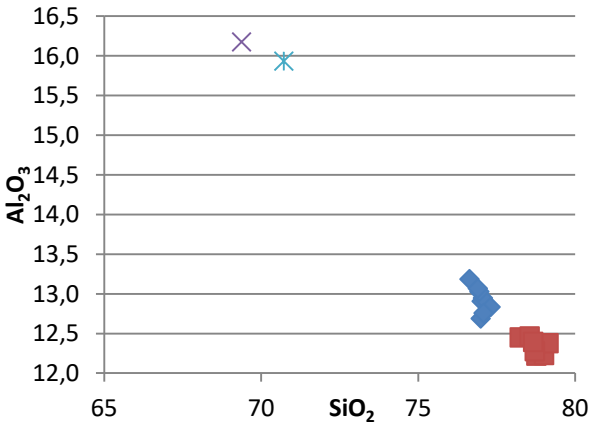
16,5
16,0
15,5
15,0
14,5
14,0
13,5
13,0
12,5
12,0
Al2O3
65
70
SiO2
75
80

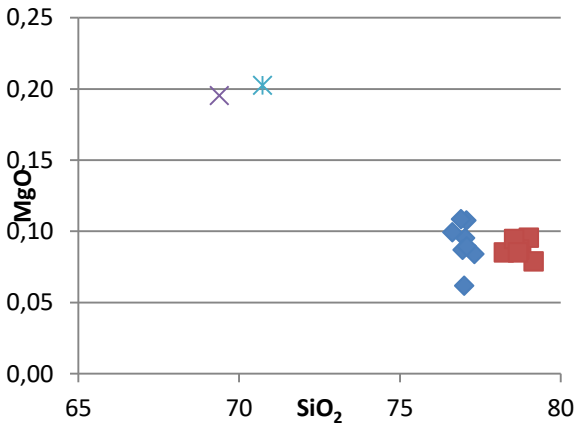
0,25
0,20
0,15
0,10
0,05
0,00
MgO
65
70
SiO2
75
80

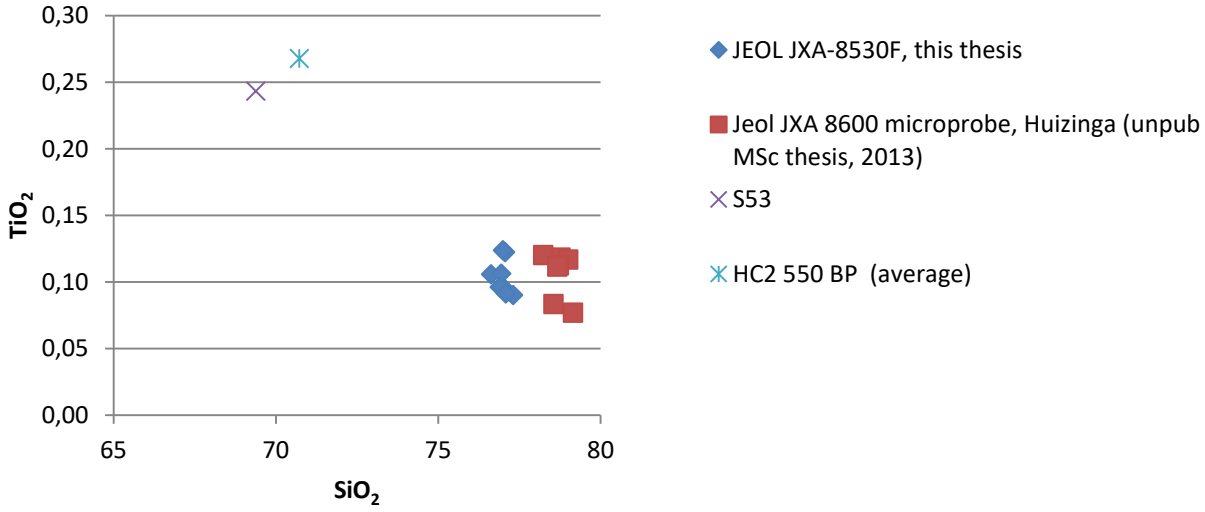

Figure 36. Comparison result of sample 193 measured by two different EPMA instruments on different dates. Blue stars: results of this thesis, red squares: results of Huizinga et al. (unpub. MSc thesis, 2013) thesis.

In the standards the same trend is see; the SiO_2 content is 2 wt.% higher for samples measured by the Jeol JXA 8600 (Appendix M). In addition, K_2O values shows higher values than the reported value. The Jeol JXA 8600 K_2O weight percentage is 5.04 wt.% and the Jeol JXA 8530F K_2O weight percentage is 5.25 wt.%, while the reported value is 4.89 wt.%. The difference between both instruments is 0.2 wt.%, which means that the standard deviation for samples used in this work will be larger than for samples from the PP1 drill core.

S53 and 550BP tephra show the same trend. Distal tephra from PP1 have higher SiO_2 weight percentages, while Al_2O3, K_2O and Na_2O have lower weight percentages than S53.

In conclusion, as mentioned in section 6.4 there is a compositional difference between distal and proximal tephra (C_1 – H_{C1}). By comparing the results of both instruments, the compositional difference between C_1 and H_{C1} can be explained by the EPMA performance difference. Since the SiO_2 content of sample 193 measured by two different instruments shows a difference of 2 wt.%, Na_2O a difference of 0.6-1 wt.% and K_2O a difference 0.4 wt.%.

It must be added that the K_2O difference between C_1 and H_{C1} is 0.6 wt.% while the results only explain a difference of 0.4%. However, from the standards (appendix M) there is a 0.2 wt.% difference reported, which explains this.

Now that the compositional difference is explained the distal and proximal clusters can be linked. Namely C_1 and H_{C1} are essentially the same. C_1 is mainly tephra from the 1982 eruption and H_{C1} also is (Huizinga, 2013 unpub. MSc thesis). For C_2 and H_{C2} this also can be concluded. However, H_{C2} consists of samples from the 1500BP eruption. C_2 samples come from various terrace with 1982 eruption products and older terraces of which the age was not derived. There are two explanations for this: one that the river terraces contain samples from older eruptions. This is not likely since multiple lines of evidence were used to find derive their age (section 6.1). The second is that these samples are part of H_{C1}. Since C_1 consist of S_{P3}, S_{P5}, S_{M17}, S_{P26}, S_{P27}, S_{P32} and S_{Pm38}, which are from the 7.5 m, 5 m 2 m and 25.7 m terraces (fig. 26, table 7). The 7.5 m, 5 m and 2 m terraces were related to the 1982 eruption and probable fall into H_{C1}. S_{Pm38} from the 25.7 m terrace, which is from an older

eruption of El Chichón most likely can be part of H_{C2}. Its composition is much different than C_1. More research is necessary to conclude this.

While the compositional difference caused by measuring with different instruments can explain the difference between C_1-H_{C1}, the difference between C_1 and the 550BP samples from Macias et al. (2003) cannot be explained this way. The K_2O and Na_2O wt.% difference is too large for this. Therefor other explanations are proposed.

Table 12. Summary of the data showing average composition measured, percentage difference and the accuracy standards of both days.

Elements	Weight percentages (averages, %)		Percentage difference	Standards Accuracy (%)	
	Jeol JXA 8600 (Huizinga et al. 2012)	Jeol JXA 8530F (this thesis)		Jeol JXA 8600 (Huizinga et al. 2012)	Jeol JXA 8530F (this thesis)
SiO_2	78.73	76.99	-2.25	0.7	0.53-0.7
Al_2O_3	12.34	12.93	4.51	-1.66	-0.73
K_2O	4.19	4.54	7.73	2.42	7.32
Na_2O	3.22	3.92	17.94	-6.93	-4.59
FeO	0.55	0.57	4.53	-6.58	-3.87
CaO	0.60	0.68	10.59	-14.91	-10.74

6.4.2 Leaching of potassium and sodium

One explanation is that the chemical composition of the magma of different events wasn't uniform. This could give rise to the fluctuations in K_2O and Na_2O. Magma's could be enriched in K_2O by supercritical fluids moving from deeper magmas which increases K_2O content (Ferlito and Lanzafame, 2010). Although this would explain the K_2O difference between the samples from 550 BP and 1982, this cannot explain the difference if the samples are from one event. Further the Holocene eruptive history volcanic products of El Chichón were very homogeneous (Macias et al. 2007, Acre et al. 2013). Making it very unlikely that the chemical composition of the magma changed in time. It is more likely that processes like alteration and weathering affect the tephra chemistry or crystal fractionation.

Weathering and alteration are very important processes changing the chemical composition of pumice rocks, glass shards and other volcanic products. They depend on soil environment, climate which are affected by ph., temperature, soil conditions, presence of water, grain size of the material, chemical composition of the glass, reaction time and age of the material (La Fuente et al. 2002, Yamado and Shoji, 1982). Further potassium, caesium, rubidium and strontium are very mobile during weathering (Chauvel et al., 2005), so they are most likely to leach from the rock. While other components are less mobile Na and K are the first compounds that leach from volcanic glass (Shipley and Sarna-Wojoicki, 1982, Cerling et al., 1985; Stefansson & Gislason, 2001; Gislason, 2008). The depletion of Na_2O may result from its preferential removal from the volcanic glass-alteration product system to the surrounding pore water.

Weathering will also show on the images of the glass shards, the tephra will not have a clear texture, have erosion rims or contain cracks. The glass shards in the matrix and pumice clasts from the river terraces did not show any signs of alteration. Their surface was in good condition (Appendix F1-5). The glass shards from the peat core show some signs of alteration (Huizinga 2013, unpublished MSc

thesis). Also these glass shards are more distal deposited. The swamp settings are much more humid, vegetated and weathering sensitive than the river terraces at the time of deposition. Tephra layers in the drill cores are very thin while very thick in the river terraces. So weathering and leaching influences the small tephra layers more than the thick volcanoclastic river terrace deposits.

Much research has been done on the alteration of tephra material by leaching and weathering. Yamado and Shoji (1982) showed that the soil environment affects the chemistry of volcanic glass. They found two types of glass alterations; one where alteration leads to a gain in potassium and loss in sodium, which is explained by an ion exchange reaction between Na and K. The other alteration processes there is a large gain of Ca and loss of K. This is explained by change in glass structure. They observed a relationship between the glass alteration mechanism, glass chemistry and soil environment.

Though most articles mentioned describe alteration processes of tephra, none of them give an explanation of only K_2O and Na_2O decreasing while other elements remain constant. Cerling et al. (1985) give this explanation. They describe low temperature alteration of volcanic glass by meteoric water where ion exchange and hydration play an important role. They found that up to 40% of the Na and K could be replaced by H ions without any measurable changes in the bulk composition of the glass. The fluid interacts with the glass and exchanges potassium and sodium ions by hydrogen ions. The potassium and sodium are then dissolved in the water and removed from the glass. Central America is a very tropical and wet climate, with a lot of rain and humid conditions, optimal for weathering. Further the amount of annual rainfall enhances the effect of leaching. Tephra is easily affected by meteoric water. This is a very suitable explanation for the K_2O difference in the tephra from El Chichón. The only problem with this explanation is that the samples used in Cerling et al. (1985) are very old (Pleistocene), meaning that the alteration process acted for quite some time. The glass shards of this work are from recent time, meaning only a short amount of time for alteration. Further there is not much known on the rate of alteration of glass shards. Wolff-Boenisch et al. (2004) did experiments where they estimated the dissolution rates of natural glass at low temperature and various ph. They found that increasing temperature increased the dissolution, which is dependent on kinetics and lower pH increase the dissolution. Their results indicate that a 1 mm rhyolite dissolved in ~4500 yr. Also Jakobsson and Moore (1986) investigated alteration rates on Iceland and found that alteration of basaltic tuff is very temperature dependant. They looked at hydrothermal alteration results from a timespan of 12 years. They took a core in the Surtsey volcanic area of 181 m deep and found that the alteration process doubles every 12 °C. At 60 °C less than 40% of the glass is altered and more than 90% is altered at a temperature of 100 °C. Stefansson and Gislason (2001) suggested that K and Mg fluxes by weathering of basalts are influenced by vegetation. Increasing vegetation increases the leaching of K and Mg.

Since the condition in the swamp are more optimal for alteration than in the river terrace; the presence of water, vegetation and warm climate, heavy rainfall all enhance the rate of the alteration process. Since the MgO concentrations measured are very low, not much of the magnesium will be removed relatively. The glass shards from 550 BP had a paleosoil on top of the tephra indicating influence of vegetation along with the fact that the alteration time is much longer, gives the low potassium and sodium content.

In conclusion the difference in K_2O and Na_2O of the tephra from the river terraces (C_1 and C_2), and Macias et al. (2003) might be due to weathering and leaching. The samples from Huizinga (2013, unpub. MSc thesis) lost relatively ~10% of its original K_2O and ~20-50% of its Na_2O content. The conditions in the peat core are more optimal for alteration than conditions in the river terraces. Further the 550 BP glass shards are much older so the alteration process acted on a much longer time scale. This is why 550 BP samples are more altered than 1982 samples. More research is needed to prove this. The assumption is made that all the condition was relatively more optimal for alteration in the swamp area than in the river terraces. The 550 BP tephra simply had more time to weather and this explains why there even lower in K_2O and Na_2O.

6.4.3 Crystal fractionation

What also could explain the difference between the distal (C_1-C_2) and proximal tephras (H_{C1-3}) and potentially explains the difference between cluster 1, 2 and the 550 BP tephras is crystal fractionation. An effort was made to relate H_{C3} to El Chichón through crystal fractionation.

6.5 Origin of H_{C3}

So far H_{C1} and H_{C2} are linked to tephra cluster 1 and 2 from the river terraces. The origin of H_{C3} could not be correlated to cluster 1, 2 and tephra data of El Chichón. Cluster 1 and 2 are both volcanic products of El Chichón and four river terraces contain tephra from the 1982 eruption. Tephra from the 12.9 m, 15.8 m and 25.7 m terraces are from older eruptions. No tephra of H_{C3} chemistry was found in the river terraces. Further most tephra from the river terraces was well preserved without any signs of weathering, except for the 12.9 m, 15.8 m and 25.7 m terraces showed weathering rims and signs of alteration. The glass shards in the H_{C3} were weathered and of less condition (Huizinga, 2013 unpub. MSc thesis) and contained no minerals. It might be possible that H_{C3} is the products of an older eruption from el Chichón, but no evidence was found for this in the older river terraces. Also no age constraint was derived for the older river terraces and so it could be that they formed from relative young eruptions (550 BP-1500BP) and that the H_{C3} is much older.

Tephra from the river terraces and the slopes of El Chichón do not show any chemical composition that resembles H_{C3}. El Chichón is known for its uniform composition of its eruption products (Espíndola et al. 2000, Macías et al. 2003, Layer et al. 2009, Acre et al. 2013), making it very unlikely that this high SiO_2 cluster found in the Usumacinta-Grijalva delta plain originates from El Chichón. Further this cluster was found throughout the drill core, not only in the lower parts, but also in the upper parts and the beach ridges were full of H_{C3} tephra. The fact that it was found at several drill depths and in the beach ridges in large amounts indicates that it must be from a huge event (Huizinga, 2013 unpub. MSc thesis). The H_{C3} was reported as accidental glass shards, that were reworked by transport and weathering processes. It is most likely that H_{C3} is not from El Chichón and originates from another rhyolitic volcano.

In order to find the source volcano, the volcanic regions of Central America tephra data are compared with H_{C3} to find the source volcanoes. Namely the H_{C3} showed in some resemblance to the TMVB tephra (Huizinga, 2013 unpub. MSc thesis). The hypothesis is that this H_{C3} might be from a large eruption of another volcano in the neighbourhood and its tephra was deposited in the drainage area of the Usumacinta-Grijalva delta plain. It was then transported to the delta plain and deposited in the swamps and beach ridges (Huizinga, 2013 unpub. MSc thesis). Finally, the source volcano

proposed in Huizinga (2013, unpub. MSc thesis); Los Chocoyos eruption from the Atitlán volcano in Guatemala is investigated in more detail.

6.5.1 Central American volcanoes

The Trans Mexican Volcanic Belt (TMVB), Tuxtlas Volcanic Field (TVF), Chiapanecan Volcanic Arc (CVA) and Central American Volcanic Arc (CAVA) are the volcanic regions of Central America (fig. 37). Not for all volcanoes tephra data is reported. Only the volcanoes with large rhyolitic eruptions or in the proximity of the Tabasco region were investigated. Their chemical compositions were compared with H_{C3} tephra in order to find its source. The magmas from these volcanoes vary from andesitic (Tacaná), andesite-dacitic (TMVB) to trachandesitic (El Chichón) with rhyolitic tephra or ash. Different magmatic processes like melting of the mantle, magma mixing, crustal assimilation and fractional crystallization have played a role in creating their compositions (Macias, 2007).

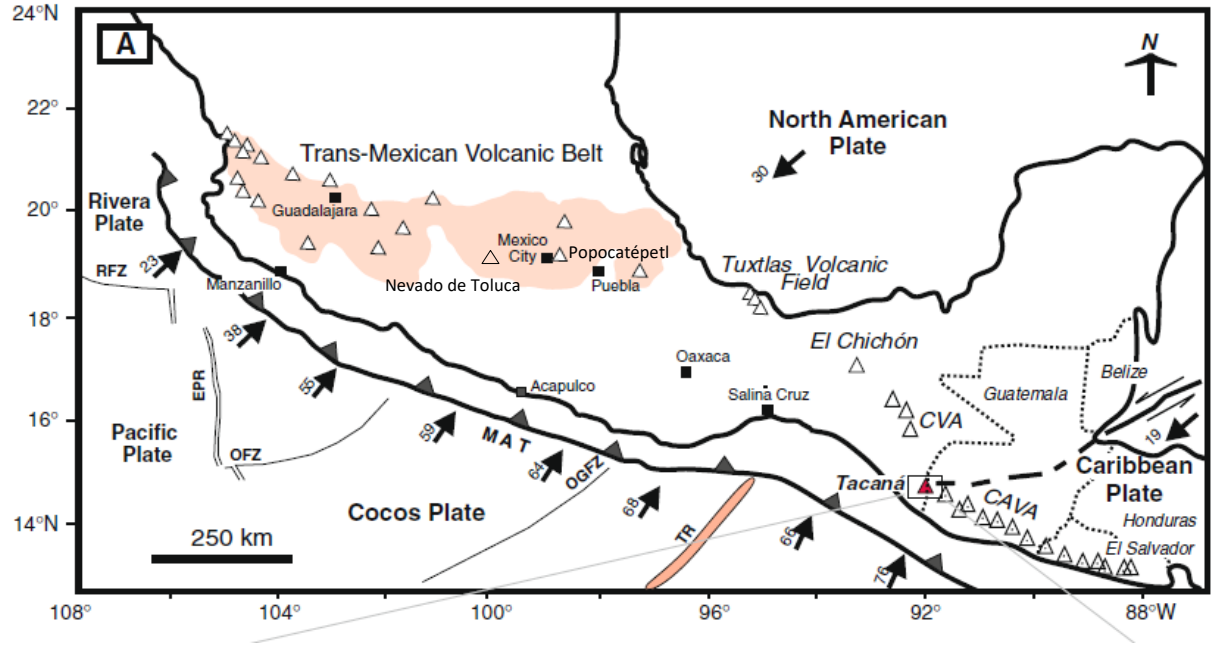

Figure 37. Major volcanic systems in Central America. From Macias et al. (2010).

6.5.2 Chiapanecan Volcanic Arc

El Chichón is not the only volcano in the CVA, Mora et al. (2007) summarises 10 volcanic structures that are part of the CVA, these are Navenchauc, Apas, Tzontehuitz, Huitepec, Amahuitz, La Iglesia, Mispia, La Lanza, Venustiano, Carranza and Santoton. The last seven are volcanic domes. The mineral composition of the CVA samples is plagioclase>amphibole>clinopyroxene>orthopyroxene>Fe-Ti oxides. Only whole rock was analysed and they belong to the calc-alkaline series with high potassium content. No glass data of any of these volcanoes is reported. Further not much is known from these volcanoes.

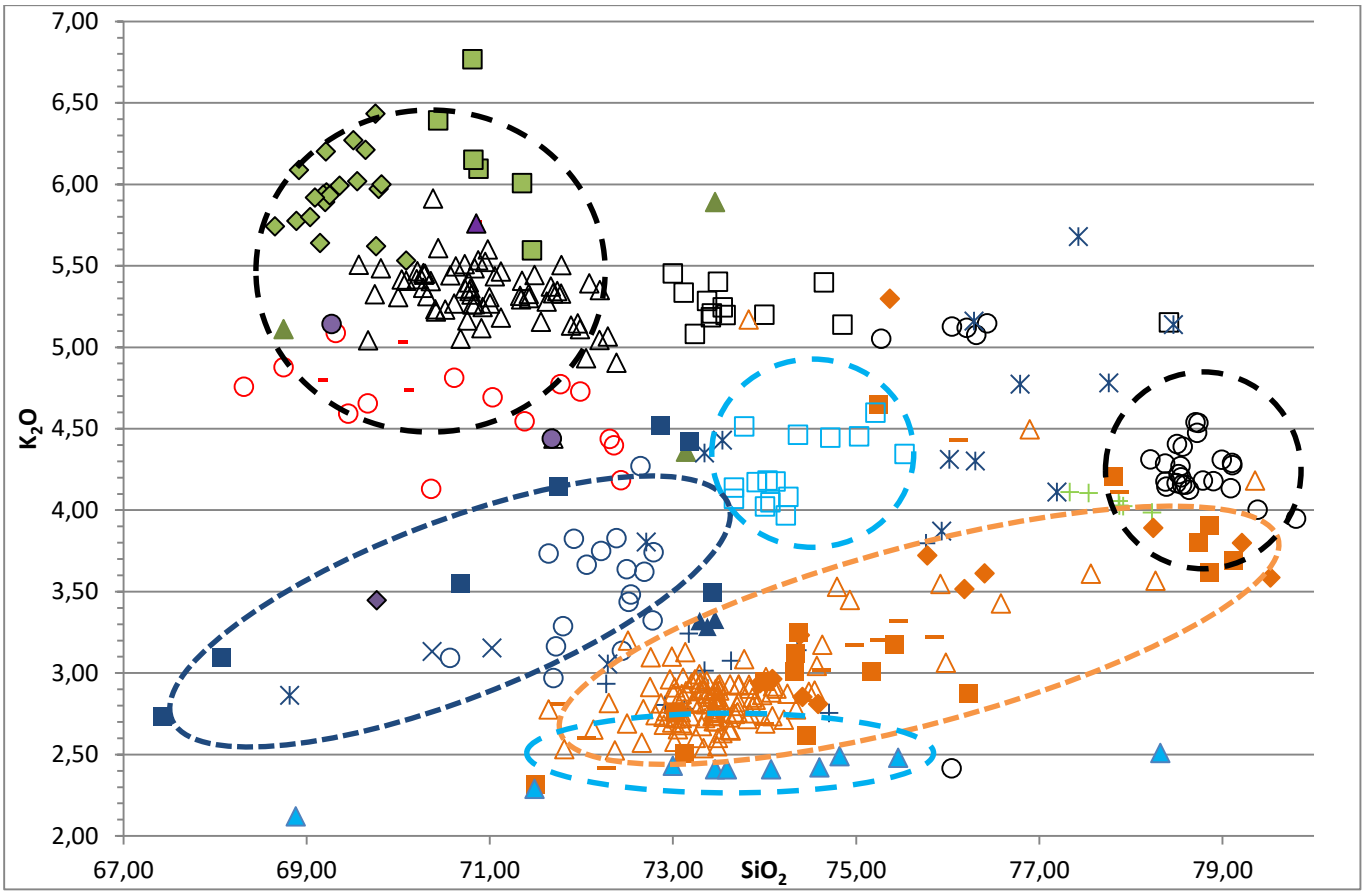

Figure 38. Harker diagram of SiO_2 against K_2O showing the major Central American volcanic belts. **Big black circle**: El Chichón, **small black circle**: cluster 3 PP1 core (Huizinga 2013, unpublished MSC thesis), **big dark blue oval**: Tephra I from TMVB (Ortega-Guerrero and Newton, 1998), **small blue circle:** San Martin tephra from Basin of Mexico (Ortega-Guerrero and Newton, 1998), **light blue circle**: Tacaná tephra (Acre et al., 2012), **light blue oval**: Santa Maria tephra (Andrew et al., 2014), **big orange oval**: TMVB tephra from Toluca basin (Newton and Metcalfe, 1999).

6.5.3 Tuxtlas Volcanic field (TVF)

The Tuxtlas Volcanic field is located in the southern Veracruz province, roughly 250 km from El Chichón and was active since the late Pliocene. Santa Marta, San Martin Pajapan and Cerro el Vigia are three of the dominant volcanoes of this area. The last eruptive event was in 1793 of the San Martin. Espíndola et al. (2010) described this eruption. They estimated an ash output of $2{,}5x10^{11}$ kg and a lava output of ~$2x10^{10}$ kg. Only whole rock and ash fall were investigated. The ash consists of very basic rocks with low SiO_2 content (42-48 wt.%). Further no large eruptions of these volcanoes were reported.

6.5.4 Trans-Mexican Volcanic Belt (TMVB)

The Trans Mexican Volcanic belt is an area of active volcanism and runs east-west at the latitude of Mexico City (~20°N). The volcanism of this complex zone is thought to be related to subduction of the Cocos plate under the North American plate (Demant, 1978). Slab melting plays a key role in the this (Gomez-Tuena et al. 2007) creating large volcanoes such as the Nevado de Toluca, Tláloc and Popocatepetl volcano. Large eruptions were reported for these volcanoes; three large Holocene eruptions were recognised for the Nevado de Toluca volcano (Acre et al. 2003), the Popocatepetl eruptions had a disastrous impact on the local inhabitants (Siebe et al. 1996, Schaaf et al. 2005). The Tlaloc was very active during the Pleistocene with a series of explosive eruptions (Rueda et al. 2013). Ortega-Guerrero and Newton (1998) found tephra layers in the Basin of Mexico, which is a large basin surrounding Mexico City. Several sites were sampled and tephra's from the Chalco and Texcoco sub-basins were linked to each other. The source of these tephra's is unknown and has to yet to be discovered. Another article further improved this first tephrabase. Newton and Metcalfe (1999) sampled tephra layers of the Toluca basin in central Mexico. They found the major element chemistry of 10 tephra layers from the late Pleistocene and Holocene. The Toluca basin was sampled in several sites and correlated with the Basin of Mexico. They suggested that several tephra layers originate from the Nevado de Toluca volcano. From these volcanoes only rhyolitic pumice clasts were included and their results shown in figure 39. Tephra from the Popocatepetl tephra is of dacite chemistry (Schaaf et al. 2005). Ruede et al. (2013) studied sections in the surroundings of the Tlaloc volcano and recognised several tephra layers with rhyolitic composition of 31 ka.

The tephra from Trans Mexican Volcanic Belt volcanoes do not have the same major element chemistry as any of the data from El Chichón reported in the papers and this thesis. The Tlaloc tephra from Rueda et al. (2013) has a very distinct chemistry. Although most major elements have similar values to the tephra from the Toluca basin (Newton and Metcalfe 1999, Ortega-Guerrero and Newton 1998), the K_2O content show high values (5 wt.%), TiO_2 content is low (0.1 wt.%), the Al_2O_3 content is low (13.5 wt.%) and the CaO content is low (0.5 wt.%).

The tephra layers described in Newton and Metcalfe (1999) show large variation in their SiO_2 content (fig. 39). The SiO_2 content varies from 71-79 wt.%, with very low K_2O values relative to cluster 1 and 2, Al_2O_3 values ranging from 12-15 wt.% and high MgO values (0.1-0.5 wt.%). Individually they also vary a lot, but no layer is related to the El Chichón volcano.

Compared to the El Chichón tephra data, the tephra's from the Toluca basin have a very low K_2O content and high MgO content. Further is the SiO_2 content much higher than the data from El Chichón. The Upper Toluca pumice has a FeO content of 2 wt.%, higher than the El Chichón tephra (~1.5 wt.%). Further does the Lower Almoloya tephra overlap with H_{C3} and tephra data from Nooren

et al. (2009). The K_2O content of the lower Almoloya tephra is 0.5 wt.% lower than H_{C3}, but the other elements fit nicely into the this high SiO_2 H_{C3} cluster. This tephra layer that might be from the Nevado de Toluca volcano (Newton and Metcalfe, 1999) could potentially be the source volcano. This tephra is dated on 12.4 Ka. However not much is known on the origin of the tephra, no trace element analysis correlation is performed and the tephra has a range in chemical composition with a few end member points to be similar with H_{C3}. More research needs to be one on this.

6.5.3 Central American Volcanic Arc (CAVA)

The Central American Volcanic Arc (CAVA) which consist of a chain of volcanoes which are related to the subduction of the Cocos plate under the Caribbean plate (Reynolds, 1987, DeMets et al. 1990, Rebollar et al. 1999, Acre et al. 2014). In this volcanic arc the Tacaná and Santa Maria are the most north western located volcanoes. The two volcanoes closest to the Tabasco province are the Tacaná and Santa Maria volcanoes. Any plinian eruption material from these volcanoes could blow into the watershed of the Usumacinta and Grijalva river which then is transported to the beach ridges.

Tacaná

The Tacaná is one of many volcanoes that make up the Central American Volcanic Arc. Glass analyses of the Tacaná and Santa Maria were compared to the El Chichón tephrabase. The two volcanoes are located in the north western part of the arc. Acre et al. (2012) took samples from outcrops around the Tacaná volcano and analysed glass, whole rock of these sites. The Sibinal pumice deposits from a plinian eruption (23,540 BP) were analysed to reconstruct the trigger mechanism and character of the eruption. Tacaná tephra has a much different chemical composition than El Chichón (fig. 39). The tephra contains less Al_2O_3, CaO and K_2O and more SiO_2 compared to El Chichón. Further ash fall was only deposited on regional scale, the eruption extent was too small to impact the Chiapas and Tabasco province. There are no reports on large eruptions from this volcano influencing the southern part of Mexico (Vogripa 2016).

Santa Maria

Andrew et al. (2014) conducted phase equilibrium experiments on pumice and phenocryst of the Santa Maria volcano in order to find magmatic storage conditions and decompression rates of the 1902 eruption. Major elements analysis was done one phenocrysts of orthopyroxene, amphibole, titanomagnetite and apatite, glass shards and plagioclase minerals. The 1902 eruption produced ~20 km^3 of tephra and let to full caldera collapse.

The Tacaná and Santa Maria tephra have quite a distinct composition. The Al_2O_3 of the Santa Maria is 1 wt.% higher, Na_2O is 0.5 wt.% higher, K_2O is much lower by almost 2 wt.% and MgO is slightly higher. Further does most data fall in the same group as the data from Newton and Metcalfe (1999) who analysed tephra's from the TMVB. The Tacaná and Santa Maria tephra are much different than H_{C3} (fig. 39).

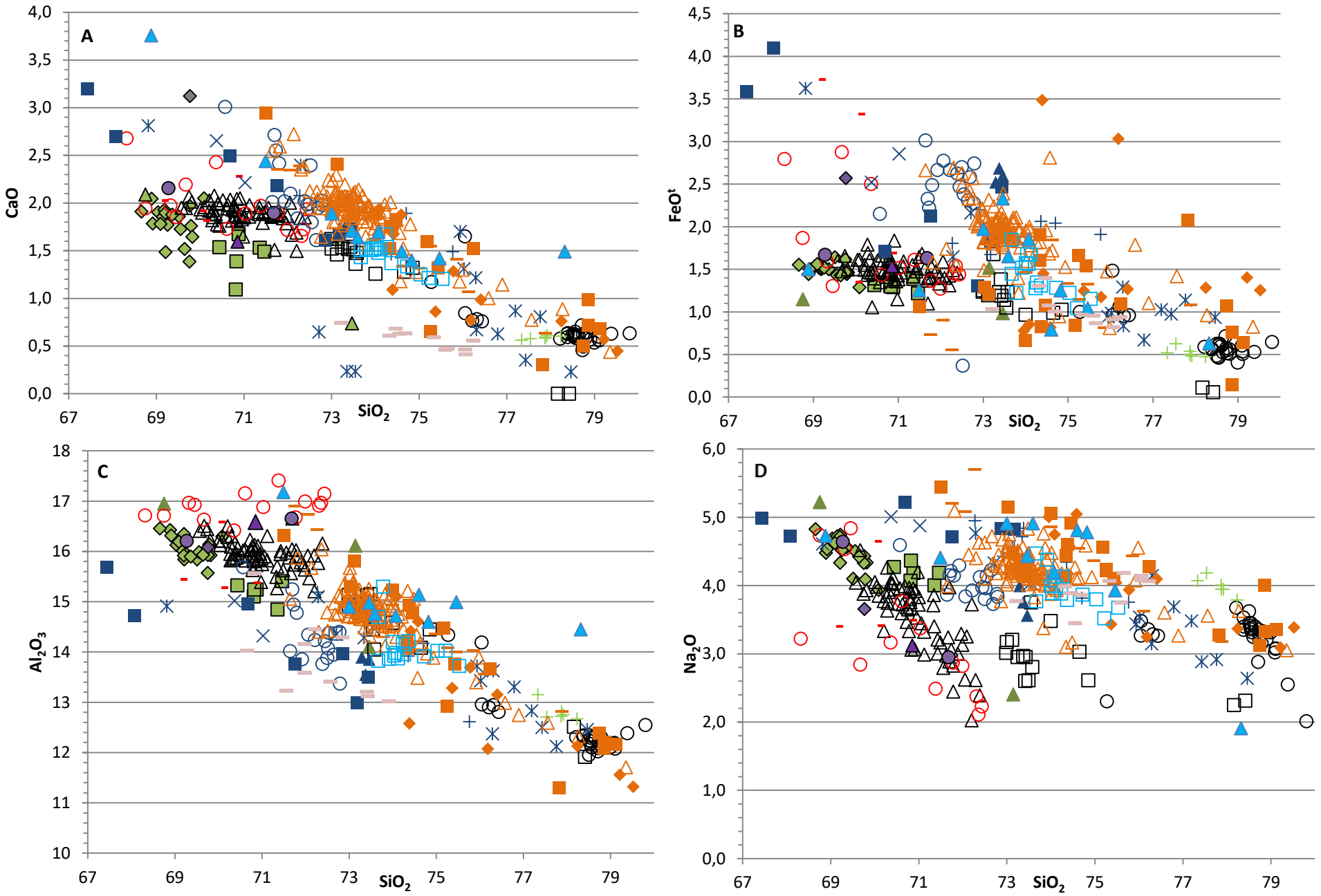
A
CaO
SiO2
B
FeOt
SiO2
C
Al2O3
SiO2
D
Na2O
SiO2

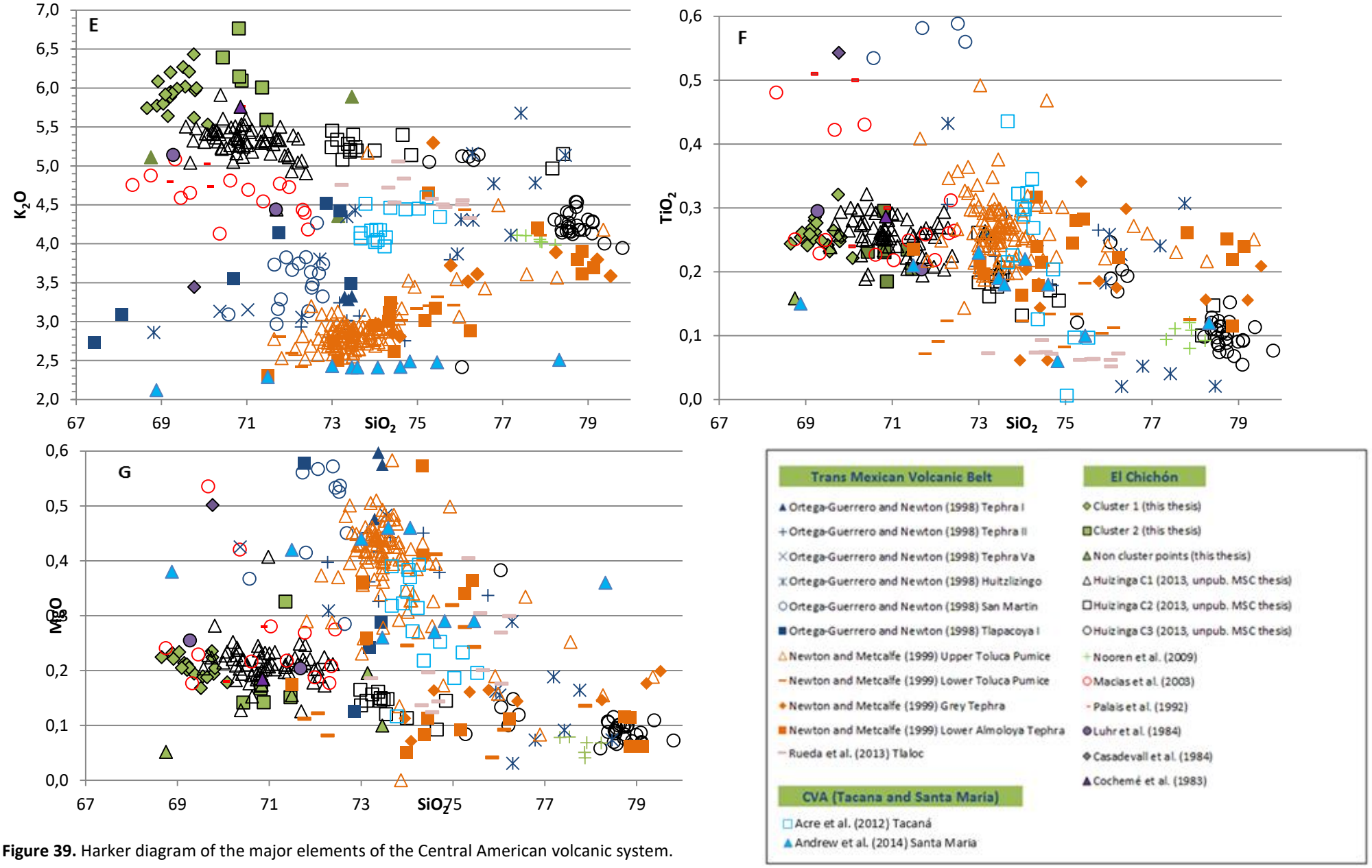

Figure 39. Harker diagram of the major elements of the Central American volcanic system.

Atitlán caldera

So far tephra data from earlier mentioned volcanic zones does not correlate with H_{C3}. Although the lower Almoloya tephra has a similar chemistry, its origin could not be derived. Therefor Huizinga (2013, unpub. MSc thesis) made a list of all large caldera forming and pre-Holocene eruptions as was reported from deep-sea cores in Kutterolf et al. (2008). From this major and trace element compositions of tephra were compared to H_{C3}. First observations recognised the Los Chocoyos eruption from 84 ka to match very well with H_{C3} (Huizinga, 2013 unpub. MSc thesis). Also Drexler et al. (1980) reported an area of $1.1x10^6$ km^3 with an isopach thickness of 10 cm. Tephra from this eruption was found in cores from the Straits of Florida to the coast of Ecuador (Dexler et al. 1980).

The Los Chocoyos eruption is one of the largest Holocene eruptions known in the history of Central America (Rose et al. 1981). Its proposed eruption date is 84 ka (Drexler et al. 1980, Reynolds et al. 1987, Rose et al., 1999) and its deposits have been found in deep sea drill cores in the Gulf of Mexico up to 22° latitude (Drexler et al. 1980) and off the coast of Guatemala, Honduras, Nicaragua, Costa Rica and Panama (fig. 40, Ledbetter et al. 1985, Kutterolf et al. 2008). The Los Chocoyos Ash is part of the San Cristobal group consisting of air fall, ash flow and surge members (Rose et al. 1987). The air fall deposit is the lowest member mentioned as H-tephra.

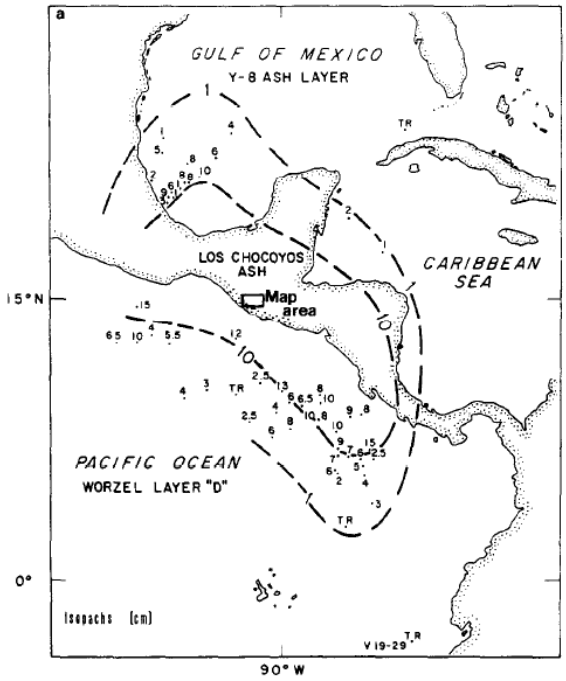

Figure 40. Isopach map of the 84 ka Los Chocoyos eruption of the Atitlán volcano (from Dexler et al. 1980).

Lager eruptions were reported for the Atitlán volcano. The biggest of these eruptions deposited the Los Chocoyos ignimbrites (84 Ka, Rose et al., 1981, 1987; Ledbetter, 1985).

Drexler et al. (1980) analysed tephra layers of several deep sea drill cores from the Gulf of Mexico and the Pacific Ocean. The D and Y-8 ash layer found in these cores were related to the Los Chocoyos Ash from trace and major element correlation. They could not conclude which of the Los Chocoyos member the ash layers represent.

Rose et al. (1981) described Quaternary Plinian tephra units from five calderas of the CAVA in Guatemala and Honduras. Los Chocoyos is one of the largest eruptions from the Atitlán caldera and they describe two members; a Plinian air fall and subsequent ash flow members. The ash flow deposits consist of two populations of volcanic rocks, a K high rhyolite bearing biotite with a similar composition as the H-tephra and the second population is more heterogeneous with low K rhyolite bearing Hornblende. The high K rhyolite population is very homogeneous composition and glass rich. Los Chocoyos Ash was found in deep sea cores from the Gulf of Mexico, Pacific Ocean and Caribbean Sea, but was not related to any deep sea tephra.

Ledbetter (1985) analysed ash layers from deep sea drill cores of the Gulf of Mexico and the Pacific Ocean. 11 tephra horizons were revealed and related to past eruption. The Los Chocoyos Ash was found in several locations. The Y-8 and D layers were correlated to the H-tephra of the Los Chocoyos Ash (fig. 41).

Rose et al. (1987) analysed Quaternary pyroclastic deposits from the Atitlán caldera. Using major and trace element compositions from the different Atitlán rhyolitic units, the eruption history was derived. Using data from Atitlán tephra units the evolution of the caldera was derived. They infer that the Los Chocoyos eruption began with a high K Plinian phase directly followed by pyroclastic flows of high and low K magmas.

Kutterolf et al. (2008) collected 56 deep sea drill cores from the seafloor of the Pacific Ocean. They found 213 ash layers which represent volcanic eruptions from volcanoes in Guatemala, El Salvador and Nicaragua. One of them being the Los Chocoyos Ash from the 84 ka Atitlán caldera. The layers consisted of white juvenile pumice bearing abundant plagioclase, biotite and quartz crystals.

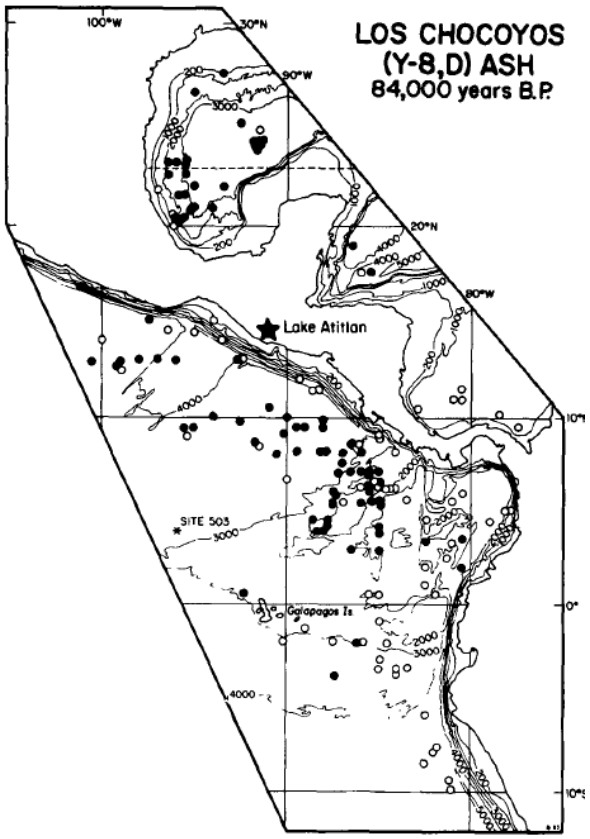

Figure 41. Distribution of deep sea drill cores in the Pacific Ocean and Gulf of Mexico. The black circles represent the locations where the Los Chocoyos ash layers (Y-8 and D) were found. From Ledbetter (1985).

If we compare the data of the previous mentioned authors with the H_{C3} there is a good fit (fig. 43). The major element plots clearly show a strong correlation between the samples from the beach ridges cores (fig. 5; Pozpetr core, Nooren et al. 2009, PP1 core, Huizinga 2013 unpub. MSc thesis) and the Los Chocoyos tephra. The Na_2O, TiO_2, K_2O, CaO, MgO and FeO weight percentages are very similar. The beach ridges tephra correlates best with H-tephra, Los Chocoyos air fall, flow and surge deposits from Drexler et al. (1980), Rose et al. (1981), Ledbetter et al. (1985), Rose et al. (1987) and Kutterolf et al. (2008). Other Atitlán units from Drexler et al. (1980) have low FeO values, but most major elements show a strong correlation.

Only the SiO_2 and Al_2O_3 content show a difference. The beach ridges tephra has lower Al_2O_3 and higher SiO_2 wt.%. Further show tephra samples from Rose et al. (1987) a strong trend in the Al_2O_3-SiO_2 and CaO-SiO_2 plot indicating plagioclase contamination (section 4.3). The high SiO_2 weight percentages from Huizinga (2013 unpub. MSc thesis) are not very surprising; since these samples show increased SiO_2 values from compositional variations caused by the instrument (section 6.5.1). Another explanation is that these tephras were reworked (Huizinga, 2013 unpub. MSc thesis).

The relative increase in the SiO_2 causes a relative decrease for the other elements which is best seen in the Al_2O_3 content. Three samples from Rose et al. (1981) are plot, which include H-tephra and Los Chocoyos ash flow deposits. Tephra from ash flow deposits show some compositional variation. The H-tephra correlates well with the beach ridges tephra. There is one low K_2O tephra sample present with a distinct composition. The CaO and FeO are much higher and the K_2O has low values. This sample is part of the heterogeneous low K_2O tephra group, which has a different chemistry as the H-tephra.

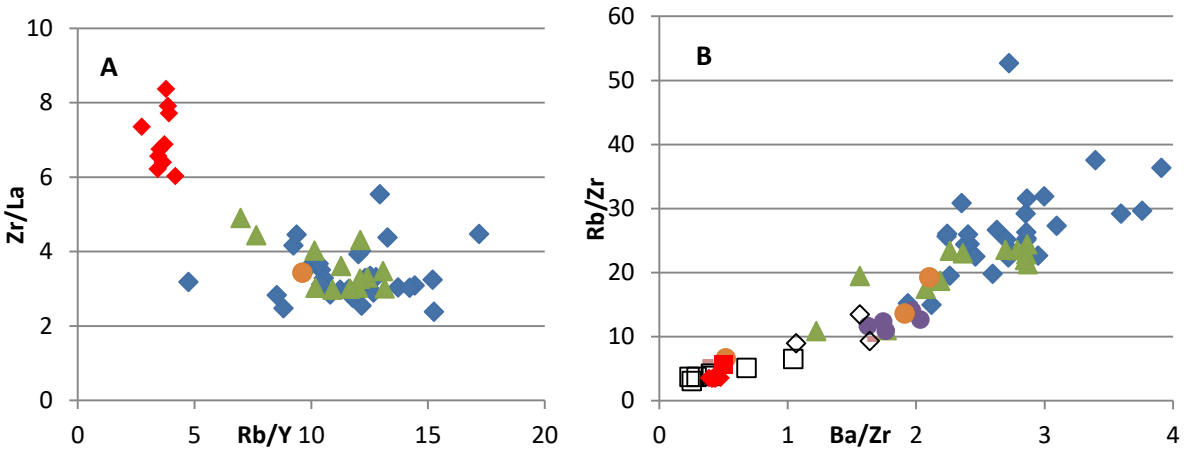

Figure 42. Trace element plots showing El Chichón and Los Chocoyos Ash. El Chichón tephra has a distinct trace element composition. Chart in figure 42 show data references.

Trace element plots show less data, because not all authors measured trace element compositions. The Los Chocoyos tephra found in the deep sea drill core (Drexler et al. 1980, Kutterolf et al. 2008) and the beach ridge tephra trace element compositions fit well with H_{C3}. The units from Drexler et al. (1980, units A-T) show a distinct trace element composition. Also the tephra from El Chichón (Rose et al. 1984, Espíndola et al. 2000) have very different trace element compositions and in the Rb/Zr – Ba/Zr plot they overlap (fig. 42).

What is also clear is from both major and trace elements is the large variation in the Los Chocoyos tephra from samples of the ash flow and surge deposits. The air fall deposits found in the Pacific and Gulf of Mexico show very uniform compositions (H-tephra, Kutterolf et al. 2008, Drexler et al. 1980), while the pyroclastic flow deposits near the caldera have a range of compositions (Drexler et al. 1980, Rose et al. 1981, 1987). The air-fall deposits which are distributed in large part of Central America and correlates best with the beach ridges tephras.

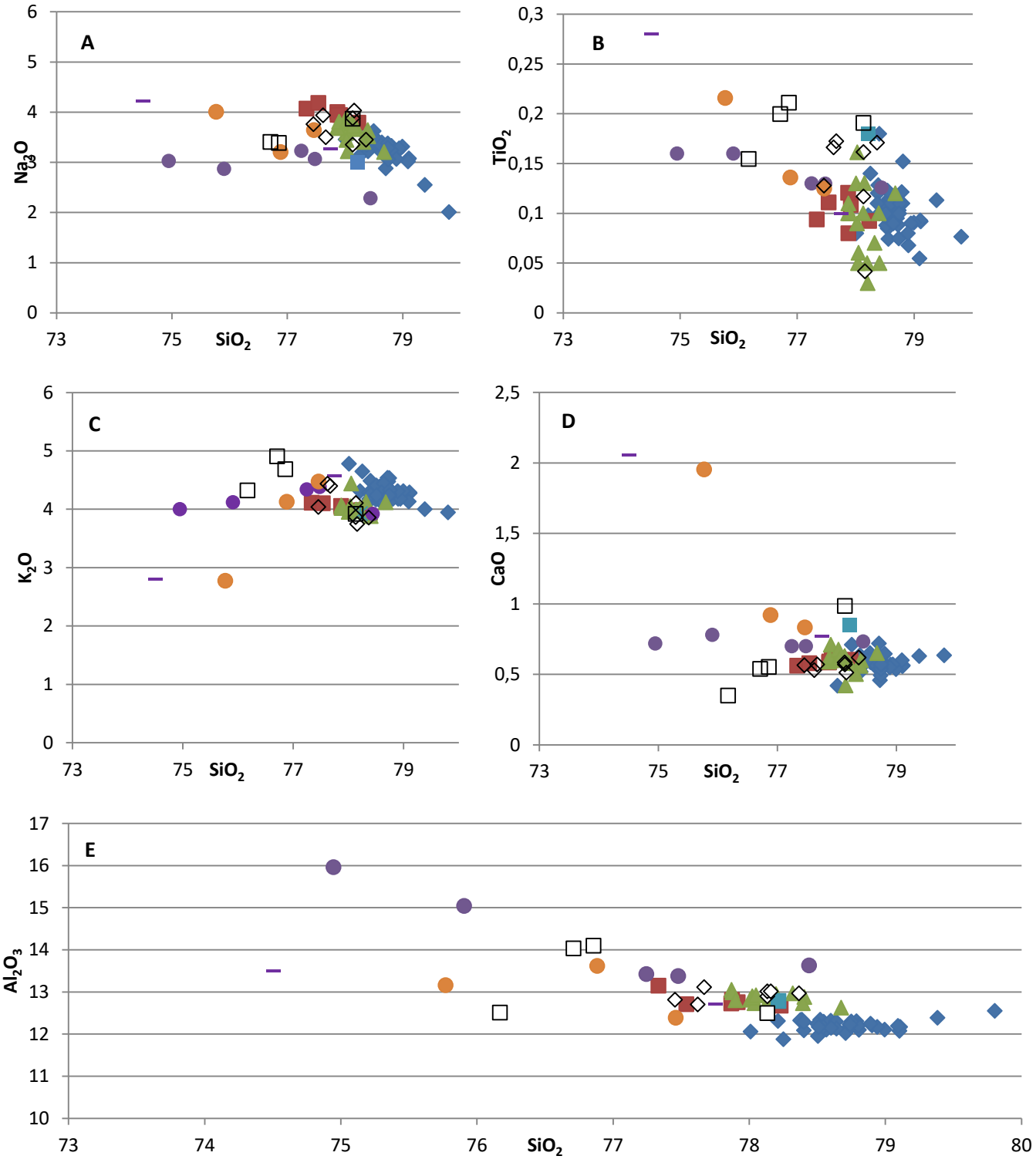
A
B
C
D
E
Na_2O
TiO_2
K_2O
CaO
Al_2O_3
SiO_2
Distal Tephra
Huizinga HC3 (2013, unpub. MSC thesis)
Nooren et al. (2009)
El Chichón tephra
Rose et al. (1984) El Chichón
Espindola et al. 2000 El Chichón
Los Chocoyos Ash
Kutterolf et al. 2008 Los Chocoyos: air, flow and surge
Rose et al. 1987 H-tephra
Rose et al. 1987 pyr. flow deposits
Ledbetter et al. 1985 H-tephra
Rose et al. 1981 Los Chocoyos: air, flow and surge
Drexler et al. 1980 units A-T
Drexler et al. 1980 Los Chocoyos: air, flow and surge

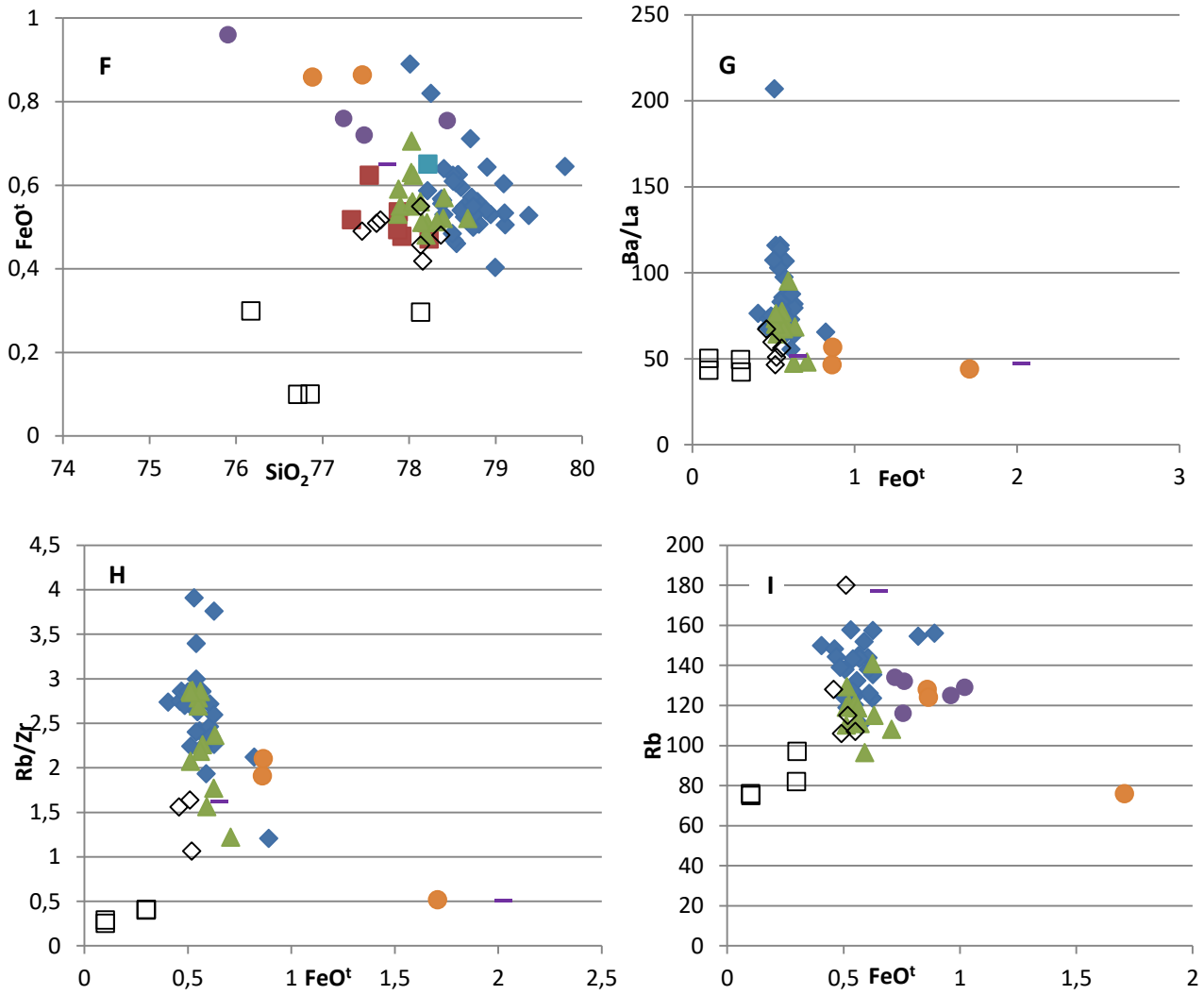

Figure 43. Major and trace element compositional plot for El Chichón, Los Chocoyos Ash from various authors. Some tephra analysis did not include trace elements. Chart below figure E shows data references.

Secondly the Lower Almoloya tephra from Newton and Metcalfe (1999) might represent the Los Chocoyos Ash deposited in the Basin of Mexico. The major element composition shows a correlation with H_{C3}. Only the K_2O content is a bit lower, but could be caused by crystal fractionation (section 6.6). The connection of the Lower Almoloya Tephra is preliminary and more research is required, since the only evidence comes from major element correlation.

The strong correlation of H_{C3} with the Los Chocoyos air fall tephra in both major and trace elements provides a good argument that H_{C3} are Atitlán 84 ka eruption products. The air-fall tephra (also mentioned as H-tephra) has a very distinct, small range chemistry different than the other members of the Los Chocoyos Ash. The variation between the tephra members is due to the different eruption stages of the eruption (Rose et al. 1981). H_{C3} best correlates with the air fall and H-tephra, which represent the tephra blown into the air.

6.6 Crystal fractionation

In the previous section the origin of H_{C3} is discussed. H_{C1} and H_{C2} originate most likely from El Chichón, but the tephra composition shows variation in K_2O. Crystal fractionation was already mentioned as explanation for this difference (section 6.5.2).

Crystal fractionation, crystal growth and magma mixing in the magma chamber change the composition of the primary magma during the eruptions. This produces magmas with different chemical compositions. In the first phase of the eruption the magma chemistry is similar to the primary melt. Then in time crystal fractionation, growth or magma mixing changes the composition of the residual melt. The deposits of the magma have slightly different chemistries. The 1982 eruption had different phases (Macias et al. 2003, De la Cruz-Reyna et al. 2009), this could have resulted in air fall and flow deposits with different compositions.

The general composition of volcanic rocks from El Chichón (550 BP and 1982) is pretty uniform (this work, Andrews et al. 2008, Macias et al. 2003, Espíndola et al. 2000, Tepley et al. 2000). This implies that the primary melt of these eruptions have similar compositions. Comparing different eruptions with each other therefor is valid for El Chichón.

So far two tephra deposits from El Chichón were found, one being proximal tephra from river terraces and the other distal tephra from the Usumacinta-Grijalva delta plain. The hypothesis is that distal tephra represents the very latest stage of evolved magma, while the more proximal tephra is from less evolved, more primary magma. This primary magma contains relatively more K_2O. Then potassium rich minerals crystalize from the melt and drops the K_2O content of the residual melt. Tephra is a representation of the residual melt. Since orthoclase was found as microliths in many glass shards (Appendix F1-5, fig. 16), this might have caused this drop.

In order to explain the K_2O difference, IGPET was used to model fractional crystallization. The tephra data of this work (proximal) was compared with tephra from the delta plain area (distal, PP1 drill core, Huizinga, unpub. MSc thesis 2013). The averages composition of the minerals found in the pumice clasts was used. The K_2O difference is assumed to be caused by crystallization of orthoclase. In this way relatively more potassium is removed from the residual melt and lowers the K_2O content. The following samples were used and summed up in the table hereunder. As parental melt the average of cluster 1 was used. The melt becomes more silica rich as it evolves. Samples with relative high SiO_2 and low Al_2O_3 weight percentages were used as daughter melt. Samples from PP1 drill core, tephra samples from this work and minerals are listed in Appendix I3. Mainly averages of H_{C1}, H_{C2} and SiO_2 rich points from H_{C1} were used. This way a good representation was made from the two clusters found in the distal swamp. Further the averages of cluster 1 and 2 were modelled to evaluate crystal fractionation formed cluster 1 and 2 from the same melt. They are listed as C_1-av, C_2-av. Since cluster 1 and 2 are very uniform, it is justified to use their average composition to compare it with the swamp tephra and tephra from Macias et al. (2003).

Table 13. List with samples used in IGPET (Appendix X3).

	River terrace samples	Swamp samples (Huizinga, unpub. MSc thesis, 2013)	550 BP dome sample (Macias et al. 2003)
Parental magma representing samples (low SiO_2, high Al_2O_3)	C_1-av	-	-
Daughter magma representing samples (high SiO_2, low Al_2O_3)	C_2-av	$Huiz_{max\text{-}C1}$, $Huiz_{max\text{-}C1\ (Na)}$, $Huiz_{avc1}$, $Huiz_{avc2}$	Mac_{av}, Mac_1

In the second part the cluster 1 and 2 were modelled with the 550 BP glass shards of Macias et al. (2003). The average of the 550 BP samples was used. It could also be that a combination of alteration and crystal fractionation caused the K_2O difference. It is important to note that this is a comparison between two events. With the assumption that the chemistry has remained uniform in time, this comparison can be made.

6.6.1 Cluster 1 and 2

As mentioned earlier there are two cluster defined in this work which have a slightly different composition. It is possible that this difference is caused by crystal fractionation. The minerals from section 5.2 were averaged and used in the IGPET. The hornblende minerals have a pretty uniform composition (fig. 31), plagioclase has a variable composition with potassium influenced minerals. Pyroxene is pretty uniform. Thus for most minerals an average will be a good representation, but for plagioclase it may vary. Since only a couple of measurements of orthoclase were done the average of these measurements were used.

Modelling cluster 1 and 2 with IGPET gave good results (table 14) using different plagioclase compositions all gave good results with sum of squares of residuals lower than 1. Also the minerals that crystalize are mainly orthoclase and plagioclase. 15% of the melt crystalizes, a small proportion of the melt is required to create C_2 from C_1. In conclusion it is possible that cluster 1 and 2 were from the same parental magma.

Table 14. Results of modelling C_1 and C_2 averages with IGPET for variable plagioclase compositions.

Fractions				**Solid cumulate (%)**				**Variables**		
0.06				42.3				Plagioclase (Pl-av)		
0.001				0.5				Hornblende (Hb-av)		
0.005				3.3				Magnetite (Mag-av)		
0.077				54.0				Orthoclase (KFSP)		
0.858								Residual liquid (C2-av)		
Major elements										
	SiO_2	TiO_2	Al_2O_3	FeO	MnO	MgO	CaO	Na_2O	K_2O	P_2O_5
Observed C_1-av	69.52	0.26	16.12	1.5	0.09	0.21	1.80	4.49	5.96	0.03
Calculated C_1-av	69.61	0.25	16.24	1.51	0.07	0.16	1.84	4.31	5.98	0.02
Difference	-0.03	0.01	-0.06	-0.01	0.02	0.05	-0.03	**0.18**	-0.02	0.01
Sum of squares of residuals: 0.041										

Fractions	**Solid cumulate (%)**	**Variables**
0.069	38.9	Albite (An0.3)
0.007	3.6	Clinopyroxene (CPX-av)
0.005	2.5	Magnetite (Mag-av)

0.098				54.6			Orthoclase (KFSP)			
0.822							Residual liquid (C2-av)			
Major elements										
	SiO_2	TiO_2	Al_2O_3	FeO	MnO	MgO	CaO	Na_2O	K_2O	P_2O_5
Observed C_1-av	69.52	0.26	16.12	1.5	0.09	0.21	1.8	4.49	5.96	0.03
Calculated C_1-av	69.58	0.24	16.23	1.51	0.07	0.22	1.79	4.4	5.94	0.02
Difference	-0.02	0.02	-0.06	-0.01	0.02	-0.01	0.01	**0.09**	0.02	0.01
Sum of squares of residuals: 0.014										

6.6.2 Cluster 1, H_{C1} and H_{C2}

Using the average plagioclase, clinopyroxene, magnetite and orthoclase mineral compositions in IGPET showed good results (Appendix L, table L-3). H_{C1} had sum of R^2 was 0.6 with the largest difference in Na_2O and Al_2O_3. For this composition to form 25% of the melt has to crystallize and primarily orthoclase crystallizes. Also the average H_{C2} chemistry gave good results, sum of R^2 of 0.8, but with 45% crystallization of melt composed of mainly orthoclase. However, one evolved H_{C1} sample IGPET gave result that did not suggests crystal fractionation ($Huiz_{max\text{-}C1}$, Appendix L, table L-3A). The sum of R^2 was 1.59, with a large difference in Na_2O and Al_2O_3. From detailed view on the data and description the tephra from the drill core, showed that a lot of these samples had Na loss during measuring. This with the possibility that these samples also undergone are more affected by alteration and leaching than the river terrace tephra (section 6.5), which lower the Na content. In order to account for this the Na_2O was increased by 1 wt.%, which gives it a more representative value. Using this adjusted sample improved the outcome by a great deal, the sum of R^2 was 0.51, with a much lower difference in Na_2O and Al_2O_3 that still are the main elements with large differences (Appendix L).

Table 15. Results of modelling C_1 with H_{C2} adjust for Na_2O (chemistry in Appendix X3).

Fractions				Solid cumulate (%)			Variables			
0.016				4.9			Plagioclase (Pl-av)			
0.016				4.8			Clinopyroxene (CPX-av)			
0.004				1.3			Magnetite (Mag-av)			
0.286				89.0			Orthoclase (KFSP)			
0.679							Na adjusted residual liquid ($Huiz_{max\text{-}C1}$, Na increase 1 wt.%)			
Major elements										
	SiO_2	TiO_2	Al_2O_3	FeO	MnO	MgO	CaO	Na_2O	K_2O	P_2O_5
Observed C_1-av	69.52	0.26	16.12	1.50	0.09	0.21	1.80	4.49	5.96	0.03
Calculated C_1-av	69.53	0.23	16.78	1.51	0.08	0.32	1.73	3.87	5.93	0.02
Difference	-0.01	0.03	-0.33	-0.01	0.01	-0.11	0.07	0.62	0.04	0.01
Sum of squares of residuals: 0.513										

It can be concluded that crystal fractionation of the parental melt, where orthoclase, plagioclase, clinopyroxene and magnetite were crystalizing, produced melts of $H_{C1\text{-}2}$ and cluster 1 and 2 compositions. IGPET indicates that mainly orthoclase crystalized (28%) and that minor amounts of plagioclase, clinopyroxene and magnetite crystalized. The residual liquid is 67% from which then the more distal beach ridge tephra is formed ($H_{C1\text{-}2}$). H_{C3} could not be produced from a cluster 1 parental magma, difference in chemistry is too large for this.

6.6.3 C_1 and 550 BP tephra

The last tephra that modelled were the 550 BP tephra samples, with relative very low K_2O, Na_2O value and high Al_2O_3 weight percentages. The results are shown in Appendix L-3. The results suggest that it is not possible to produce the 550 BP tephra by crystal fractionation from a cluster 1 melt composition. Na_2O, Al_2O_3, SiO_2 and MgO difference were large and contributed to a sum of R^2 of 1.3-1.7 (Appendix L, table L-3) and 33-40% of the melt has to crystalize to produce this tephra composition. The 550 BP tephra low K_2O and Na_2O values are more likely to be the result of alteration and leaching.

In conclusion IGPET is a good tool to model crystal fractionation of magma from El Chichón. The proximal tephra (C_1 and C_2) originate from the same parental magma, where crystal fractionation formed the composition of C_1 and C_2. In a broader scale the orthoclase microliths present in the pumice clasts were formed at one stage of the eruption producing a K_2O depleted melt that has was deposited in the distal Grijalva-Usumacinta delta plain area. The primary melt evolved producing tephra with different compositions; one was deposited in the river terraces and one in the delta plain area near the Gulf of Mexico. Further the difference in the 550 BP tephra is most likely cause by alteration and leaching of elements, from which Na_2O and K_2O are the first elements that were removed.

6.7 Magmatic processes

Here the processes are described that occur in the magma chamber of El Chichón. One way of changing the chemical composition in a melt are crystal fractionation and magma mixing (section 6.6). These two are the most important processes occurring in a magma chamber. Magma mixing can occur when magma is injected from the mantle. This brings new heat that can melt the surrounding wall rock and is incorporated into the new formed melt. Crystal fractionation occurs when a melt cools and minerals crystallize. The crystallization process provides heat to the magma maintaining its high temperatures and might even melt the surrounding crust. It is a very complex system with many factors influencing the composition of the melt and growth of minerals. Several authors investigated the magmatic system of El Chichón (Tepley et al. 2000, Andrew et al. 2008, Macias et al. 2003).

The isotope composition of magma can be only changed through assimilation or recharge, whereas fractional crystallization not changes the isotope ratio. The two processes have different effects; assimilation of wall rock increases the strontium ratio and recharge might decrease the ratio (Tepley et al. 2000, Davidson et al. 2001, Andrew et al. 2008). Phenocrysts which are compositionally zoned give a record of crystallization, recharge and assimilation because the major and trace element compositions are strongly dependant to composition and temperature (Holland and Blundy 1994, Holtz et al. 2005, Andrew et al. 2008).

Tepley et al. (2000) investigated plagioclase phenocrysts of the 200 Ka and 1982 eruptions. The $^{87}Sr/^{86}Sr$ ratio from core to rim in plagioclase phenocrysts was measured. To strontium ratio increased towards the rim which is an indication of a changing magma system. Zoning is present in the plagioclase. Larger phenocrysts had a larger difference in their strontium ratio than smaller ones. These observations gave implications for magma mixing and recharge. They concluded that that the change observed in the plagioclase was caused by either an irregular shaped magma chamber or multiple magma chambers. In this way different isotope ratios in plagioclase can form from similar

parental magmas. Further they infer that fractional crystallization occurs although they not give clear evidence for this.

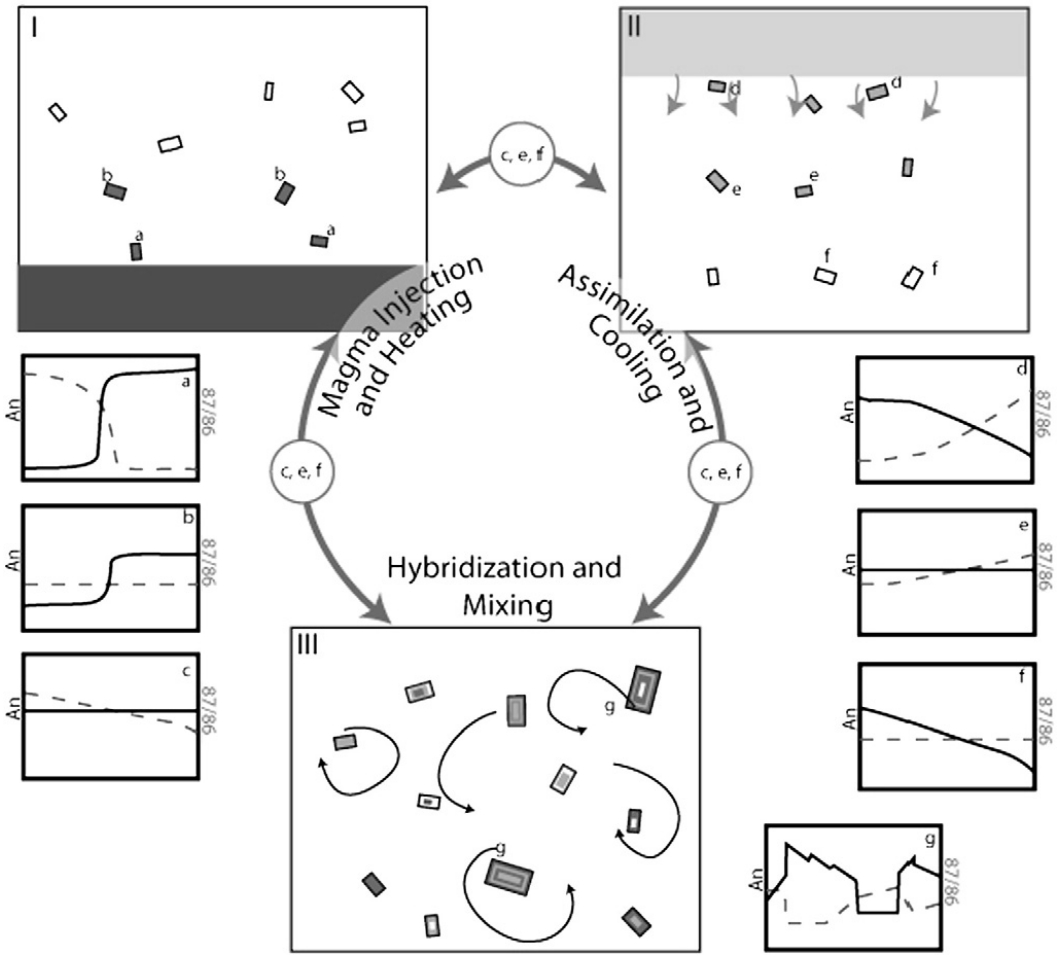

Figure 44. Description by Andrew et al. (2008). "Diagram showing formation of different zoning types. In figure A, interval 1, crystals a, b, and c all crystallize with invariant An and 87Sr/86Sr ratios. As hotter, more primitive magma (dark grey) is injected in interval 2, crystal a is engulfed by the intruding magma and forms a Type I zone. Crystal b, on the other hand, is far enough from the intruding magma that it experiences an increase in temperature, but no change in isotopic composition, and c is far enough away that it remains entirely unchanged. During interval 3, the two magmas hybridize (light grey), producing a Type II zone in crystal a, and lowering the isotopic ratio of b. Crystal c remains far enough from the intrusion that it records only very minor changes in An and 87Sr/86Sr ratio. Interval 1 of figure B is identical to that of figure A. In interval 2, however, assimilation of country rock (grey) begins to occur and is recorded by the crystal closest to the wall (d) as a Type II zone. In interval 3, host magma contaminated by country rock penetrates further into the chamber recorded as a type II zone in crystal e, and eventually, as a small amplitude Type IV zone in crystal f. It is important to consider the processes depicted in figures A and B together, such that the heat required for assimilation of wall rock (B) may be provided by a hot intruding magma (A). Furthermore, mixing of the system will move crystals through the chamber resulting in a single crystal, for example, perhaps developing Type I zones in one magma injection, and Types II, III, or IV in a later event when the crystal is farther from the injection. "

Macias et al. (2003) investigated the processes behind the 550 BP eruption. They analysed whole rock, pumice clasts and phenocrysts of plagioclase, hornblende of unit B (Espíndola et al. 2000). The 550 BP eruption was the result of an injection of hotter, more basaltic magma into the trachandesitic

magma residing beneath El Chichón. Evidence for this comes from the presence of mafic enclaves, zoning patterns and chemical variations in plagioclase phenocrysts. They estimated that before the eruption the magma had a temperature of 820-830 °C and a pressure of 2-2.5 Kbar, the 550 BP eruption was one order magnitude larger than the 1982 eruption.

Andrew et al. (2008) continued on the work of Tepley et al. (2000) and analysed plagioclase and amphibole phenocrysts from 7 eruptions that occurred in the last 3100 years. Both the amphiboles and plagioclases showed zonation and four types of zoning patterns were recognised. The whole rock assemblages were mainly potassic trachandesites dominated by plagioclase and hornblende phenocrysts, further clinopyroxene was present. Augite, magnetite, titanite and apatite were present in smaller amounts.

The bulk composition and the isotope ratios of the plagioclase and amphibole were analysed and the bulk shows a homogeneous isotope composition. However, plagioclase and amphibole phenocrysts had complex zonation shown from their anorthite content and isotope ratio. Type I had increasing anorthite (An) and decreasing $^{87}Sr/^{86}Sr$ ratios from core to rim. Type II had a decreasing An and increasing $^{87}Sr/^{86}Sr$ ratio. Type III had a changing An content and a constant $^{87}Sr/^{86}Sr$ ratios and type IV a constant An content and changing $^{87}Sr/^{86}Sr$ ratios. The anorthite content shows the maturity of a rock, more An means that the parental melt was less evolved, possibly hotter and wetter. Injection of new magma from the mantle or fractional crystallization were thought to be the process behind an increasing An in phenocrysts, but these two processes give different $^{87}Sr/^{86}Sr$ ratios. Mantle derived rocks have lower strontium ratio values than crust derived ones. Magma injection would lower the ratio whereas assimilation of wall rock would increase the ratio. Further if crystallization occurs the $^{87}Sr/^{86}Sr$ ratio would be constant but the An could variate. The anorthite content is also temperature dependant (Holland and Blundy 1994, Holtz et al. 2005, Andrew et al. 2008). In order to explain the four types of zonation Andrew et al. (2008) created a model for the magma system of El Chichón in which cycles of recharge, assimilation and hybridization occur (fig. 44). In the first stage magma injection from the mantle occurs which lowers the $^{87}Sr/^{86}Sr$ ratio and increases the temperature. The phenocrysts that form during the injection will be progressively An richer and the $^{87}Sr/^{86}Sr$ ratio decreases. In the next period heat melts the wall rock where it mixes with the magma in the chamber, as the magma cools the minerals crystallize and will have increasing $^{87}Sr/^{86}Sr$ ratios and decreasing An. As the magma is entirely mixed and cools further the $^{87}Sr/^{86}Sr$ ratio will not variate much while the An decreases as the temperature goes down. Also if the magma is entirely mixed after the magma injection and temperature goes up the anorthite will go up in the phenocrysts while the $^{87}Sr/^{86}Sr$ ratio remains the same. Then during wall rock assimilation, the contaminated magma mixes with the main host magma, during this the temperature will not change much while $^{87}Sr/^{86}Sr$ ratio changes to the $^{87}Sr/^{86}Sr$ ratio of the contaminated magma.

6.8 Recommendation for using tephra from event terraces

River terraces are a very useful tool identifying the chemical fingerprint of a volcano and even its events. In this work the tephra from river terraces were used to identify the chemical fingerprint of the 1982 eruption and the El Chichón volcano. However, in order to use river terraces for chemical fingerprinting several conditions have to be met. They are explained in here and a list of recommendations is made to make future research easier.

First the event related river terraces need to be identified. There are several ways to identify them; LIDAR maps, features from the stratigraphy, articles describing the terraces and tephra chemical fingerprint. It is important to use multiple lines of evidence, because one approach will often not be sufficient to identify event related river terraces. Second after recognizing the event terraces it is important to derive an age constraint. This is very important if you want to compare different eruptions with each other and is the most reliable method for linking river terraces to eruptions. Third collecting tephra from multiple river terraces give you information on the extent of the eruption. Fourth a detailed understanding of the river valley, water runoff and number of terrace levels makes it easier to recognise event river terraces. Fifth is it necessary to take samples from different positions in the stratigraphy of the terrace. There can still be some contamination of accidental lithic rocks that are not related to the eruption, which need to be excluded. Some river terraces can be part of the same eruption or have deposits from several eruptions. Geomorphology, mineral textures and compositions give you this information. Lastly a list with recommendations is made based on experience gained during this research. This list provides helps recognizing and describing event river terraces.

Recommendations

- Age constraints from river terraces, preferentially from different multiple height in the terrace
- Multiple sampling at different positions in the stratigraphy
- Careful examination the condition of the tephra
- Sample several river terraces of the same eruption
- Use multiple lines of evidence for identifying eruption related river terraces; geomorphology, mineral compositions and textures, tephra condition, LIDAR images
- Detailed logging of river terrace stratification

7. Conclusions

Research questions of this study addressed the potential of river terraces as indicators of eruption events of El Chichón. The principal issue was:

Are river terraces of the Magdalena and Platanar rivers suitable for tephrochronology and does each river terrace level represent a single eruption?

The findings indicate that the terraces are suitable to obtain tephrochronological and geochemical information on El Chichón eruptions. However, not every terrace level represents a separate eruptive event. For example, both the 5 m and the 8.5 m terrace in the Magdalena River are constituted by 1982 eruption products.

> *Did these river terraces form during or shortly after an eruption so that they can be considered as short-lived volcanic events?*

The river terraces in the valleys of the Platanar and Magdalena rivers formed shortly after eruptions of El Chichón. The eruptions produced large amounts of new material in a short time interval so that they choked the valleys of the two rivers. Following an eruption of mainly pyroclastic material, a massif hyper-concentrated, debris or pyroclastic flow passed through the valleys and was eventually deposited as an 'event' terrace, consistent with evidence from Lidar images. Failure of natural dams promoted the mobility hyper-concentrated debris flows (Macias et al., 2004). Morphological features in the terrace stratigraphy include inverse grading, coarsening upward of pumice layers, and cataclastic signatures. Geochemical fingerprints of seven terraces, five from the Platanar River and two from the Magdalena River were obtained by electron-microprobe analysis of glass shards, mineral phases and microliths from matrices and pumices. The combined evidence points to event-related terrace formation in the valleys of the Magdalena and Platanar rivers.

> *Is the tephra from the river terraces uniform or do different events have different chemical compositions?*

Although the tephra is quite uniform in composition, the data fall into two clusters with slightly different SiO_2 contents. Cluster-1 contains 68.2-70.2 wt.% and represents the large majority of analysed material, whereas cluster-2 contains 70.5-71.5 wt.% of SiO_2. Most of the analysed terraces are related to the 1982 eruption. This conclusion is consistent with depositional maps for the 2 m, 5 m and 8.5 m terraces (Smid, 2015) and literature data on the 5 m terrace (Macias et al., 2004). Terraces at higher levels that often show signs of weathering are probably associated with the 550BP and 1500BP or other older eruptions. Age uncertainties and overall chemical uniformity of erupted material of El Chichón pose limitations to tephrochronological applications of the terraces and the reconstruction of the compositional evolution of the volcano's products throughout its eruption history.

> *Is there a difference between proximal and distal tephra?*

In general, the chemical compositions of the proximal tephra fit well with distal tephra such as described from the distal delta plain area in Tabasco (PP1 core) and other available data for El Chichón.

The presence of the clusters 1 and 2 in the proximal terraces, previously defined from glass compositions of distal tephra in drill cores, supports this. The data show minor differences in SiO_2, Na_2O and K_2O contents between the distal, proximal and 550BP tephra data. One explanation might be an analytical bias due to sample preparation or because the comparison is made with older data obtained with a different instrument and with different matrix-correction software. Alternatively, post-depositional leaching and alteration in the distal tephra, which was deposited in a swamp area, may have removed Na_2O and K_2O from the glassy material. It is also possible that the small differences are due to some heterogeneity in the magma body and reflect the effect of crystal fractionation of primary magma.

Is the high-SiO_2 tephra group (77-79 wt.%) found in the distal delta plain area in Tabasco also present in the river terraces and is it linked to El Chichón?

This group (H_{C3}) was not found in the river terraces. El Chichón is most likely not the source of this tephra. Instead, its chemical composition is similar to that of the Los Chocoyos tephra, which represents a major explosive eruption from Atitlán volcano (Guatemala) 84 ka ago.

8. References

Andrew, B.J., Gardner, J.E. and Housh, T.B. (2008). Repeated recharge, assimilation, and hybridization in magmas erupted from El Chichón as recorded by plagioclase and amphibole phenocrysts. Journal of Volcanology and Geothermal Research 175, p. 415-426.

Arce, J.L, Macías, J.L. and Vásquez-Selem, L. (2003). The 10.5 ka Plinian eruption of Nevado de Toluca volcano, Mexico: Stratigraphy and hazard implications. Geological Society of America 115, p. 230–248.

Arce, J.L., Macías, J.L., Gardner, J.E. and Rangel, E. (2012). Reconstruction of the Sibinal Pumice, an andesitic Plinian eruption at Tacaná Volcanic complex, Mexico-Guatemala. Journal of Volcanology and Geothermal Research 217-218, p. 39-55.

Arce, J.L., Walker, J. and Keppie, J.D. (2014). Petrology of two contrasting Mexican volcanoes, the Chiapanecan (El Chichón) and Central American (Tacaná) volcanic belts: the result of rift- versus subduction-related volcanism. International Geology Review 56, p. 501-524.

Brian M. Tissue, Accuracy and Precision. (1996). http://elchem.kaist.ac.kr/vt/chem-ed/data/acc-prec.htm (consulted on 16-11-2015).

Brendryen, J., Haflidason, H., Sejrup, H.P. (2010). Norwegian Sea tephrostratigraphy of marine isotope stages 4 and 5: prospects and problems for tephrochronology in the North Atlantic region. Quaternary Science Reviews 29, p. 847-864.

Burbach, V.G., Frohlich, C., Pennington, D.W. and Matumoto, T. (1984). Seismicity and Tectonics of the subducted Cocos plate. Journal of Geophysical Research 89, p. 7719–7735.

Canul, R.F. and Rocha, V.L. (1981). Informe geologico de la zona geotermica de 'El Chichonal'. Chiapas Comision Federal de Electricidad, Morelia, Mexico. Informe 38, 32-81.

Canul, R.F., Razo, A.M. and Rocha, V.L. (1983). Geologica e historia volcanologica del volcan Chichonal, Estado de Chiapas. Revista del Instituto de Geologia, U.N.AM., Mexico 3-22.

Capaul, W.A. (1987). Volcanoes of the Chiapas Volcanic Belt, Mexico [Master's thesis]: Houghton, USA, Michigan Technological University, 93 p.

Casadevall, T.J., De la Cruz-Reyna, S., Rose, W.I., Bagley, S., Finnegan, D.L. and Zoller, W.H. (1984). Crater lake and Post-eruption hydrothermal activity, El Chichón volcano, Mexico. Journal of Volcanology and Geothermal Research 23, p. 169-191.

Carey, S., and Sigurdsson, H. (1986). The 1982 eruptions of El Chichón volcano, Mexico (2): Observations and numerical modelling of tephra-fall distribution. Bulletin of Volcanology 48, 127-141.

Cerling, T.E., Brown, F.H. and Bowman, J.R. (1985). Low-temperature alteration of volcanic glass: Hydration, Na, K, ^{18}O and Ar Mobility. Chemical Geology 52, p. 281-293.

Chatterjee, Nilanjan. Electron Microprobe Analysis, course 12.141. January 2012. http://ocw.mit.edu/courses/earth-atmospheric-and-planetary-sciences/12-141-electron-microprobe-analysis-january-iap-2012/lecture-notes/MIT12_141IAP12_coursenotes.pdf (consulted 9-11-2015).

Chauvel, C., Dia, A.N., Bulourde, M., Chabaux, F., Durand, S., Ildefonse, P., Gerard, M., Derualle, B. and Ngounouno, I. (2005). Do decades of tropical rainfall affect the chemical compositions of basaltic lava flows in Mount Cameroon. Journal of Volcanology and Geothermal Research 141, p. 195-223.

Cocheme, J.J. and Silva-Mora, L. (1983). Les eruptions de Mars-Avril 1982 du Volcan Chichonal. Bulletin of Volcanology 46-1, p. 1-15.

Damon, P. and Montesinos, E. (1978). Late Cenozoic volcanism and metallogenesis over and active Beniofff zone in Chiapas, Mexico. Arizona Geological Society Digest 11, 155-168.

Davidson, J., Tepley, F., Palacz, Z. and Meffan-Main, S. (2001). Magma recharge, contamination and residence times revealed by in situ laser ablation isotopic analysis of feldspar in volcanic rocks. Earth And Planetary Science Letters 184(2), p. 427-442.

De la Cruz-Reyna, S., Martin Del Pozzo, A.L. (2009). The 1982 eruption of El Chichón volcano, Mexico: Eyewitness of the disaster. Geofisica Internacional 48, p. 21-31.

De La Fuente, S., Cuadros, J. and Linares, J. (2002). Early stages of volcanic tuff alteration in hydrothermal experiments: formation of mixed-layer illite-smectite. Clays and Clay minerals 50, p. 578-590.

DeMets, C., Gordon, R.G., Argus, D.F., Stein, S. (1990). Current plate motions. Geophysical Journal International 101, p. 425–478.

Demant, A. (1978). Características del Eje Neovolcánico Transmexicano y sus problemas de interpretación: Revista Instituto de Geología 2, p. 172–187.

Drexler, J. W., W. I. Rose Jr., R. S. J. Sparks, and M. T. Ledbetter (1980). The Los Chocoyos Ash, Guatemala: A major stratigraphic marker in Middle America and in the three ocean basins. Quaternary Research 13, p. 327–345.

Duffield, W.A., Tilling, R.I. and Canul, R. (1984). Geology of El Chichón volcano, Chiapas, Mexico. Journal of Volcanology and Geothermal Research 20, 117-132.

Duffield, W.A. (2001). At least Noah had some warning. EOS 82, p. 305-309.

Espíndola, J.M., Macías, J.L., Tilling, R.I. and Sheridan, M.F. (2000). Volcanic history of El Chichón Volcano (Chiapas, Mexico) during the Holocene, and its impact on human activity. Bulletin of Volcanology 62, 90-104.

Ferlito, C. and Lanzafame, G. (2010). The role of supercritical fluids in the potassium enrichment of magmas at Mount Etna volcano (Italy). Lithos 119, p. 642-650.

Froggatt, P. C. (1982). Review of methods of estimating rhyolytic tephra volumes; application to the Taupo volcanic zone. Journal of Volcanology Geothermal Research 14, p. 301–318.

Gislason, S.R., Oelkers, E.H., Eiriksdottir, E.S., Kardjilov, M.I., Gisladottir, G., Sigfusson, B., Snorrason, A., Elefsen, S., Hardardottir, J., Torssander, P. and Oskarsson, N. (2008). The feedback between climate and weathering. Mineralogical Magazine 72, p. 317-320.

Goldstein, J.I., Newbury, D.E., Echlin, P., Joyce, D.C., Fiori, C. and Lifshin, E. (1981). Scanning Electron Microscopy and X-ray Microanalysis: New York (Plentum).

Gomez-Tuena A., Langmuir, C.H., Goldstein, S.L., Straub, S. and Ortega-Gutiérrez, F. (2007). Geochemical evidence for slab melting in the Trans-Mexican Volcanic Belt. Journal of Petrology 48, p. 537–562.

Huizinga A. (2013). Reconstructing El Chichón eruptive history using tephrostratigraphy of the Usumacinta-Grijalva delta plain, Tabasco, México, unpublished MSc thesis.

Jakobsson, S.P. and Moore, J.G. (1986). Hydrothermal minerals and alteration rates at Surtsey volcano, Iceland. Geological Society of America Bulletin 97, p. 648-659.

Kim, Y.H., Clayton, R.W., and Keppie, F. (2011). Evidence of a collision between the Yucatán Block and Mexico in the Miocene. Geophysical Journal International 187, p. 989–1000.

Kuehn, S.C., Froese, D.G. and Shane, P.A.R. (2011). The INTAV intercomparison of electron-beam microanalysis of glass by tephrochronology laboratories: Results and recommendations. Quaternary international 246, p.19-47.

Kutterolf, S., A. Freundt, W. Peréz, T. Mörz, U. Schacht, H. Wehrmann, and H.-U. Schmincke (2008). Pacific offshore record of plinian arc volcanism in Central America: 1. Along-arc correlations. Geochemisty, Geophysiscs and Geosystems 9.

Layer, P.W., Garcia-Paloma, A., Jones, D., Macias, J.L., Arce J.L. and Mora, J.C. (2009). El Chichón volcanic complex, Chiapas, Mexico: stages of evolution based on field mapping and 40Ar/39Ar geochronology. Geofisica International 48, p. 33-54.

Ledbetter, M. T. (1985). Tephrochronology of marine tephra adjacent to Central America. Geological Society American Bulletin 96, p. 77–82.

Lowe, D.J. (2011). Tephrochronology and its application: A review. Quaternary Geochronology 6, p. 107-153.

Lowe, D.J. (1986a). Revision of the age and stratigraphic relationships of Hinemaiaia Tephra and Whakatane Ash, North Island, New Zealand, using distal occurrences in organic deposits. New Zealand Journal of Geology and Geophysics 29, p. 61-73.

Luhr, J.F., Carmichael, I.S.E. and Varekamp, J.C. (1984). The 1982 eruptions of El Chichón volcano, Chiapas, Mexico: mineralogy and petrology of the Anhydrite-bearing pumice. Journal of Volcanology and Geothermal Research 23, p. 69-108.

Luhr, J. (1990). Experimental phase relations of water-and-sulphur saturated arc magmas and the 1982 eruption of El Chichón volcano, Journal of Petrology 31, p. 1071– 1114.

Macías, J.L. (1994). Violent short-lived eruptions from small-size volcanoes: El Chichón, Mexico (1982) and Shtyubel, Russia (1907). Ph.D. dissertation, State University of New York, Buffalo.

Macías, J.L., Sheridan, M.F. and Espíndola, J.M. (1997). Reappraisal of the 1982 eruption of El Chichón volcano, Chiapas, Mexico: new data from proximal deposits. Bulletin of Volcanology 58, 459-471.

Macías JL (1994) Violent short-lived eruptions from small-size volcanoes: El Chichón, Mexico (1982) and Shtyubel, Russia (1907). Ph.D. dissertation, State University of New York, Buffalo.

Macías J.L., Sheridan M.F. and Espíndola J.M. (1997). Reappraisal of the 1982 eruption of El Chichón volcano, Chiapas, Mexico: new data from proximal deposits. Bulletin of Volcanology 58, p. 459–471.

Macías, J.L., Espíndola, J.M., Bursik, M. and Sheridan, M.F. (1998). Development of lithic-breccia's in the 1982 pyroclastic flow deposits of El Chichón volcano, Mexico. Journal of Volcanology and Geothermal Research 83, 173-196.

Macías, J.L., Arce, J.L., Mora, J.C., Espíndola, J.M. and Saucedo, R. (2003). A 550-year-old Plinian eruption at El Chichón Volcano, Chiapas, Mexico: Explosive volcanism linked to reheating of the magma reservoir. Journal of Geophysical Research 108, p. 2569-2586.

Macías, J.L., Capra, L., Scott, K.M., Espíndola, J.M., García-Palomo, A and Costa, J.E. (2004). The 26 May 1982 breakout flows derived from failure of a volcanic dam at El Chichón, Chiapas, Mexico. Geological Society of America Bulletin 116, p. 233-246.

Macias, J.L. (2007). Geology and eruptive history of some active volcanoes of Mexico. Geographical Society of America 422, p. 183-232.

Macías, J.L. (2010). Geology and eruptive history of some active volcanoes of Mexico. in Alaniz-Álvarez, S.A., and Nieto-Samaniego, Á.F., eds., Geology of México: Celebrating the Centenary of the Geological Society of México. Geological Society of America 422, p. 183-232.

Macías, J.L., Arce, J.L., García-Palomo, A., Mora, J.C. and Espíndola, J.M. (2010). Late-Pleistocene flank collapse triggered by dome growth at Tacaná volcano, México-Guatemala, and its relationship to the regional stress regime. Bulletin of Volcanology 72, p. 33-53.

Mora, J.C., Jaimes-Viera, M.C., Garduno-Monroy, V.H., Layer, P.W., Pompa-Mera, V. and Godinez, M.L. (2007). Geological and geochemistry characteristics of the Chiapanecan Volcanic Arc (Central Area), Chiapas Mexico. Journal of Volcanology and Geothermal Research 162, p. 43-72.

Newton, A.J. and Metcalfe, S.E. (1999). Teprhochronology of the Toluca Basin, Central Mexico. Quaternary Science Reviews 18, p. 1039-1059.

Nielsen, C.H. and Sigurdsson, H. (1981). Quantitative methods for electron microprobe analysis of sodium in natural and synthetic glasses. American Mineralogist 66, p. 547-552.

Nixon, G.T. (1982). The relationship between Quaternary volcanism in central Mexico and the seismicity and structure of the subducted ocean lithosphere. Geological Society American Bulletin 93, p. 514– 523.

Nooren, C.A.M., Hoek, W.Z., Tebbens, L.A. and Del Pozzo, A.L.M. (2009). Tephrochronological evidence for the late Holocene eruption history of El Chichón Volcano, Mexico. Geofísica Internacional 48, p. 97-112.

Ortega-Guerrero, B. and Newton, A.J. (1998). Geochemical characterization of Late Pleistocene and Holocene tephra layers from the Basin of Mexico, Central Mexico. Quaternary Research 50, p. 90-106.

Palais, J.M., Germani, M.S. and Zielinski, G.A. (1992). Inter-hemispheric transport of volcanic ash from a 1259 AD. Volcanic eruption to the Greenland and Antarctic ice sheets. Geophysical research letters 19, p. 801-804.

Payne, R.J., Gehrels, M.J., 2010. The formation of tephra layers in peatlands: an experimental approach. Catena 81, p. 12-23.

Pearce, N.J.G., Bendall, C.A., Westgate, J.A. (2008a). Comment on "Some numerical considerations in the geochemical analysis of distal microtephra" by A.M. Pollard, S.P.E. Blockley and C.S. Lane, Applied Geochemistry, vol. 21, p. 1692-1714. Applied Geochemistry 23, p. 1353-1364.

Rebollar, C.J., Espíndola, V.H., Uribe, A., Mendoza, A., Pérez-Vertti, A. (1999). Distribution of stress and geometry of the Wadati–Benioff zone under Chiapas, Mexico. Geofísica Internacional 38, p. 95–106.

Reynolds, J. H. (1987). Timing and sources of Neogene and Quaternary volcanism in south-central Guatemala, Journal of Volcanology and Geothermic Research 33, p. 9–22.

Rose, W.I., Hahn, G.A., Drexler, J. W., Malinconico, M. L., Peterson, P. S., Wunderman., R.L. (1981). Quaternary tephra of Northern Central America. Tephra Studies, p. 193-211.

Rose, W. I., F. M. Conway, C. R. Pullinger, A. Deino, and K. McIntosh (1999). An improved age framework for late Quaternary silicic eruptions in northern Central America. Bulletin of Volcanology 61, p. 106–120.

Rueda, H., J.L. Macías, J.L. Arce, J.E. Gardner, P.W. Layer. (2013). The ~ 31 ka rhyolitic Plinian to sub-Plinian eruption of Tlaloc Volcano, Sierra Nevada, central Mexico, Journal of Volcanology and Geothermal Research 252, p 73-91.

Schaaf, P., Stimac, J., Siebe, C. and Macías, J.L. (2005). Geochemical Evidence for Mantle Origin and Crustal Processes in Volcanic Rocks from Popocatépetl and Surrounding Monogenetic Volcanoes, Central Mexico Journal of Petrology 46, p. 1243–1282.

Scolamacchia T. and Macias, J.M. (2015). Active volcanoes of Chiapas (Mexico): El Chichón and Tacaná. In active volcanoes of the world. Springer-Verslag Berlin Heidelberg, Berlin.

Shane, P.A.R., Doyle, L.R., Nairn, I.A., 2008b. Heterogeneous andesite-dacite ejecta in 26-16.6 ka pyroclastic deposits of Tongariro Volcano, New Zealand: the product of multiple magma-mixing events. Bullletin of Volcanology 70, p. 517-536.

Shipley, S. and Sarna-Wojcicki, A.M. (1982). Distribution, Thickness and mass of Late Pleistocene and Holocene tephra from major volcanoes in the north western United States: a preliminary assessment

of hazard from volcanic ejecta to nuclear reactors in the Pacific Northwest. US Geological Survey Miscell. Field Studies Map MF-1435.

Siebe, C., Abrams, M., Macías, J.L., and Obenholzner, J. (1996). Repeated volcanic disasters in Prehispanic time at Popocatépetl, central Mexico: Past key to the future? Geology 24, p. 399–402.

Stefansson, A. and Gislason, S.R. (2001). Chemical weathering of basalts, Southwest Iceland: effect of rock crystallinity and secondary minerals on chemical fluxes to the ocean. American Journal of Science 301, p. 513-556.

Smits, K. (2015). Environmental change since AD 1080 in the Grijalva watershed, México, inferred from Lake Chicuacan sediments, Unpublished MSc thesis.

Smid, E. (2015). Amount of eroded sediment originating from the Platanar and Magdalena rivers (Tabasco, Mexico), since the eruption of El Chichón in 1982, unpublished MSc thesis.

Summering. (2010). LIDAR Analysis in ArcGIS® 9.3.1 for Forestry Applications, an Esri White paper chapter 3. From: http://www.esri.com/library/whitepapers/pdfs/lidar-analysis-forestry.pdf. (Consulted on 20-11-2015).

Tepley, F.J., Davidson, J.P., Tilling, R.I. and Arth, J.G. (2000). Magma mixing, Recharge and eruption histories recorded in plagioclase phenocrysts from El Chichón volcano, Mexico. Journal of Petrology 41, p. 1397-1411.

Tilling, R., Rubin, M., Sigurdsson, H., Carey, S., Duffield, W. and Rose, W.I. (1984). Holocene eruptive activity of El Chichón volcano, Chiapas, Mexico. Science 224, p. 747-749.

Tilling, R.I. (2009). El Chichón's 'suprise' eruption in 1982: Lessons for reducing volcano risk. Geofisica Internacional 48, p. 3-19.

VOGRIPA (2013). Database historic activity Tacaná, from various authors. www.bgs.ac.uk/vogripa/. (Consulted march 2016).

Vogripa, 2015. Database of El Chichón for eruption properties and date. Data based on several authors. http://www.bgs.ac.uk/vogripa/searchVOGRIPA.cfc?method=detail&id=2035. (Consulted on 9-11-2015).

Wittke, James H. Electron Microprobe. 2015. http://nau.edu/CEFNS/Labs/Electron-Microprobe/GLG-510-Class-Notes/Detection-of-Signals/. (Consulted 9-11-2015).

Yamada, I. and Shoji, S. (1983). Alteration of volcanic glass of recent Towada ash in different soil environments of North-eastern Japan. Soil science 135, p. 316-321.

Zielinski, G. A., Mayewski, P. A., Meeker, L. D., Grönvold, K., Germani, M. S., Whitlow, S., Twickler, M. S., Taylor, K. (1997). Volcanic aerosol records and tephrochronology of the Summit, Greenland, ice cores. Journal of Geophysical Research 102, p. 26625–26640.